PHYSIOLOGY OF THE PULMONARY PACEMAKER: A NEW REGULATOR OF LUNG GROWTH

Thesis submitted in accordance with the requirements of the University of Liverpool for the degree of Doctor in Philosophy

by

Neil Christopher Featherstone

1st August 2009

ABSTRACT

Physiology of the pulmonary pacemaker: a new regulator of lung growth

NC Featherstone

Background: Pulmonary hypoplasia and pulmonary hypertension account for the high mortality in Congenital Diaphragmatic Hernia (CDH). Factors involved in determining lung growth are thus of interest: spontaneous contractility of embryonic airway smooth muscle (ASM) is one such mechanical factor.

Aim: To examine the physiological mechanisms underpinning spontaneous airway contractility ('airway peristalsis') in normal and hypoplastic lung and relate these to pulmonary development.

Methods: Sprague-Dawley rats were fed 100mg nitrofen on Day 9.5 of pregnancy to induce lung hypoplasia in offspring (controls had vehicle alone). Normal and hypoplastic lung primordia were cultured from Day 13.5 of gestation at 37°C in 5% CO_2 and loaded at 54 or 78 h with calcium (Ca^{2+})-sensitive indicators: Fluo-4 for confocal imaging and Indo-1 or Fura-2 for photometric measurements of Ca^{2+}_i.

Results: Peristalsis of the embryonic airways was driven by spontaneous, regenerative, temperature-sensitive Ca^{2+}_i waves. These Ca^{2+}_i waves propagated between individual ASM cells coupled by gap junctions, were likely to be action potential-mediated, and were dependent on not only extracellular Ca^{2+} (Ca^{2+}_o) entry via L-type voltage-gated channels but also intracellular stores. Hypoplastic lung also featured spontaneous propagating ASM Ca^{2+}_i transients, but with reduced frequency, increased amplitude, and significantly prolonged plateau duration, relative to control lung.

Conclusions: Spontaneous prenatal Ca^{2+}_i waves underpin airway peristalsis in embryonic rat lung. If as recent data suggest, airway peristalsis regulates prenatal lung growth, then we can assert intercellular Ca^{2+}_i oscillations in turn regulate antenatal lung development. Early ASM dysfunction in lung hypoplasia is apparent as specific anomalies of Ca^{2+}_i transients and may suggest key problems in the ASM ion channels / action potential generation. These changes accompany early hypoplasia and precede visceral herniation; they may underlie, in part, later post-CDH ASM abnormalities (airway hyperactivity).

DECLARATION

This thesis is the result of my own work. The material contained in this thesis has not been presented, nor is currently being presented, either wholly or in part for any other degree or other qualification.

The research was carried out at the Institute of Child Health, Royal Liverpool Children's Hospital (Alder Hey); the Department of Physiology; and the School of Biological Sciences, University of Liverpool, UK.

CONTENTS

Chapter 5

CYCLOPIAZONIC ACID (CPA) REVERSIBLY ABOLISHES LUNG BRANCHING MORPHOGENESIS AND AIRWAY PERISTALSIS 132

LIST OF FIGURES

ACKNOWLEDGMENTS

I should like to acknowledge the input and support of numerous colleagues during the undertaking of these studies. In particular, I should like thank Ted Burdyga for his enthusiasm and dedicated teaching in Ca^{2+}_i imaging techniques; Susan Wray and David Fernig for continuous encouragement in their respective laboratories; David Spiller and Mike White for assistance in the Centre for Cell Imaging; Gwen Connell for her friendship and unrelenting assistance during dissection, lung culture, photography, and histological processing; Harriet Corbett for her friendship and support; Edwin Jesudason for his friendship, dedication, enthusiasm, encouragement, and reflection and reasoning; and Paul Losty for his continuous enthusiasm, friendship, suggestions and assistance. Their contributions all played a role in these studies resulting in two publications in the American Journal of Respiratory Cell and Molecular Biology and awards from the British Association for the Advancement of Science and The Medical Research Society / Academy of Medical Sciences.

I should also like to acknowledge the financial support provided by the Royal College of Surgeons of England (One Year Research Fellowship) and The Medical Research Council (MRC) which supported these studies.

Finally, I would like to thank my family and Lynne Kirby for their love and support during these studies. Lynne's diagnosis of Hodgkin's Lymphoma during this time reminds us that being in good health is often unappreciated. Basic science research can drive new clinical treatment and bring hope to patients and their families.

Chapter 1

INTRODUCTION

1.1 Congenital diaphragmatic hernia

1.1.1 Definition and Classification

Congenital diaphragmatic hernia (CDH) comprises the posterolateral Bochdalek diaphragmatic malformation (Figure 1.1), intra-thoracic herniation of abdominal viscera and pulmonary hypoplasia (Bochdalek 1848). The malformation is left sided in 78% of cases, right sided in 21% and bilateral in 1% (Clark *et al.* 1998; Neville *et al.* 2003).

CDH differs from the rarer Morgagni hernia in which the diaphragmatic defect lies anteriorly in a retrosternal position (Baran *et al.* 1967). This thesis only considers the commonest form, the Bochdalek defect due to its more severe prognosis; it continues to challenge neonatologists and paediatric surgeons despite advances in care.

1.1.2 Epidemiology

Determining the true incidence of CDH is problematic. A number of fetuses with CDH will be lost antenatally either spontaneously or though termination. Some CDH newborns will die before transfer to the surgical centre for definitive repair. CDH detected outside the perinatal period may not be included in epidemiological studies resulting in errors of estimation. Lastly, population-based studies may be affected by ascertainment bias (Beresford *et al.* 2000; Stege *et al.* 2003; Ontario Congenital Anomalies Study Group 2004; Colvin *et al.* 2005; Dillon *et al.* 2000). Different countries and regions differ in their abilities to ascertain data and create

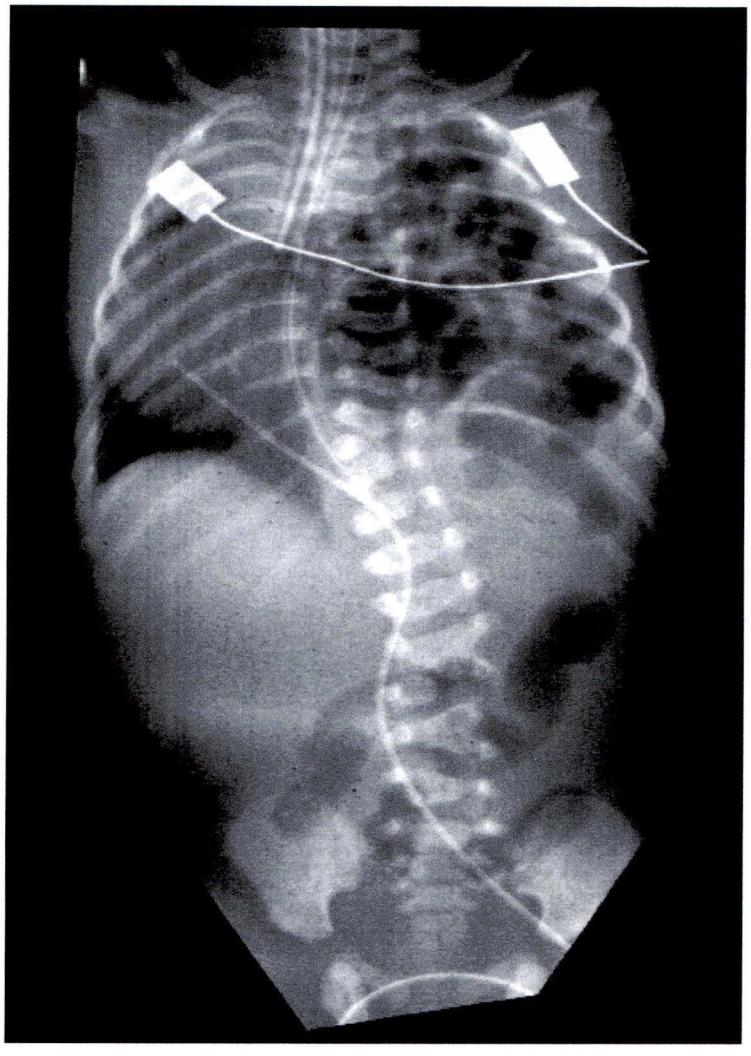

Figure 1.1. Chest and abdominal radiograph showing a newborn with left congenital diaphragmatic hernia (CDH). Loops of bowel can be seen the left hemithorax. The heart is displaced to the right. Vertebral defects can also be seen. Radiograph courtesy of Dr David Pilling (Consultant Radiologist at The Royal Liverpool Children's Hospital, Alder Hey).

registries of antenatally and postnatally detected cases of CDH (Garne *et al.* 2005; Rankin *et al.* 2005). Given these caveats, it has been estimated that CDH has an incidence of approximately 1 in 2500 births such that a new case is born in the United Kingdom every 24-36 hours (Smith *et al.* 2002).

1.1.3 Aetiology

Although the aetiology is largely unknown, CDH has been reported in conjunction with the maternal administration of thalidomide and phenometrazine (Hobolth 1962; Powell *et al.* 1962). A small number of cases exhibiting familial inheritance exist within the literature (Tibboel et al. 1996; Kufeji *et al.* 1999).

CDH occurs as an isolated defect in the majority of cases; however, it may co-exist with other major anomalies (cardiac and neural tube being particularly prominent) in one quarter to one third of cases (Benjamin *et al.* 1988; Sweed *et al.* 1993). However, in approximately 10%, it forms a component of a syndromic genopathy (Witters *et al.* 2001). Genetic syndromes include Fryn's, Denys-Drash, Goldenhar's, Brachmann-de-Lange, Beckwith-Wiedemann and Pallister-Killian (Dillon *et al.* 2000; Borys *et al.* 2004; Ahn *et al.* 2005; Slavotinek 2007). Associated anomalies increase mortality markedly; 93% of newborns with CDH and major anomalies have been reported to die, either antenatally or early within the postnatal period (Beresford *et al.* 2000).

1.1.4 Pathology

There is a clinical spectrum of disease in CDH ranging from newborns that do well with conventional mechanical ventilation, to the sickest requiring advanced stabilization strategies for the opportunity to survive.

Hypoplastic lungs are morphologically abnormal; CDH results in a reduction in lung weight, volume, airway generation and alveolar number. There is also abnormal development of bronchiolar cartilage, abnormal muscularisation of the pulmonary arteriolar wall and decreased cross-sectional area of the pulmonary vascular bed (Nakamura *et al.* 1991; Kitagawa *et al.* 1971; Adzick *et al.* 1985). In addition, the lungs may be stiff, non-compliant and atelectatic as a result of surfactant deficiency (Moya *et al.* 1995; Alfanso *et al.* 1996; Valls-i-Soler *et al.* 1996). Pulmonary vascular adaptation to postnatal life has been demonstrated to be delayed in CDH newborns; normally, pulmonary artery pressures fall rapidly at birth, however in CDH, it may take weeks to normalize (Haugen *et al.* 1991). The resulting elevation in pulmonary vascular resistance produces right to left shunting and hypoxaemia. Hypoxia results from these anatomical, biochemical and physiological abnormalities of the CDH lung.

1.1.5 Animal Models for Congenital Diaphragmatic Hernia

Four types of animal models for CDH can be identified 1) naturally occurring 2) surgically created 3) teratogen-induced and 4) transgenic. They provide investigators with tools with which to study pulmonary

development in CDH; they may provide insights into the pathogenesis of this lethal condition, which may then be translated to the clinical setting. However, certain caveats must be borne in mind when using these experimental models.

1.1.5.1 Naturally occurring CDH

CDH was reported to occur naturally in a herd of pigs that was bred to produce anorectal malformations (Ohkawa *et al.* 1992). Symptoms occurred 1 to 4 months postnatally. Despite herniated organs being found within the thoracic cavity, the lungs do not exhibit the hypoplasia that is characteristic of human CDH.

1.1.5.2 Surgically created CDH

Surgically created models of CDH are based on the traditional thesis that lung hypoplasia results from compression by the herniated abdominal viscera. The first model was described in 1967 and involved creating a diaphragmatic hernia in third trimester fetal lambs (De Lorimier *et al.* 1967). Subsequently, many investigators have used a variety of techniques based upon this principle in a variety of species (mainly ovine) to investigate the pathophysiology of CDH (Haller *et al.* 1976; Harrison *et al.* 1980; Adzick *et al.* 1985; Fauza *et al.* 1994; Wu *et al.* 2002; Roubliova *et al.* 2004). Usually, time-dated ewes are operated upon at mid-gestation to expose the fetus; a diaphragmatic defect is created via a posterolateral

thoracotomy. Stomach, omentum and small intestine are then placed in the chest. The thoracotomy is closed and the pregnancy maintained with tocolytics.

This model produces several similarities to human CDH; the lungs exhibit hypoplasia, reduced number of airway branches and alveoli, diminished pulmonary vasculature and increased muscularisation of the pulmonary arteries (Lipsett *et al.* 2000; Ting *et al.* 1998). Prenatal 'repair' of the surgically created defect resulted in reversal of the pulmonary hypoplasia (Harrison *et al.* 1980). As a consequence, paediatric surgeons investigated in-utero repair of congenital diaphragmatic defects; a prospective randomised trial showed no benefit in humans compared with standard postnatal management (Harrison *et al.* 1997).

New trials of temporary tracheal occlusion commenced following the finding that congenital laryngeal obstruction resulted in hyperplastic lungs (Silver *et al.* 1988). Initially, the trachea was occluded using clips that required surgical removal prior to birth, and later, via an inflatable detachable balloon (Skarsgard *et al.* 1996). However, temporary balloon occlusion did not prevent the development of lung pathology associated with pulmonary hypoplasia (Harrison *et al.* 2003), nor did it improve survival or morbidity rates (Heerema *et al.* 2003). Despite this, human fetal programmes in North America and Europe continue to investigate fetal endoscopic techniques in selected high-risk fetuses (Keller *et al.* 2004; Deprest *et al.* 2005; Saura *et al.* 2007).

There are a number of problems associated with surgically created models of CDH. Ovine fetuses undergo antenatal surgery exposing them to pharmaceutical agents / mechanical ventilation. The fetuses are otherwise normal and lack the associated defects (e.g. cardiac or chromosomal) which are often seen in human CDH and may contribute to its high mortality. Large animal studies are inherently expensive due to the costs of maintaining the stock, operative costs and drugs. Economic costing and a high rate of fetal loss following antenatal surgery limit the size of experimental groups. The timing of surgery is also pertinent in that according to the compression theory herniated viscera should inhibit growth from the early pseudoglandular stage. However, the ovine surgical model of CDH is usually created during the late pseudoglandular or canalicular stages of lung development (de Lorimier *et al.* 1967; Adzick *et al.* 1985). As a result, the resulting pulmonary defects may be dissimilar to human CDH. Lastly, the surgically created model is not able to provide any insights into the pathophysiology of CDH at an embryonic level.

1.1.5.3 Teratogen-induced CDH

A number of chemicals have been described that induce CDH in rodents (Taleporos *et al.* 1978; Iritani 1984). Vitamin A deprivation in rodents also results in CDH in the offspring (Wilson *et al.* 1953). Perhaps the most popular teratogen used to induce CDH is nitrofen (2,4-dichloro-4'-nitrodiphenylether). It is administered to pregnant rats (single gavage feed)

on a specific point in gestation to induce CDH in a proportion of the offspring (Kluth *et al.* 1990; Kluth *et al.* 1993; Kluth *et al.* 1996a; Kluth *et al.* 1996b). It provides the singular opportunity to study CDH at an embryological level (prior to closure of the diaphragm).

However it is unclear how nitrofen actually induces CDH (e.g. it is unknown whether nitrofen itself or one of its metabolites is the active teratogen) (Noble *et al.* 2007). Nitrofen has similarities to thyroid hormone and it has been suggested that it may work through disruption of thyroid metabolism (Figure 1.2) (Tovar *et al.* 1997). However, nitrofen does not appear to alter thyroid hormone signalling or receptor function (Noble *et al.* 2007). Neither does it seem to involve the oxidative effects of nitrofen (Noble *et al.* 2007). Rather, it appears to inhibit the rate-limiting enzymes that control retinoic acid synthesis (Greer *et al.* 2003; Noble *et al.* 2007). Nitrofen-exposed pups without CDH also exhibit pulmonary hypoplasia compared to controls (Kluth *et al.* 1990; Kluth *et al.* 1993; Brandsma *et al.* 1995; Losty *et al.* 1996b). As a consequence, there are some concerns that the pulmonary abnormalities may arise as a direct effect of nitrofen itself. Also, there appears to be no correlation between nitrofen exposure and CDH in humans (Bos *et al.* 1994). Nor does nitrofen necessarily produce CDH in non-Sprague-Dawley rat strains, raising questions regarding its species-dependent method of action (Kang *et al.* 1986). Despite these concerns, nitrofen remains popular as it is cheap, simple to administer and

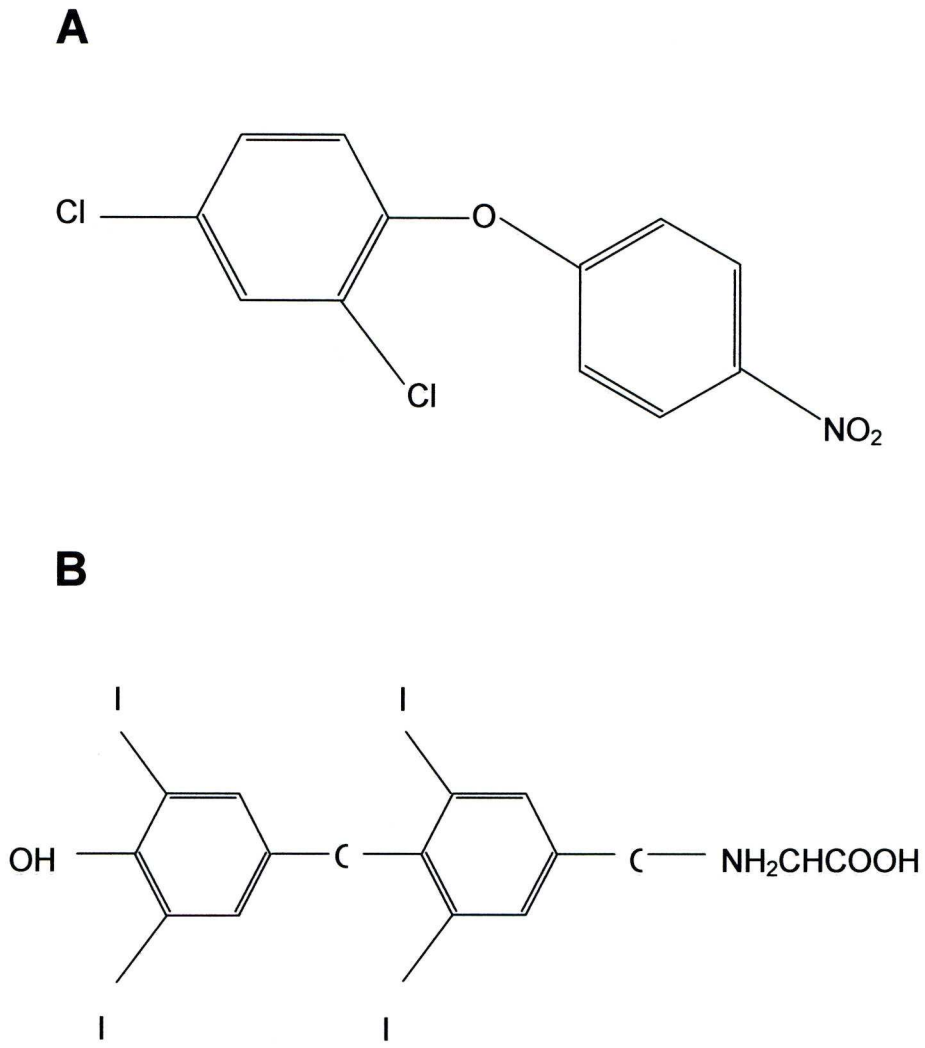

Figure 1.2. Schematic diagram depicting the molecular structure of A) nitrofen (2,4-dichloro-4'-nitrodiphenylether) and B) thyroxine. Nitrofen exhibits stereochemical structural similarity to thyroid hormone and its teratogenic effects have been speculated to be a consequence of altered thyroid hormone metabolism.

permits investigation of pulmonary development during CDH embryogenesis.

1.1.5.4 Transgenic models of CDH

More recently, the use of rodent genetic technology has provided new tools with which to investigate diaphragm development and CDH. Several mutant phenotypes have been described in which CDH features. However, they often frequently exhibit other malformations that result in them being phenotypically different from human CDH. Deletion of both murine retinoic acid receptors (RARs) results in a high incidence of cranial, vertebral, limb, cardiac, foregut and pulmonary malformations but only yields a low frequency of CDH (Lohnes *et al.* 1994; Mendelsohn *et al.* 1994). Mice with Hlx gene mutations (a homeobox transcription factor gene) have CDH, but, have large lungs and small liver and intestine (Hentsch *et al.* 1996). Homozygous inactivation of WT-1 (Wilms' Tumour suppressor gene) results in CDH, but the mice are severely deformed and have severe urogenital anomalies (Kreidberg *et al.* 1993). Mice homozygous for Slit3 (slit homolog 3 [drosophila]) deficiency exhibit CDH, but the hernia is located within the central tendon, rather than the posterolateral diaphragm (Liu *et al.* 2003). In these mice, the hernias contain the liver and gallbladder, and a large proportion of mice exhibit urogenital anomalies (renal / ureteral agenesis). Murine COUP-TFII-null mutants (COUP-TFII is a member of nuclear receptor superfamily that

plays a critical role during mouse development) exhibit Bochdalek-type CDH and the stomach and liver protrude into the thoracic cavity (You *et al.* 2005).

These models may in time, permit investigation of the pathophysiology of CDH. Like the nitrofen model of CDH, they would allow study at the embryological stage. However, at present many phenotypic differences exist between the models and human CDH which currently limits their use on a wide scale.

1.1.6 Pathogenesis

The causation of the hypoplastic lung in CDH remains unknown. Several explanations have been proposed; these have been derived from clinical observation and studies of developmental biology utilising animal models.

Herniated abdominal viscera may compress the developing lung and prevent normal development. Evidence supporting this arises from the sheep model of CDH, in which a surgically created defect and manual herniation of the viscera result in lung hypoplasia (De Lorimier *et al.* 1967). Reduction of the herniated material and repair of the defect whilst in utero produces lung enlargement (Harrison *et al.* 1980a; Harrison *et al.* 1980b).

Alternatively, an abnormality of pulmonary development may already exist prior to closure of the diaphragm at 8 weeks of age in the human fetus. Various teratogens that induce CDH have been utilised in animal models to

test these hypotheses (Taleporos *et al.* 1978; Iritani 1984; Kang *et al.* 1986). Nitrofen (2,4-dichloro-4'-nitro diphenyl ether) murine (mouse or rat) models of CDH are one of the most commonly used (see section 1.1.5.3). At day 13.5 of gestation, 24 hours after lung primordia develop from the foregut, the normal lung and two thirds of nitrofen-exposed lungs have $\geq$ 6 buds, in contrast, one third of nitrofen exposed lungs have less than six buds. When followed longitudinally utilising organ culture techniques, the nitrofen lungs show reduced bud counts, area and perimetry (Jesudason *et al.* 2000). These findings suggest branching morphogenesis is disrupted prior to diaphragmatic closure.

However, lung hypoplasia may occur through a combination of these hypotheses. Keijzer et al. suggested that there may be a 'dual hit' upon the developing lung. He postulated that: 1) the lungs were intrinsically abnormal prior to closure of the diaphragm, and; 2) growth was further impaired through compression by herniated viscera (Keijzer *et al.* 2000).

Diaphragmatic defects may also result in fluid loss from the lungs through dysfunction of the diaphragm. Studies have shown drainage of lung fluid at regular intervals during pregnancy results in lung hypoplasia, whereas perfluorocarbon instillation and fetal tracheal occlusion produces fetal lung enlargement (Fauza *et al.* 2001; Alcorn *et al.* 1977; Moessinger *et al.* 1990; DiFiore *et al.* 1994; Adzick *et al.* 1985).

1.1.7 Management

The first successful neonatal CDH repair was performed in 1946 by Robert Gross (Gross 1946). During the last half-century, several stabilisation techniques (extracorporeal membrane oxygenation (ECMO), high frequency oscillatory ventilation (HFOV), nitric oxide (NO) inhalation, and permissive hypercapnia) and advances in prenatal therapy have been introduced. Novel therapies such as liquid ventilation (LV), surfactant therapy and steroids have also been investigated (Hirschl *et al.* 2003; Van Meurs 2004; Lally *et al.* 2006; Logan *et al.* 2007).

Despite these developments, mortality has changed little when the 'hidden mortality' (antenatal and early postnatal deaths prior to transfer to the definitive paediatric surgery centre) is considered; mortality remains as high as 60% (Stege *et al.* 2003; The Ontario Congenital Anomalies Study Group 2004; Colvin *et al.* 2005; Dillon *et al.* 2000). The majority of these deaths result from the associated pulmonary hypoplasia and accompanying pulmonary hypertension (Skari *et al.* 2000).

Approximately 50 – 60% of cases are detected antenatally via routine obstetric ultrasound scanning (often prior to 25 weeks gestation) (Thilaganathan 2002; Garne *et al.* 2002; Dillon *et al.* 2000). In the UK, most antenatally detected cases of CDH are detected upon the 20-week routine anomaly scan. It is possible to diagnose CDH as early as the 11th week of gestation, but a European multi-centre study has shown the mean age at diagnosis is 24.2 weeks (Garne *et al.* 2005). Visualisation of the

stomach, liver or intestines within the thoracic cavity confirms the diagnosis. Mediastinal shift away from the side of the defect may also be noted. Antenatally detected cases should ideally be referred to a specialist centre such that a multi-disciplinary medical team, consisting of obstetrician, neonatologist and paediatric surgeon may then counsel the parents and plan delivery and management options.

However, predicting the outcome and survival for antenatally detected CDH cases is difficult; many parameters have been proposed and evaluated over time. For example, polyhydramnios (Adzick *et al.* 1989), presence of stomach herniation (Burge *et al.* 1989) and abdominal circumference at the level of the umbilical cord (Teixeira *et al.* 1997) have all been associated with poor outcome in studies (Metkus *et al.* 1996); but none are absolutely predictive of postnatal death.

Lung head ratio (LHR) was suggested as a marker of prognosis by Harrison's group in San Francisco (Lipshutz *et al.* 1997). It is the ratio of the area of the lung contralateral to the hernial defect to the fetal head circumference. Measured via ultrasonography at the level of the atria (so-called 'four-chamber view of the heart') it minimizes discrepancy owing to gestational age. LHR levels have been subdivided into categories: <1, 1-1.4, and >1.4. They have been reported to show good applicability in the prediction of fetal outcome within retrospective and prospective study populations, with 100% survival if LHR >1.4 and 100% mortality if LHR <1 (Laudy *et al.* 2003; Keller *et al.* 2003; Lipshutz *et al.* 1997); the

outcome is not so clear for those with a mid-range LHR. More recently, the relationship between LHR and gestational age has been investigated; it has been suggested that LHR predicts postnatal survival in fetuses at 24-34 weeks of gestation, but less reliably at 20-24 weeks (Yang *et al.* 2007). However, others have reported that a LHR of <1 does not predict postnatal survival and as such, should not be used as a factor for choosing fetal intervention (Arkovitz *et al.* 2007). Indeed, a recent meta-analysis of the current prognostic use of LHR in fetal surgery shows lack of a sufficient evidence base and is impaired by overlapping and methodologically diverse reporting (Ba'ath *et al.* 2007). There is a paucity of information available on normal LHR values and inter-observer and inter-institution variations in its measurement may exist (Ba'ath *et al.* 2007). Further evaluation of LHR is therefore required.

Both prospective and retrospective studies have determined that liver herniation ('liver up cases') and early diagnosis (less than 25 weeks gestation) markedly reduce survival (Adzick *et al.* 1985; Albanese *et al.* 1998). It may be that large symptomatic hernias are detected easily on ultrasonographic scanning resulting in lead-time bias.

Antenatal magnetic resonance imaging (MRI) holds promise in CDH assessment; it has been shown to yield information additional to that gained by ultrasonography in fetuses with thoracic abnormalities (Levine *et al.* 2003; Hubbard *et al.* 1999; Neff *et al.* 2007; Cannie *et al.* 2008).

If CDH is not diagnosed antenatally, the majority will present with signs of respiratory distress within the first few minutes of life. A small subset of patients may present at a later date, often with insidious clinical signs that may not be related to the hernia itself ('late presentation CDH').

A team of paediatric surgeons, neonatologists and anaesthetists should care for the baby once born. Elective intubation should be performed (avoiding barotrauma or volutrauma to the hypoplastic lung) and a nasogastric tube passed to prevent dilatation of the bowel and resulting compromise of respiratory function.

Radiographic investigations confirm the diagnosis: chest radiographs may show loops of bowel within the thoracic cavity, mediastinal shift or occasionally abnormal position of a naso-gastric tube indicating displaced viscera. Rarely, an upper gastrointestinal contrast study may be required to provide further information. Alternative pathologies, such as cystadenomatous lung lesions, can normally be excluded with the aid of ultrasonography.

Historically, repair was undertaken as an emergency, but over time, practice has gradually shifted to a policy of stabilization using a variety of ventilatory strategies before operation. It was recognised early surgery did not necessarily result in an improved outcome. Randomized prospective studies and retrospective studies have been performed to determine optimal timing of surgery for infants with congenital diaphragmatic hernia. Many have demonstrated no benefit in undertaking immediate surgery (Nio *et al.*

1994; Shanbhogue *et al.* 1990; Langer *et al.* 1988). The Cochrane collaboration concluded similar findings, but stated a large, multicenter randomized trial would be needed to fully answer this question (Moyer *et al.* 2002). Newborns undergo physiological remodelling following birth to prepare for postnatal life. Permitting these adaptations to take place, whilst in an intensive care setting and prior to surgery, may result in improved outcomes.

It is now recognised that is important to use ventilatory strategies that exploit low tidal volumes and pressures to minimise volutrauma and barotrauma ('gentilation'). High ventilation pressures, high-end expiratory volumes and repeated opening and closing of alveoli during the respiratory cycle have been shown to cause lung injury (Wung *et al.* 1985; Boloker *et al.* 2002; Downard *et al.* 2003; Smith *et al.* 2002).

Extracorporeal membrane oxygenation (ECMO) is a heart-lung bypass technique utilised for severe but potentially reversible respiratory failure and cardiac failure in children and adults. It was first utilised in a neonate in 1975 (Bartlett 1976). It may be employed for pre-operative stabilisation, or post-operative rescue in CDH newborns. Surgery may even be performed whilst on ECMO, although care must be taken with regards to anticoagulation. Early retrospective studies from single institutions, using historical controls for comparative data, suggested ECMO may improve survival (Weber *et al.* 1987; D'Agostino *et al.* 1995; Atkinson *et al.* 1991). Likewise, the Congenital Diaphragmatic Hernia Study Group reported that

ECMO significantly improved survival rates for newborns with CDH with a predicted mortality of $\geq$ 80% (The Congenital Diaphragmatic Hernia Study Group 1999). Conventional mechanical ventilation (CMV) and ECMO were compared to CMV and high frequency oscillatory ventilation (HFOV), as rescue therapies, in two large tertiary care paediatric centres ('A tale of two cities'); CMV with ECMO resulted in an overall survival similar to CMV with HFOV (Wilson *et al.* 1997; Azarow *et al.* 1997). The Cochrane Group concluded ECMO provided short-term benefits for the CDH newborn; however, the overall effect was not clear (Elbourne *et al.* 2002). In comparison, it led to significantly improved survival in mature infants with potentially reversible respiratory failure, who did NOT have CDH (Elbourne *et al.* 2002). Previously, the UK Collaborative ECMO Trial Group had reported that ECMO was beneficial and should be actively considered for neonates with severe but potentially reversible respiratory failure (UK Collaborative ECMO Trial Group 1996).

High frequency oscillatory ventilation (HFOV) operates at low airway pressures, tidal volumes and end-expiratory volumes; consequently, it avoids barotrauma and volutrauma. Anecdotal reports from centres suggest CDH patients show benefit with this technique, compared to conventional mechanical ventilation (Azarow *et al.* 1997; Karl *et al.* 1983; Arnold 2000). One such report from Italy stated that HFOV had improved survival from 67% using CMV to 94% (Cacciari *et al.* 2001). However, as yet, no randomised controlled evidence exists to support its widespread use.

Nitric oxide is an endogenous, free radical that has vasodilatory effects via cyclic GMP on the pulmonary vasculature in both animal models and humans. Identified as endothelial derived relaxing factor (EDRF) in 1987 (Palmer *et al.* 1987), it has a short half-life and is rapidly oxygenated to nitrates and nitrites. Inhaled nitric oxide (iNO) was introduced as an alternative to systemic vasodilators such as tolazoline and prostacyclin, for the treatment of persistent pulmonary hypertension (and thereby avoid their side effect profile, including marked systemic hypotension) (Stevens *et al.* 1980; Bloss *et al.* 1980). Theoretically, iNO is beneficial for treating pulmonary hypertension in CDH as it is directed to well-ventilated areas of lung, resulting in targeted vascular relaxation and decreased pulmonary hypertension. Only a few studies have investigated the use of iNO as a selective vasodilator in CDH. The Neonatal Inhaled Nitric Oxide Study Group (NINOS) reported that although NO provided short-term improvements in oxygenation, it did not reduce the proportion of patients requiring ECMO or mortality rates (The Neonatal Inhaled Nitric Oxide Study Group (NINOS) 1997). Similarly, a Cochrane systematic review concluded that iNO did not improve the outcome of newborns with CDH (Finer *et al.* 2000).

Permissive hypercapnia was developed to avoid lung damage through avoidance of high ventilatory pressures and high tidal volumes. The technique permits neonates to breathe spontaneously at a high rate achieving a normal minute volume. Low airway pressures prevent

compromise of venous return and cardiac output. An elevated P_aCO_2 is accepted within regulated limits. Hypercapnia may be beneficial as it maintains cerebral blood flow by avoiding hypocapnic-mediated vasoconstriction, and aids CO_2 elimination from the lungs as a higher concentration of CO_2 is exhaled per breath. Elevated levels of CO_2 produce a right shift in the oxygen dissociation curve, decreasing affinity of haemoglobin for oxygen, resulting in increased release of O_2 in the peripheries. Conversely, this may also reduce oxygen uptake within the alveoli. Excessive hypercapnia should be avoided to prevent severe metabolic acidosis.

In 1985, Wung *et al.* from New York, reported impressive survival rates utilising this novel technique (Wung *et al.* 1985). The majority of infants (84.4%) survived to discharge and showed little in the way of pulmonary morbidity. Preductal PaO_2 is maintained in the range 50 – 70mmHg and permits $PaCO_2$ to rise to 60mmHg, whilst maintaining spontaneous respiration on the ventilator. Hyperinflation and alkalisation were avoided to prevent lung barotrauma and exacerbation of pulmonary hypertension (Wung *et al.* 1995; Boloker *et al.* 2002). Similarly, Wilson's Boston group reported survival rates of 93% using this approach (Downard *et al.* 2003).

The technique for open repair has changed little over time; classically, the defect is approached via a thoracic or abdominal (subcostal) incision. Herniated viscera are reduced carefully into the abdomen, the defect being closed either primarily (Figure 1.3) or using a patch. Prosthetic material

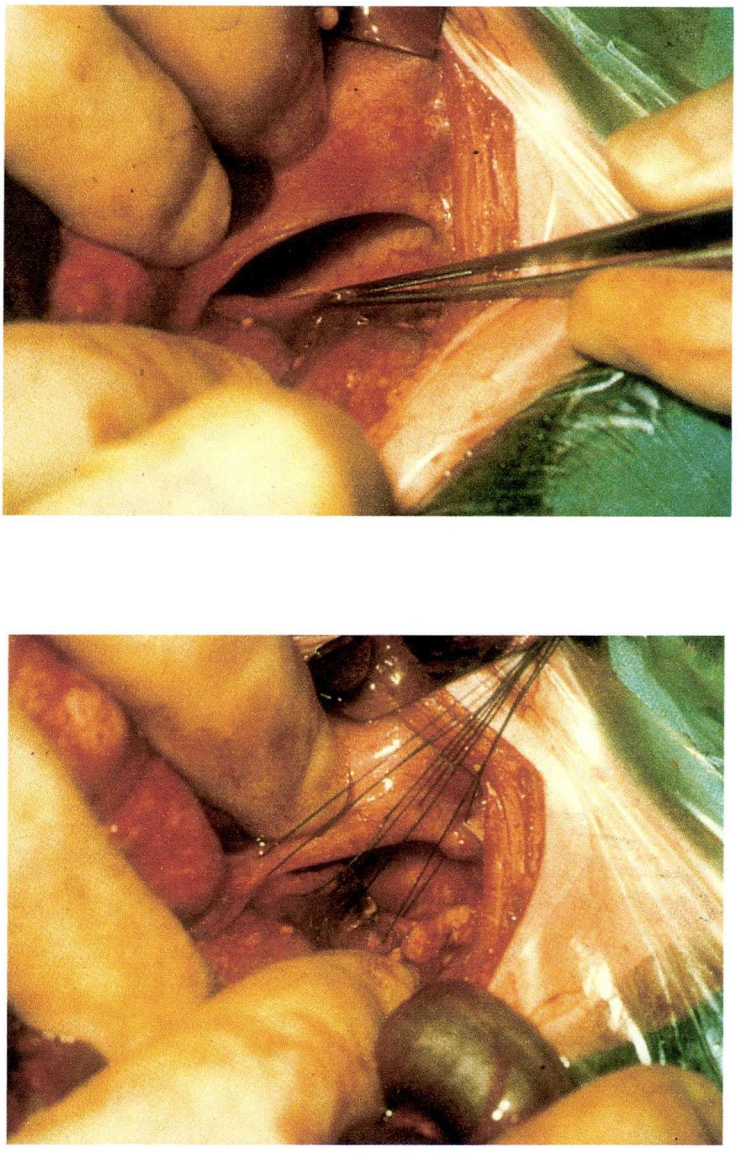

Figure 1.3. Intra-operative repair of congenital diaphragmatic hernia (CDH). In the upper image, the defect has been defined. The anterior and posterior rims are evident. In the lower image, the defect is being closed with interrupted sutures. Images courtesy of Professor Paul Losty, The Royal Liverpool Children's Hospital, Alder Hey.

includes polytetrafluoroethylene (PTFE; Gore-Tex [W.L. Gore and Associates, Flagstaff, AZ]), SILASTIC® (Dow Corning, Midland, MI), Dacron, and polypropylene. Muscle flaps based on the latissimus dorsi (Bianchi *et al.* 1983; Sydorak *et al.* 2003), internal oblique and transversalis (Scaife *et al.* 2003) have been used to patch the defect and recurrences. These autologous techniques may have benefit in the long-term, as up to 40% of hernias recur when repaired with prosthetic patches, necessitating re-repair (Moss *et al.* 2001). Others have reported the use of SILASTIC® mesh to enlarge the abdominal cavity, preventing an increase in intra-abdominal pressure when herniated viscera are reduced (Michalevicz *et al.* 1989).

A few groups have utilised the endosurgical approach in selected cases of CDH with favourable results (Shah *et al.* 2002; Taskin *et al.* 2002). Advances in neonatal endosurgery, including smaller instruments and optics have facilitated such operations. Insufflation pressures need to be kept low to prevent respiratory embarrassment and reduced venous return. Studies have been published stating laparoscopy should not be considered for newborn with CDH as the failure rate is high and there are problems relating to the pneumoperitoneum and rising PCO_2 levels (Arca *et al.* 2003). However, the thoracoscopic approach may be beneficial as it allows spontaneous reduction of the herniated viscera into the abdomen and permits diaphragmatic suture with minimal visceral handling (Schaarschmidt *et al.* 2005).

Fetal surgery was introduced in the 1970's as conventional therapies available at that time did little to improve the outcome for CDH newborns (Lipshutz *et al.* 1997). Early repair of CDH in-utero in an experimental lamb model revealed improved lung growth (Harrison *et al.* 1980a; Harrison *et al.* 1980b). Fetal surgery has been limited to fetuses with a prediction of poor outcome. However, as discussed above, selecting 'high-risk' fetuses for prenatal surgery requires accurate prognostic scoring. At present, there is a lack of evidence base to support the use of LHR in selecting fetuses for prenatal surgery (Ba'ath et al. 2007). Initially, open fetal repair was performed, but abandoned due to high mortality, mainly through premature labour, but also due to obstructed venous return, when attempts were made to reduce the herniated liver (Harrison *et al.* 1993). The observation that congenital laryngeal obstruction in infants resulted in hyperplastic lungs, led to attempts at tracheal occlusion (Silver *et al.* 1988). This technique became known as PLUG ('Plug the LUng until it Grows') (Hedrick *et al.* 1994; Bealer *et al.* 1995; Skarsgard *et al.* 1996; VanderWall *et al.* 1996; Beierle *et al.* 1996). The trachea was occluded at 24 – 26 weeks gestation using clips placed via the fetal endoscopic route (Fetendo Clip); the technique was modified later to balloon occlusion (Fetendo balloon) because of high morbidity resulting from tracheal dissection required to place the clips. These techniques appeared to result in augmented lung growth (Harrison *et al.* 2003), and a National Institutes of Health (NIH) randomized controlled trial ensued. However, fetal tracheal

ligation did not prevent the development of pulmonary hypoplasia in human CDH (Harrison *et al.* 2003), nor did it improve survival or morbidity rates (Heerema *et al.* 2003). Radiographic increases in lung size achieved with fetal tracheal occlusion may have been in part due to emphysematous change and fluid pooling. Human fetal programmes in North America and Europe continue to investigate fetal endoscopic techniques reserving them for fetuses considered at the highest risk: however selecting such cases remains problematic (Keller *et al.* 2004; Deprest *et al.* 2005; Saura *et al.* 2007).

1.1.8 Outcome

Survival rates are hard to determine due to 'hidden mortality' i.e. antenatal and early postnatal deaths prior to transfer to the definitive paediatric surgery centre (Beresford *et al.* 2000; Stege *et al.* 2003; The Ontario Congenital Anomalies Study Group 2004; Colvin *et al.* 2005; Dillon *et al.* 2000). Many dedicated centres now report 80–90% survival for CDH (Wilson *et al.* 1997; Boloker *et al.* 2002; Kays *et al.* 1999; Wung *et al.* 1995). However, when the 'hidden mortality' is considered it appears that mortality remains as high as 60% (Beresford *et al.* 2000; Stege *et al.* 2003). In addition, centres performing more than 5-6 cases per year appear to achieve better survival compared with smaller-volume centres (Skari *et al.* 2004).

In long-term follow-up studies of children requiring ECMO, either prior to, or following CDH repair, a proportion suffer from significant hearing loss, the aetiology of which is not clear (Rasheed *et al.* 2001; Robertson *et al.* 1998); others exhibit mild neuromotor and cognitive delay in their development (Ahmad *et al.* 1999; McGahren *et al.* 1997; Lund *et al.* 1994). A proportion of patients remain oxygen dependent, some being affected by chronic lung disease and infection (Schoeman *et al.* 1999). Many have problems with growth and nutrition. Gastro-oesophageal reflux, possibly related to diaphragmatic dysfunction may often require fundoplication (Kieffer *et al.* 1995).

1.2 Lung development

Human lung development begins during the fourth week of gestation when the lung bud forms as a ventral outgrowth of the foregut; the process is held to conclude during early childhood (Boyden 1977).

Although investigators have studied the human lung, much of our understanding of pulmonary development has arisen from the study of animal models due to their availability and accessibility. The ability to create genetic knock-out and knock-in models has permitted the function of several genes and transcription factors to be elucidated. Despite the duration / timing of the stages of pulmonary development differing between species, it appears that the major mechanisms of development are

well conserved, such that insights gained from animal models, including invertebrates such as *Drosophila melanogaster*, can be cautiously translated to the human fetal lung (Ghabrial *et al.* 2003).

1.2.1 The mature lung

Normal lung development is complete by approximately 2-3 years of age. At completion, there are 300-600 million alveoli, approximately 1000 per acinus (Thurlbeck 1982). The adult lung contains more parenchymal air spaces (86.5% in the adult vs. 74% at birth), less tissue (13.5% in the adult vs. 26% at birth), but much more capillary blood (42% in the adult vs. 16% at birth) (Zeltner *et al.* 1987a; Zeltner *et al.* 1987b; Gehr *et al.* 1978; Crapo *et al.* 1982). Lung development and growth represent well-balanced processes which occur in keeping with the requirements of the organism for an adequate and undisturbed supply of oxygen.

1.2.2 Morphological stages of lung development

Five stages of pulmonary development (Figure 1.4) have been described: (1) the embryonic period, (2) the pseudoglandular stage, (3) the canalicular stage, (4) the saccular stage and (5) the alveolar stage (Zeltner *et al.* 1987a). Some of these phases overlap and their duration / timing differ between species.

During the fourth week of human gestation, the laryngotracheal grooves appear laterally on both sides and deepen, such that the lung bud begins to

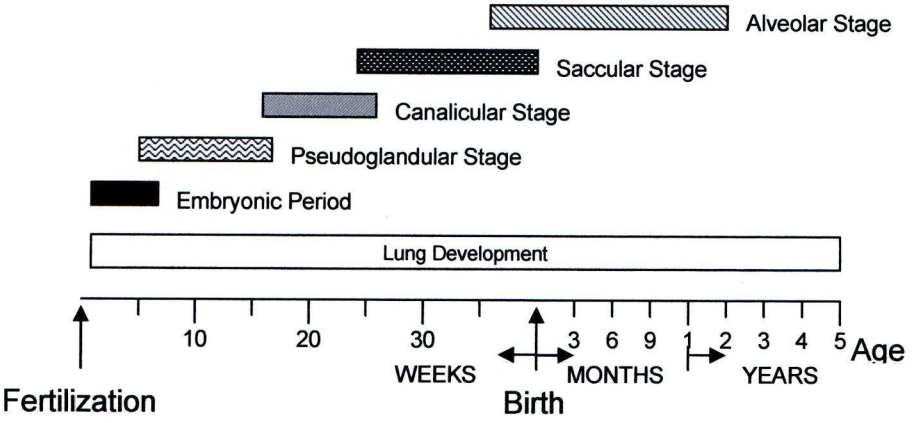

Figure 1.4. Stages of human lung development. Adapted from Zeltner et al. 1987a.

separate from the oesophagus. Following elongation of the lung bud, it divides dichotomously and invades the surrounding mesenchyme, whereupon it undergoes further dichotomous branching (Figure 1.5). Epithelial-mesenchymal interactions play a critical role (see section 1.2.3) in regulating lung development (Alescio *et al.* 1968; Taderera 1967; Spooner *et al.* 1970; Wessells 1970; Metzger *et al.* 2008).

During the pseudoglandular phase, the developing lung undergoes further stereotypical branching and vascular development such that at its completion (week 17 in the human fetus), the patterning of the preacinar airways and vasculature matches that of the adult lung.

The canalicular stage is characterised by gas-exchanging tissue becoming visible under the light microscope (Boyden 1977), the lung parenchyma being 'canalised' by capillary development, and surfactant production commencing.

During the saccular stage, the peripheral airways distal to the terminal bronchioles lengthen and widen, the last generations of air spaces are formed, and the peripheral airways form groups of widened air spaces called saccules. As a consequence, the future gas-exchanging regions increase exponentially.

Finally, the human lung enters the alveolar stage at around week 36 of gestation, which is completed by 18–24 months postnatal age (Langston *et al.* 1984). During this stage, the alveoli are formed and the capillary network becomes single layered.

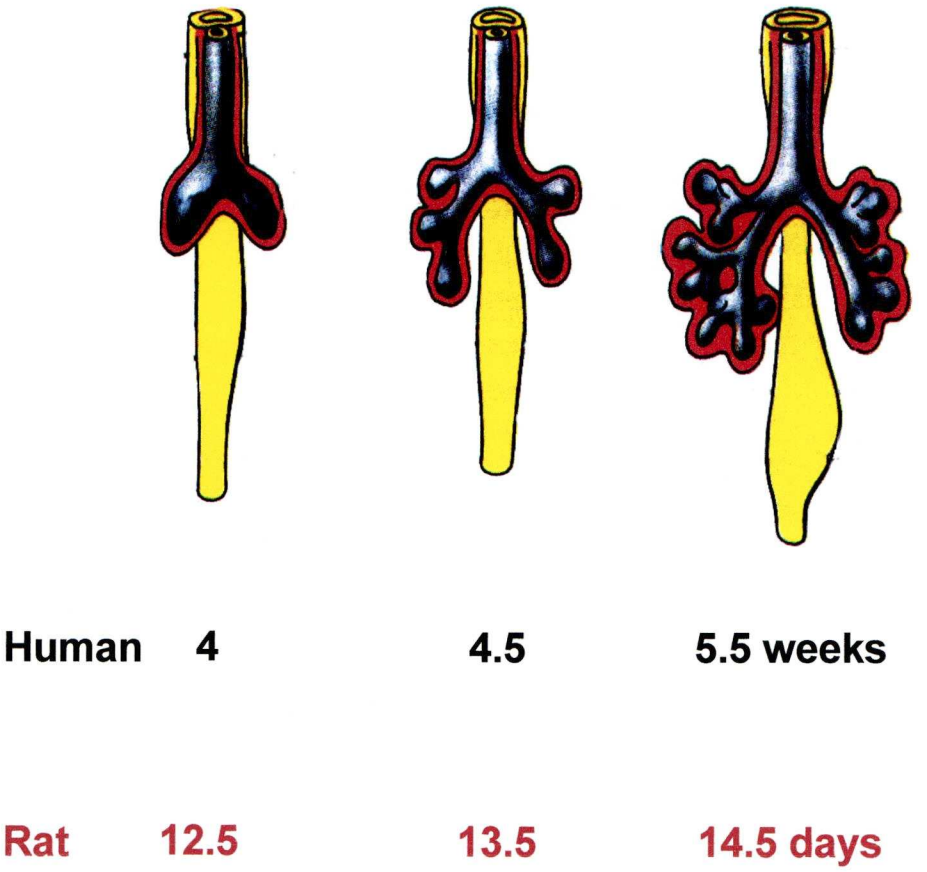

Figure 1.5. Human lung development begins during the fourth week of gestation when the lung bud (black) forms as a ventral outgrowth of the foregut (yellow). Following elongation of the lung bud, it divides dichotomously and invades the surrounding mesenchyme (red), whereupon it undergoes further dichotomous branching. Lung development occurs in an analogous manner in the rat, albeit, over a different time frame. Figure courtesy of Mr Edwin Jesudason, Consultant Paediatric Surgeon, The Royal Liverpool Children's Hospital, Alder Hey (adapted from Larson et al. Human Embryology).

1.2.3 Epithelial-mesenchymal interactions in the developing lung

Lung morphogenesis is complex; the process is tightly regulated by a genetic programme (which involves transcription factors, growth factors, epithelial-mesenchymal interactions and hormones). These factors interact along the proximal-distal axis of the respiratory tract and direct endodermal patterning, lung branching morphogenesis, left-right asymmetry and vascular development (Copland *et al.* 2004).

It is only possible to briefly review some of these factors in this introductory chapter. Epithelial-mesenchymal interactions are central to branching morphogenesis (Masters 1976; Bluemink *et al.* 1976). Factors such as hepatocyte nuclear factor-3 beta (HNF3β [foxf2a]) (Zhou *et al.* 1996; Zhou *et al.* 1997), GATA binding protein 6 (GATA-6) (Keijzer *et al.* 2001), thyroid transcription factor-1 (TTF-1 [Nkx2.1]) (Zhou *et al.* 1996; Ikeda *et al.* 1995; Kimura *et al.* 1996) and *Iroquois* homeobox genes (Irx) (van Tuyl *et al.* 2006) are found within the epithelium and regulate epithelial specification. Members of the Gli gene family, Gli2 and Gli3 (Motoyama *et al.* 1998; Quaggin *et al.* 1998) and basic-helix-loop-helix proteins, Pod-1 (Quaggin *et al.* 1998) are located in the mesenchyme and control epithelial patterning. A number of morphogens are produced by the epithelium and mesenchyme; sonic hedgehog (Shh) (Miller *et al.* 2001; Urase *et al.* 1996) and platelet-derived growth factors (PDGFs) (Buch *et al.*

1991) are produced in the epithelium while fibroblast growth factors (FGFs) (Lebeche *et al.* 1999) and epithelial growth factors (EGFs) (Ruocco *et al.* 1996) are mainly produced by the mesenchyme. Shh (Pepicelli *et al.* 1998) and fibroblast growth factor 10 (FGF10) (Sekine *et al.* 1999) play a crucial role in branching morphogenesis.

Vascular development is likewise controlled by a number of growth factors, transcription factors, cell-extracellular matrix and cell-cell interactions. Vascular endothelial growth factor (VEGF) (Healy *et al.* 2000; Bhatt *et al.* 2000; Gebb *et al.* 2000), angiopoietin (Colen *et al.* 1999; Koblizek *et al.* 1998; Maisonpierre *et al.* 1997) and ephrin families (Hall *et al.* 2002) have been implicated in its regulation.

1.2.4 Mechanical factors in the developing lung

It is now evident that the process of lung growth and development not only requires a genetic programme but also many physical factors. A variety of physical factors have been implicated in lung development: (i) lung liquid secretion by the pulmonary epithelium (Alcorn *et al.* 1977; Fewell *et al.* 1983), (ii) retention of lung liquid by the fetal glottis and upper airways resulting in a positive intraluminal pressure (Vilos *et al.* 1982; Harding *et al.* 1986), (iii) fetal breathing movements (Kitterman 1986), (iv) maintenance of sufficient intrathoracic and amniotic liquid volumes (Harrison *et al.* 1980b; Potter 1946) and more recently, (v) airway

peristalsis (spontaneous contractility of the prenatal airways) (Jesudason *et al.* 2005).

Drainage of lung liquid by tracheostomy in fetal lambs results in pulmonary hypoplasia; conversely, tracheal ligation results in lung growth and pulmonary maturation (Alcorn *et al.* 1977; Fewell *et al.* 1983). These experiments alter both intraluminal liquid volumes and pressures; therefore, lung liquid secretion and maintenance of a positive intraluminal pressure may be interrelated in their effects. In a similar manner, congenital laryngeal obstruction in the fetus results in hyperplastic lungs due to the retention of lung liquid (Griscom *et al.* 1969; Silver *et al.* 1988).

Fetal breathing movements begin as early as the eighth week of gestation in the human fetus and continue until parturition (de Vries *et al.* 1986). They result in changes in intrathoracic volume which prevent lung liquid loss from the developing lung (during periods of upper airway relaxation and glottic opening) and may also distend the developing airspaces (Harding 1991). When fetal breathing movements are abolished through phrenic nerve section, cervical cord lesions, or neurological conditions, the resulting lung is hypoplastic (Wigglesworth *et al.* 1979; Goldstein *et al.* 1980; Liggins *et al.* 1981a; Liggins *et al.* 1981b). Fetal breathing movements therefore provide mechanical signals that influence lung growth and development.

1.3 Airway smooth muscle and peristalsis

1.3.1 Airway smooth muscle development

Pulmonary development commences on embryonic day 10 (E10) in the mouse; the two lung buds arise from the foregut (Spooner *et al.* 1970; Ten Have-Opbroek 1981). During the following days (E11-14) the lung undergoes dichotomous branching (branching morphogenesis) to form the bronchial tree. Airway smooth muscle (ASM) becomes apparent on day E11; parallel bundles of ASM cells are arranged circumferentially around the long axis of the airways and stain positively for α-smooth muscle actin and calponin (Tollet *et al.* 2001). At branch points, airway smooth muscle fibres bend or curve around the tubules following the structural contours. At higher magnification, the bundles do not constitute a continuous sheet, but intermittently cross over to join neighbouring bundles. However, the layer is continuous, forming a syncitium or meshwork of interlocking airway smooth muscle over the developing lung.

ASM cells develop from the mesenchyme directly underlying the epithelium at the base of the epithelial buds (Sparrow *et al.* 2003; Mailleux *et al.* 2005). Initially, the newly formed ASM bundles form a thin ring around the base of the epithelial bud. As the epithelial tubule progresses into the mesenchyme, new cells are added distally. In general, smooth muscle myogenesis requires transformation of mesenchymal cells into SM myoblasts; these subsequently become immature SM cells (Mitchell *et al.* 1990; Wright *et al.* 1999). Mesenchymal cell shape plays a strong role in

visceral myogenesis; if mesenchymal cells are plated under conditions that maintain cell rounding or permit elongation, it is those cells that elongate that differentiate into smooth muscle (Yang *et al.* 1999).

The interlocking nature of the smooth muscle bundles permits electrical continuity and may facilitate coordinated rhythmic contractions of the tubules via low resistance gap junctions (Sparrow *et al.* 2003). The circumferential arrangement of airway smooth muscle provides radial stiffness and the discontinuity of neighbouring bundles may assist longitudinal extensibility, helping length changes that occur during spontaneous narrowing (Sparrow *et al.* 2003).

Stretch appears to be a prerequisite for smooth muscle myogenesis (Schuger 1997; Yang *et al.* 1998; Zhang *et al.* 1999; Yang *et al.* 1999; Yang *et al.* 2000). Mesenchymal cells need to spread on their basement membranes. Blocking laminin polymerisation prevents the spread of mesenchymal cells and abolishes synthesis of smooth muscle cell proteins (Schuger 1997; Yang *et al.* 1998; Zhang *et al.* 1999). Serum response factor (SRF) may induce the expression of smooth muscle-specific proteins within mesenchymal cells (Belaguli *et al.* 1997; Kim *et al.* 1997; Browning *et al.* 1998). Sustained stretch induced by increasing intraluminal pressure using dextrans in cultured mouse lungs results in an increase in the production of SRF in favour of its inhibitory isomer SRFΔ5 (Yang *et al.* 2000). When SRFΔ5 is over-expressed under the same conditions, stretch-induced myogenesis was blocked (Yang *et al.* 2000).

1.3.2 Spontaneous airway contractility (airway peristalsis)

Airway smooth muscle is a central component of the developing lung. Spontaneously contractile (Figure 1.6) throughout gestation; it is pharmacologically responsive at an early stage. Its phasic activity is associated with maintenance of a positive intraluminal pressure within the developing lung (McCray 1993). This positive pressure may act as a stimulus to lung growth via forces applied across the airway wall and neighbouring parenchyma. This activity may also be central to smooth muscle myogenesis.

Spontaneous smooth muscle contractility was first noted in the fetal airway and air sacs within chick embryos and cultured chick lung explants; contractility was temperature dependent, had a frequency of ~2 per minute at 38^0C and occurred without histological evidence of innervation (Lewis 1924). Schopper reported similar findings in chick and guinea pig lung explants (Schopper 1935; Schopper 1937). Solman *et al.* reported spontaneous airway smooth muscle activity in preparations from puppies and midgestation human fetal lung (Solmann *et al.* 1937). They also documented the pharmacologic responses to adrenergic and cholinergic stimuli and other agents.

Sparrow *et al.* described spontaneous contractility in fetal pigs and the responses to a range of pharmacological agents; prenatal airways

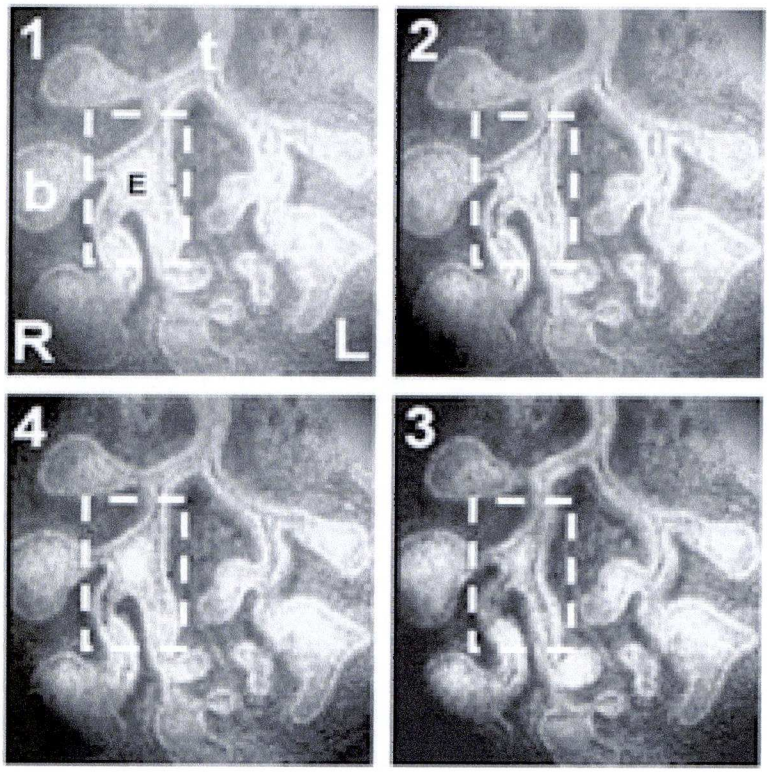

Figure 1.6. Airway peristalsis in embryonic lung. View clockwise from top-left. Epithelium (E) in dashed box constricts in panels 2 and 3 before relaxation. t-=trachea; b=end-bud; R=right; L=left. Images courtesy of Miss Nikki Smith, The Royal Liverpool Children's Hospital, Alder Hey.

contracted in response to application of acetylcholine, depolarising high-K^+ solution, histamine and substance P (Sparrow *et al.* 1995). The β-adrenergic agonist, isoprenaline, relaxed the airways and abolished spontaneous contractility (Sparrow *et al.* 1995). Verapamil, a Ca^{2+} antagonist, similarly abolished spontaneous contractile activity (Sparrow *et al.* 1995).

Schittny *et al.* investigated spontaneous contractility in fetal pigs and rabbits, noting spontaneous contractility throughout gestation, to within 100 μm of the terminal sacs (Schittny *et al.* 2000). Contractility was transient, initiating in one part of the bronchial tree before subsiding and beginning in another portion.

Spontaneous airway contractility also occurs *in vitro*. Sorokin noted that spontaneous airway contractions were present in rat lung cultures after 2-3 days and considered that distension of the terminal buds produced by such contractions might relate to pulmonary development (Sorokin 1961). Sparrow *et al.* documented contractility in pig lung explants (Sparrow *et al.* 1994). Roman and Schittny *et al.* noted spontaneous contractility in mice (Roman 1995; Schittny *et al.* 2000). McCray noted spontaneous contractility in human fetal lung tissue when cultured (McCray 1993). Epithelial tubules were spontaneously contractile and could be contracted by cholinergic agents (acetylcholine), dilated by adrenergics (isoprotenerol) and the contractions reduced or abolished by Ca^{2+} antagonists (cadmium chloride or nifedipine) or activation of potassium

channels (lemakalim) (McCray 1993). Abolition of spontaneous contractile activity using Ca^{2+} antagonists suggested it requires Ca^{2+} influx via voltage-operated channels (McCray 1993). Fetal airway smooth muscle must contain functional cholinergic receptors given that carbachol application resulted in an increase in contractility and tetany (McCray 1993). Isoprotenerol application resulted in relaxation (McCray 1993) suggesting that the sympathetic nervous system or circulating catecholamines could affect fetal airway contractility. Lemakalim activates K^+ channels in adult airway smooth muscle, resulting in relaxation of carbachol-induced contractions; here (McCray 1993) it abolished airway contractility and carbachol-induced tetany suggesting K^+ channels are also involved in the control of spontaneous activity. Contractile activity originated from within the same region in explants, generally propagated in a proximal to distal direction, and occurred regularly (inter-contractile interval 54 ± 5 sec (mean ± SEM)) (McCray 1993). Contractile strength was variable; sometimes contractions were easily seen, but at other times could only be documented on video recordings played at high speed (McCray 1993).

Contractile activity is highly temperature dependent as first noted by Margaret Reed Lewis (Lewis 1924). McCray similarly documented a gradual weakening of contractile force and increase in the inter-contractile interval upon cooling from 37°C to 22°C (McCray 1993).

Given that airway smooth muscle contractility has been documented throughout gestation in several species in embryos, cultured fetal lung explants and isolated smooth muscle preparations, it suggests it is a highly conserved mechanism and supports the thesis that such activity is a physiological function of the developing lung *in vivo*. It also suggests that contractility is not an artefact of the culture system.

In vitro, spontaneous contractility begins within 24 hours and is evident by the airways narrowing over short distances (McCray 1993; Roman 1995; Jesudason *et al.* 2005). By 48 hours, strong airway contractions are propagated from the central tubules to the periphery (Schittny *et al.* 2000). Embryonic ASM contractility is phasic, contrasting with its postnatal tonic activity (Boyle *et al.* 1992; Somlyo *et al.* 1994; Bergner *et al.* 2002). Similar to peristalsis within the gastrointestinal tract, prenatal mechanical contractility of airway smooth muscle may be driven by bursts of action potentials (Featherstone *et al.* 2005).

Contractility is peristaltic-like, propelling lung liquid through the principal airways and distending the distal buds. Perhaps this spontaneous activity is not so surprising given the common embryological origin of the lung and the gastrointestinal tract.

Video-microscopy has permitted airway peristalsis to be quantified in the lungs of fetal pigs and rabbits, and murine lung explants (Schittny *et al.* 2000). Airway narrowing was reported to occur intermittently (lasting for several minutes) in the large and small diameter tubules; the luminal

diameter reducing to as much as 46% of the relaxed size. The peristaltic wave was propagated over several generations of airways in a proximal to distal direction.

Although the embryological lung contains nerve fibres, spontaneous contractility occurs even in the presence of atropine (cholinergic antagonist) or tetrodotoxin (an inhibitor of sodium currents in excitable cells and action potentials that are dependent on sodium ion influx), demonstrating that the activity is myogenic, i.e. the activity arises from the muscle itself or potential tetrodotoxin-insensitive pacemaker cells (McCray 1993; Sparrow *et al.* 1995). In some smooth muscles, spontaneous activity is generated from groups of smooth muscle cells (Lang *et al.* 2006; Lang *et al.* 2007). In others, such as the gastrointestinal tract, it arises from the interstitial cells of Cajal (Der-Silaphet *et al.* 1998; Ward *et al.* 2001), and recently it has been shown that some smooth muscle activity appears to originate from Cajal-like cells (Metzger *et al.* 2004; Ciontea *et al.* 2005; McHale *et al.* 2006; Lavoie *et al.* 2007).

The prenatal airway smooth muscle is pharmacologically responsive (similar to postnatal airway); embryonic airways narrow rapidly to within 80 μm of the epithelial buds in response to acetylcholine and histamine (Sparrow *et al.* 1994; Sparrow *et al.* 1995). Electrical field stimulation (EFS) also results in rapid narrowing mediated by cholinergic innervation as it is reversibly blocked by both atropine and tetrodotoxin, but not hexamethonium (Sparrow *et al.* 1994). Prenatal airway smooth force

generation is comparable with postnatal ASM when normalised for ASM content (Booth *et al.* 1992).

Spontaneous contractility of the embryological airways results in mechanical stretching or distortion of the fetal pulmonary epithelium (Sparrow *et al.* 2003). Mesenchymal cells adherent to the basement membrane within this region would consequently be stretched and then relax as the lung liquid returned centrally with dilatation of the principal airways. Wirtz and Dobbs reported that a single mechanical stretch of adult rat alveolar type II cells resulted in a release of surfactant and a sustained increase in intracellular calcium, and suggested that phasic distension of the alveolar epithelium is a mechanical signal for surfactant release mediated via calcium-induced exocytosis (Wirtz *et al.* 1990).

Phasic lung distension within the embryological lung may provide a mechanical signal that governs growth factor release, signalling molecules or gene expression, resulting in lung growth. ASM tone may be responsible for the maintenance of a positive intraluminal pressure within the fetal lung (McCray 1993). If the ASM lacked tone, the airway wall would be compliant and distend with the secretion of lung liquid during the fetal period. Airway peristalsis may also serve to maintain an even positive-pressure within the developing lung or to prevent cellular debris from settling in any particular portion of the lung, hence preventing obstruction (Sparrow *et al.* 1994).

Phasic mechanical stretching of fetal lung organotypic cultures or cells has been shown to induce changes that may affect lung growth. For example, intermittent stretch of fetal lung organotypic cultures or cells has been shown to enhance prostacyclin production and increase cyclic adenosine monophospahate (cAMP) production and increase lung growth (Skinner *et al.* 1992; Liu *et al.* 1992). Mechanical stretch also increases expression of extracellular matrix components, surfactant protein (SP) mRNAs (SP-A, SP-B and SP-C) and parathyroid hormone-related peptide (Nakamura *et al.* 2000; Sanchez-Esteban *et al.* 1998; Torday *et al.* 1998). It appears that the cellular changes mediated by mechanical stretch may occur through activation of the tyrosine kinase $pp60^{src}$ and be mediated via phospholipase C and protein kinase C (Liu *et al.* 1995; Liu *et al.* 1996). Thus it appears that a pulsatile mechanical stimulus is better than static forces when stimulating lung growth *in vitro*.

As yet, it remains unclear as to when the transition occurs from a phasic to tonic activity. If action potentials drive spontaneous airway contractility (Featherstone *et al.* 2005), the airways will need to lose their capacity to generate such activity if it is to become tonic. Perhaps, tonic activity may result from increased autonomic activity from central neurones acting via the vagus that increases with the approach of parturition (Featherstone *et al.* 2005).

1.3.3 Airway peristalsis and lung growth

Recently, it has been demonstrated that airway peristalsis (AP) appears to be coupled to lung growth *in vitro* (Jesudason *et al.* 2005). Modulation of peristaltic frequency resulted in parallel changes in lung growth and vice versa. Stimulation of lung growth using 5% fetal calf serum or the classical morphogen FGF-10 resulted in increased frequency of airway peristalsis (Jesudason *et al.* 2005). Increasing airway peristalsis frequency using the cholinergic agonist, nicotine (0.1 μM), resulted in increased lung growth (Jesudason *et al.* 2005). Likewise, blockade of airway peristalsis using nifedipine (5 μM) reduced lung growth (Jesudason *et al.* 2005). Inhibition of lung growth using UO126 (a MEK1/2 inhibitor) impaired airway peristaltic frequency (Jesudason *et al.* 2005). These data lend further support to the thesis that airway smooth muscle may have a purpose rather than purely being the 'appendix of the lung' (Mitzner 2004).

Further studies supporting this hypothesis have been published more recently (Jesudason *et al.* 2006). The nitrofen model of congenital diaphragmatic hernia (see section 1.1.5) allows investigation of the embryonic lung prior to closure of the diaphragm. These studies have demonstrated that the hypoplastic lung exhibits abnormal smooth muscle function and uncoupling of growth and airway peristalsis.

1.4 Ca^{2+}_i signalling in smooth muscle

1.4.1 Smooth muscle

The majority of smooth muscle is located within the walls of hollow organs and tubes of the body. Cells are spindle-shaped, have a single nucleus and measure approximately 2-10 μM in diameter and 50-400 μM in length (Stephens 2002). Cells are arranged in sheets throughout the length of the muscle.

Smooth muscle cells contain three types of filaments: thick myosin filaments, thin actin filaments and intermediate filaments (Stephens 2002). Unlike skeletal muscle, smooth muscle filaments do not from myofibrils and are not arranged in a sarcomere pattern. Thick myosin and thin actin filaments are arranged obliquely within an elongated diamond lattice; sliding of the thin filaments past the thick filaments results in cellular contraction. During smooth muscle excitation, there is an increase in intracellular Ca^{2+} (Ca^{2+}_i). Ca^{2+} binds with calmodulin and the resulting complex binds to and activates myosin kinase, which in turn phosphorylates myosin. This then binds with actin such that cross-bridge cycling and contraction can begin (Stephens 2002).

Ca^{2+} either enters the cell from the extracellular space (e.g. via voltage-gated L-type Ca^{2+} channels) or from the Ca^{2+}_i store, the sarcoplasmic reticulum (SR). Smooth muscle relaxation is achieved through removal of Ca^{2+}_i; it is actively transported across the plasma membrane or returned to the SR via the SR Ca^{2+}-ATPase (SERCA pump)(Sanders 2001; Taylor *et*

al. 2002). When Ca^{2+}_i is removed, myosin is dephosphorylated and muscle relaxation occurs.

There are two main types of smooth muscle: multiunit or single unit (Burnstock 1979). Multiunit smooth muscle is composed of multiple discrete units that exhibit independent function. Each muscle subunit is stimulated by nerves with resultant contraction (neurogenic action). However, most smooth muscle is single unit (also known as visceral smooth muscle) and located within the walls of tubular organs or viscera. Gap junctions link the cells and allow the propagation of action potentials throughout the muscle (functional syncitium) such that when cells become excited, the muscle contracts as a whole (Hashitani *et al.* 2001; Hashitani *et al.* 2004). This form of smooth muscle is myogenic; specialised pacemaker cells generate spontaneous activity (pacemaker potentials)(Hirst *et al.* 2003). Pacemaker cells spontaneously depolarize and initiate an action potential which is then propagated throughout the muscle via gap junctions. Pacemaker cells are usually located at specific anatomical locations within the muscle itself (Hirst *et al.* 2003). There is also an intermediate category of smooth muscle (e.g. canine tracheal smooth muscle) which has sparse innervation and few gap junctions (Burnstock 1979).

Normally, smooth muscle has sufficient baseline levels of Ca^{2+}_i to maintain a low level of contraction (tension / tone). An increase in Ca^{2+}_i results in a contractile response. Airway smooth muscle is also innervated by the

autonomic nervous system which can enhance or inhibit contraction (Stephens et al. 2002).

1.4.2 Ca^{2+}_i sensors

Ca^{2+}_i dynamics and corresponding physiological phenomena have interested researchers for over fifty years. Development of probes and instrumentation has made this research a possibility (the relationship between Ca^{2+}_i and excitation-contraction coupling in a wide variety of smooth muscle types has been investigated as a result). Probes need to be able to measure the temporal and spatial changes of Ca^{2+}_i within cells and tissues (ranging from nanomolar to micromolar concentrations) such that the biological response to stimulation can be determined (Rudolf *et al.* 2003).

Ca^{2+} probes (indicators, reporters or sensors) are molecules that are able to: (1) form selective and reversible complexes with Ca^{2+} ions; and (2) exhibit different physicochemical characteristics when bound / unbound. These abilities permit the relative concentrations of free and bound probe (rather than absolute Ca^{2+}_i concentrations) to be measured.

For example, the excitation (or emission) spectra of the ratiometric dyes, Indo-1 or Fura-2, as used in our studies alter according to the free Ca^{2+}_i concentration (Grynkiewicz *et al.* 1985). The Ca^{2+}_i concentration is measured as the ratio between the two fluorescence intensity values that are obtained at two wavelengths (λ_1 and λ_2). Ratiometric dyes are valuable

as they correct for uneven loading, photobleaching and changes in the focal plane (through movement) as the ratio does not rely on the absolute intensity of the fluorescent signal. Non-ratiometric dyes, e.g. Fluo-4 as used in our studies, measure the $Ca^{2+}{}_i$ concentration through the relative increase in fluorescence intensity upon an increase in free $Ca^{2+}{}_i$ (Gee *et al.* 2000). However, these dyes are more susceptible to photobleaching and movement artefact.

Absolute $Ca^{2+}{}_i$ concentration can be calculated through measurement of the maximal or minimal fluorescence (F_{max} and F_{min} respectively) necessitating exposure of the loaded cells or tissue to a known Ca^{2+} concentration via biochemical methods, e.g. ionophores (Kao 1994). These techniques are often incompatible with cell or tissue survival.

The first dyes were discovered during the 1960's and 1970's; the spectral properties of the organic coloured compounds murexide, the azo dyes and chlortetracycline were noted to change upon binding Ca^{2+} (Rudolf *et al.* 2003). However, it was not until the late 1970's that the first rationally designed fluorescent Ca^{2+} probe was synthesised for intracellular use (Tsien 1980). The prototype polycarboxylate dye (BAPTA) was a derivative of the Ca^{2+} chelator EGTA; Ca^{2+} binding resulted in structural changes / alteration of spectral properties (Tsien 1980). This group of dyes gained popularity as synthesis of their acetoxymethyl (AM) esters permitted trapping of the dye within living cells, no specific technology

was required to load cells or tissues, and they were effective in most cell types with minimal side effects (Tsien 1981).

In the 1960's, aequorin (AEQ) and green fluorescent protein (GFP), were discovered during investigation of the medusa *Aequorea victoria* (Shimomura *et al.* 1962; Morise *et al.* 1974). These proteins have impacted greatly upon Ca^{2+}_i signalling research during recent years. Cloning of AEQ complementary DNA has permitted recombinant expression of AEQ protein in heterogeneous systems (Prasher *et al.* 1985). Probes can be targeted to specific cellular locations by the insertion of specific signal sequences into cells, or to specific proteins such that their spatio-temporal distribution and interactions can be studied (Rizzuto *et al.* 1992; Rizzuto *et al.* 1994).

Similarly, recombinant probes based on GFP were developed after it was demonstrated that heterogeneously expressed GFP maintains its strong fluorescence upon excitation in cells (Chalfie *et al.* 1994; Miyawaki *et al.* 1997; Romoser *et al.* 1997). These probes, of which there are three main types ('cameleons', 'camgaroos' and 'pericams') use calmodulin (CaM) as a molecular switch, which changes its conformation on the binding of Ca^{2+} (Miyawaki *et al.* 1997; Baird *et al.* 1999; Nagai *et al.* 2001). These conformational changes alter the fluorescence properties permitting calculation of $[Ca^{2+}_i]$. However, CaM is important in many physiological processes, and its over-expression within cells may alter Ca^{2+}_i-dependent reactions. As a consequence, transgenic models expressing GFP probes

have been only described in lower organisms e.g. *Drosophila* (Diegelmann *et al.* 2002; Fiala *et al.* 2002; Reiff *et al.* 2002; Yu *et al.* 2003). $Ca^{2+}{}_i$ imaging using CaM-GFP probes may also be affected by photobleaching of GFP and the loss of kinetics of the conformational changes of CaM upon the binding of Ca^{2+}.

These techniques may permit the analysis of highly complex organisms and perhaps in time, whole living organisms. To undertake this, it will not only require the development of new probes, but also instrumentation (e.g. camera systems, filters, software and hardware) that will permit their investigation. The genetically encoded probes are becoming more popular as genetic manipulation readies the organism for *in vivo* $Ca^{2+}{}_i$ signalling studies.

1.4.3 In-situ $Ca^{2+}{}_i$ signalling

$Ca^{2+}{}_i$ sensitive indicators are most often used in single cell preparations necessitating enzymatic digestion. More recently, it has been possible to perform imaging of structures without enzymatic treatment or extensive dissection (Burdyga *et al.* 2003). These preparations are perhaps 'more physiological' as they retain cell to cell contact with neighbouring tissue rather than being isolated. Through pioneering techniques it has been possible to image larger structures (e.g. mouse lungs and brain) through tissue slicing techniques (Bergner *et al.* 2002; Yuan *et al.* 2007).

1.5 Closing remarks and aims of the thesis

This study aims to investigate the basic biology of spontaneous fetal airway smooth muscle contractility. Firstly, it aims to study the mechanisms underlying this physiological activity and secondly, to relate them to lung growth in normal development and hypoplastic lung development (the nitrofen model of lung hypoplasia). Thus far, there is good evidence to suggest that spontaneous airway contractility requires the entry of extracellular calcium (Ca^{2+}_o) via voltage operated channels and that AP may be regulated via K^+ channels. We aim to specifically test whether AP is underpinned by Ca^{2+}_i activity, and if so, the role of Ca^{2+}_o entry and Ca^{2+}_i release in its generation.

Chapter 2

METHODS

2.1 Introduction

CDH has an incidence of approximately 1 in 2500 births and despite advances in healthcare mortality remains as high as 60% (Stege *et al.* 2003). The majority of these deaths result from the associated pulmonary hypoplasia and accompanying pulmonary hypertension (Skari *et al.* 2000). Accordingly, many researchers have chosen to investigate early pulmonary development in order to gain insights into factors that influence pulmonary growth. To undertake these studies, a variety of techniques are required; some are already well-established (e.g. lung culture) whilst others (e.g. confocal and photometric measurement of Ca^{2+}_i) have been used with success in other tissues, but require innovative ideas and refinement to permit their use in small tissues such as the embryonic lung (< 1mm diameter).

This study aims to investigate the basic biology of spontaneous fetal airway smooth muscle contractility with particular emphasis on Ca^{2+} signalling. The work necessitates knowledge of organ culture techniques, Ca^{2+}-sensitive dyes and imaging techniques.

2.2 Materials and methods

2.2.1 Embryonic lung culture

Morphological development *in vitro* depends on the physiological conditions (Nogawa *et al.* 2002). Consistent adhesion is essential to ensure

reproducible branching morphogenesis. We have utilised translucent polytetrafluorethylene membrane culture-dish inserts (Millicell, Millipore Corp, Bedford, MA) for these reasons (Figure 2.1). Reproducible adhesion is achieved and lungs undergo branching morphogenesis in a pseudo 2-dimensional manner. Lungs are supported by the membrane and bathed by medium on their undersurface at 37°C in 5% CO_2 for periods up to 78 hours; oxygenation occurs by diffusion. Translucency of the membrane permits photography (Figure 2.2) and subsequent morphometric analysis (Figure 2.3) using computer software (specimen perimeter, specimen area and total bud count). The membrane also permits easy loading of explants with calcium sensitive dyes prior to undertaking confocal and photometric measurements of Ca^{2+}_i.

Other investigators have utilised alternative methods for organ culture, these include pre-scratching of plasticware to allow adhesion of explants or their submersion within collagen gels (Gross *et al.* 1983; McAteer *et al.* 1983). However, previous experience of these techniques showed unacceptable variation in branching morphogenesis (Jesudason 2001). Lung branching morphogenesis within collagen gels occurs in a 3-dimensional manner which results in difficulty in quantifying lung growth and division. Furthermore, 3-dimensional growth may impair the ability of lung explants to be optically sectioned using confocal microscopy and finally, submersion within collagen gels would impair the ability to load with Ca^{2+}_i sensitive indicators.

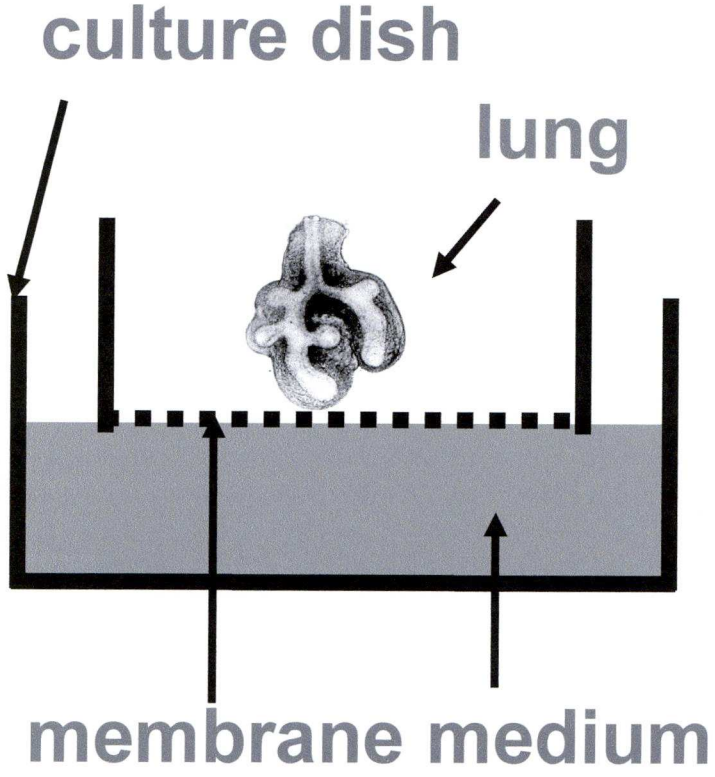

Figure 2.1. Schematic diagram of the lung culture system. Lung rudiments were positioned on translucent polytetrafluorethylene membrane culture-dish inserts with serum-free culture medium incorporating penicillin (100 IU/ml) and streptomycin (100 μg/ml). Lung explants were incubated at 37°C in 5% CO_2 for periods up to 78 hours. Diagram courtesy of Mr Edwin Jesudason, Consultant Paediatric Surgeon, The Royal Liverpool Children's Hospital, Alder Hey.

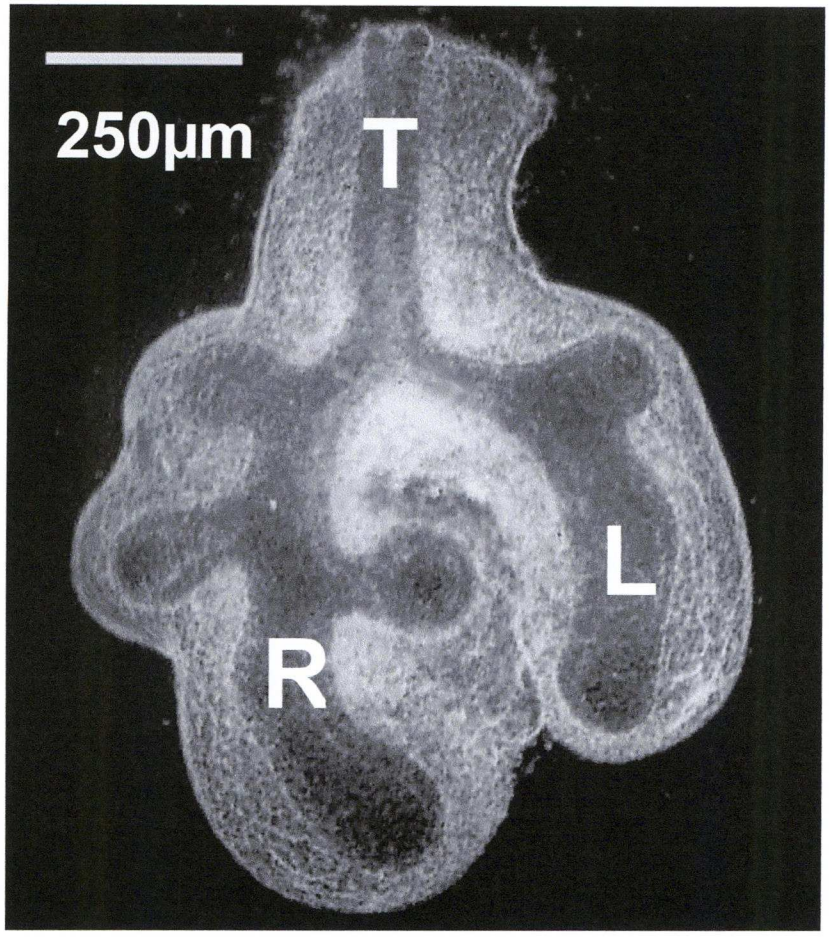

Figure 2.2. Photomicrograph of an embryonic rat lung following microdissection. The trachea (T), left lung bud (L) and right lung bud (R) are shown. The scale bar shows 250 µm. Image courtesy of Mr Edwin Jesudason, Consultant Paediatric Surgeon, The Royal Liverpool Children's Hospital, Alder Hey.

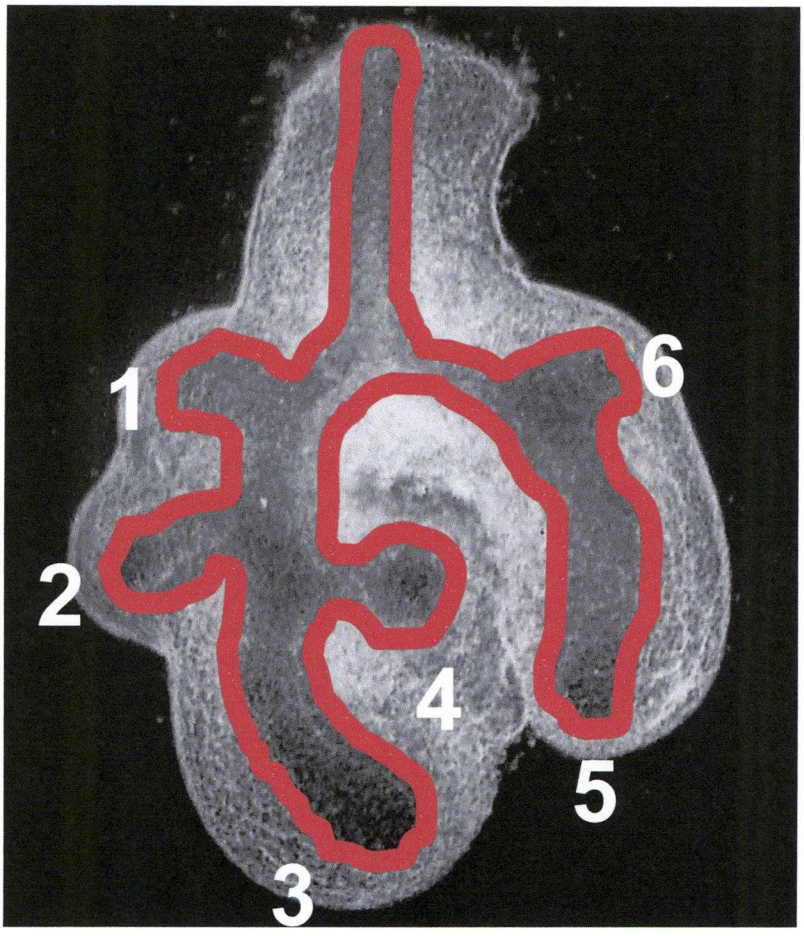

Figure 2.3. Lung morphometry. Scion Image Beta 4.03 software (Scion Corporation, Frederick, Maryland, USA) was used to trace the epithelial contour (red line) around each image of cultured lungs in order to calculate the individual lung epithelial area and perimeter. The number of terminal buds was also recorded (as shown).

Alternative tissues (sheep or rabbit) could have been considered for investigation in these studies. However, the rodent model was favoured as: 1) the model is well-established in our laboratory; 2) nitrofen (2,4-dichloro-4'-nitro diphenyl ether) can be administered to pregnant rats on day 9.5 of gestation to generate embryonic lung hypoplasia permitting comparison between controls and hypoplastic lungs (Kluth *et al.* 1990; Kluth *et al.* 1993; Kluth *et al.* 1996a; Kluth *et al.* 1996b); and 3) the small size of the lungs (< 1 mm in diameter) permits the whole lung to undergo confocal imaging of intercellular Ca^{2+}_i waves. Should the ovine or rabbit models of CDH have been used, it would have not been possible to image the whole of the embryonic lungs (as we have been able to do in these studies) and research would have been limited to sections of airway. Given the larger size of the lungs of these species, it may not have been possible to optically section them as to the same extent as rodent lungs. Finally, the numbers in experimental cohorts would have been less than with the rodent model as it is expensive to maintain the stock and perform antenatal surgery in order to create CDH.

2.2.2 Ca^{2+}_i sensitive indicators

The ratiometric dyes Indo-1 AM (Figure 2.4) and Fura-2 AM were chosen for photometric studies and the non-ratiometric dye Fluo-4 AM (Figure 2.5) for confocal imaging. The excitation (or emission) spectra of the ratiometric dyes (Indo-1 or Fura-2) alter according to the free Ca^{2+}_i

concentration; they were invaluable for these studies as they correct for uneven loading, photobleaching and changes in the focal plane (through movement) as the ratio does not rely on the absolute intensity of the fluorescent signal. As a consequence, prolonged investigations (e.g. 90 minutes) examining the responses of lung explants to a variety of pharmacologic agonists / antagonists could be undertaken with no loss of signal. Non-ratiometric dyes (e.g. Fluo-4) measure the Ca^{2+}_i concentration through the relative increase in fluorescence intensity upon an increase in free Ca^{2+}_i. However, these dyes are more susceptible to photobleaching and movement artefact. As a result measurement of Ca^{2+}_i transients were limited to not more than 90 seconds to reduce the effects of photobleaching. However, Fluo-4 AM was essential to the ability to perform simultaneous in-situ measurement of Ca^{2+}_i signals in ASM within whole embryonic lung explants.

The acetoxymethyl (AM) esters permit trapping of the dye within living cells; no specific technology is required to load cells or tissues (Tsien 1981) (Figure 2.6). These dyes have been previously reported to be effective in most cell types with only minimal side effects.

Lungs were cultured for 54 or 78 hours before loading with Ca^{2+}_i sensitive indicators. Following loading (see subsequent chapters for full details) the explants were allowed to equilibrate for 30 minutes in physiological saline solution at 37°C for washing and de-esterification of the dye.

Alternative techniques that could have been theoretically considered for

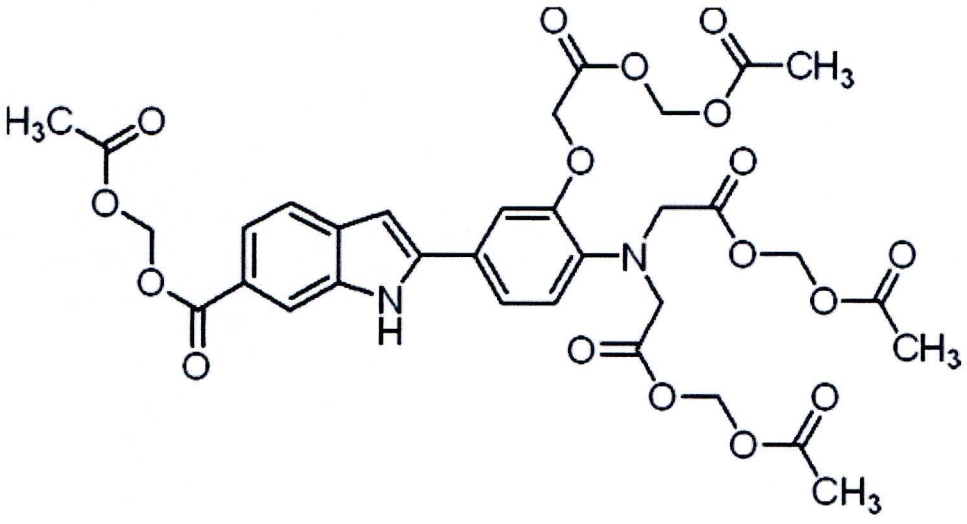

Figure 2.4. Schematic diagram depicting the molecular structure of Indo-1 AM.

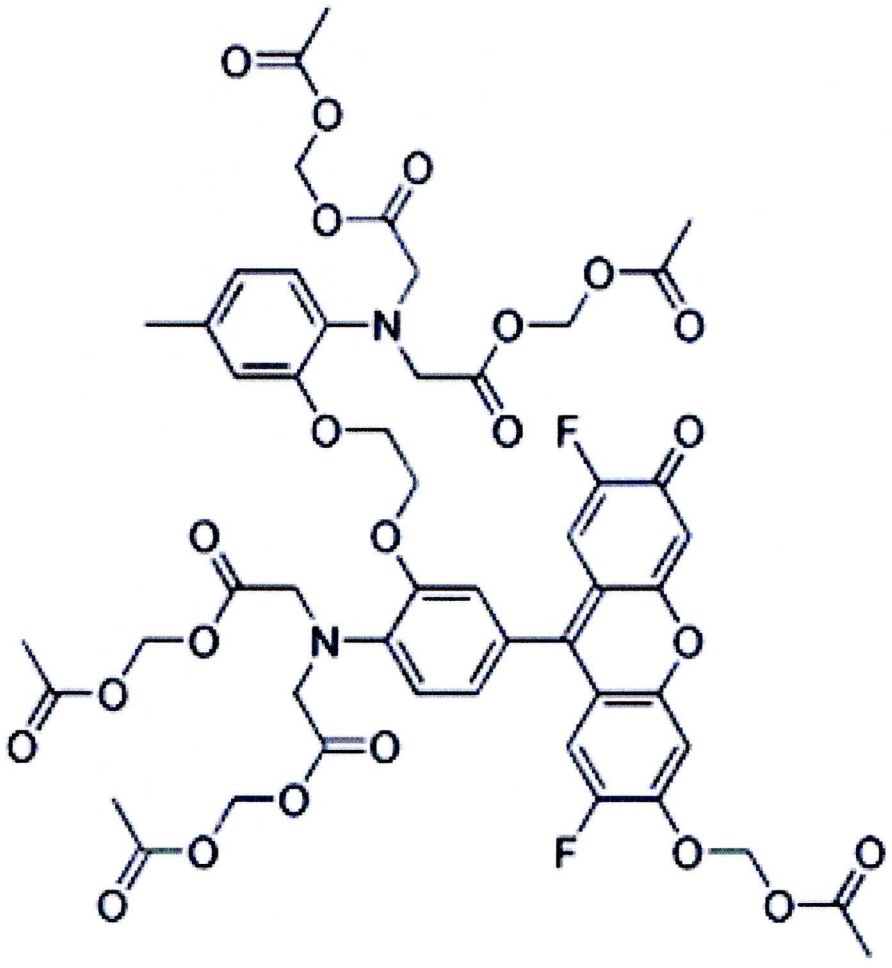

Figure 2.5. Schematic diagram depicting the molecular structure of Fluo-4 AM.

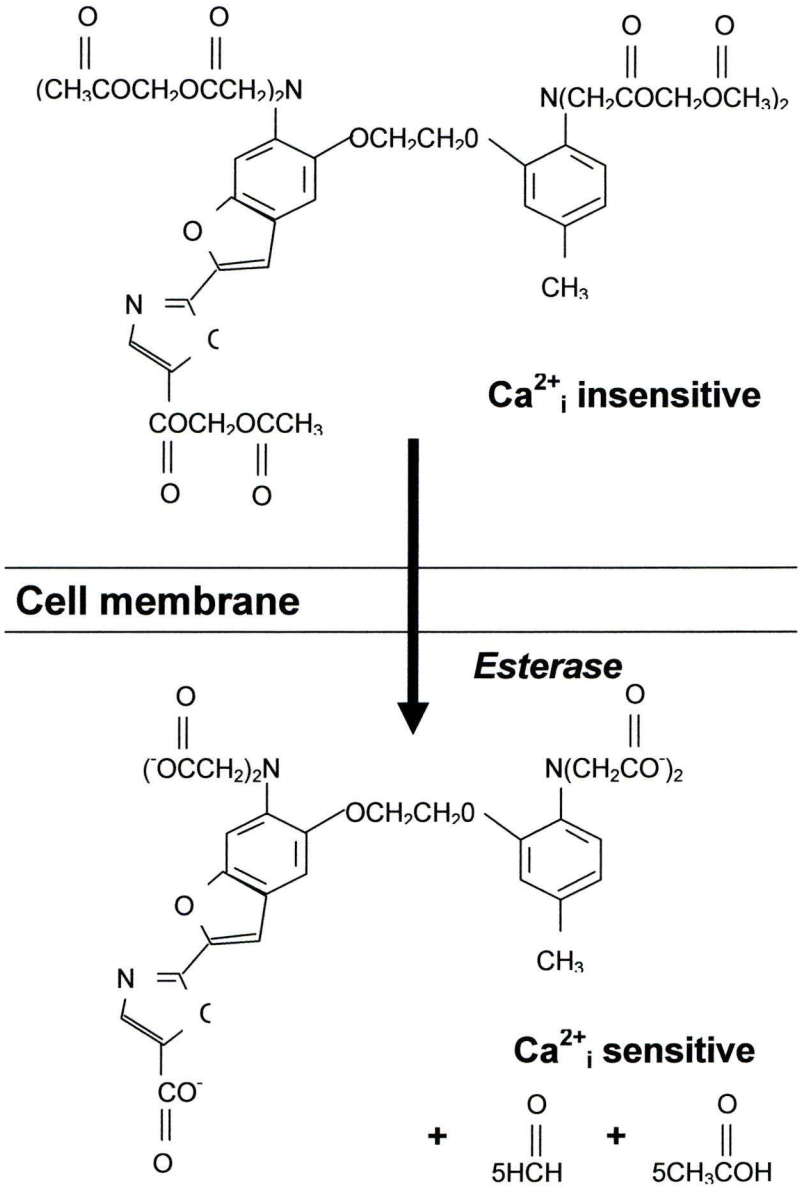

Figure 2.6. Schematic diagram of the processes involved in loading cells using membrane-permeant acetoxymethyl (AM) ester derivatives of fluorescent indicators, in this case fura-2. Note the generation of potentially toxic by-products (formaldehyde and acetic acid).

measurement of Ca^{2+}_i include targeting of recombinant probes based on AEQ or GFP to developing ASM (Prasher *et al.* 1985; Rizzuto *et al.* 1992; Rizzuto *et al.* 1994; Chalfie *et al.* 1994; Miyawaki *et al.* 1997; Romoser *et al.* 1997). Although this technique has been used with some effect in the sarcoplasmic reticulum of rat tail artery (Rembold *et al.* 1997), infection of the embryonic ASM would necessitate generation of adenoviral vectors. To design such a vector and successfully infect the ASM to permit measurement of Ca^{2+}_i would be extremely technically challenging and exceed the timescales available for this work. Additionally, the use of adenoviral vectors could potentially alter the culture system and / or spontaneous contractile activity.

2.2.3 Perfusion chamber

Once loaded with Ca^{2+}_i sensitive dyes, the explants were secured within a perfusion chamber. This provided stability (to reduce movement artefact), allowed easy access to the tissue under study (should manipulation be required during an experimental protocol) and allowed perfusion / rapid exchange of solutions at a constant rate of known temperature. Lung explants are of small size (< 1mm diameter) necessitating development of a custom-built chamber to fulfill these requirements. It was imperative that any structure designed to hold the lung explants did not impair the spontaneous contractile activities noted during *in vitro* culture.

Initially lung explants were placed on glass coverslips to determine whether adherence would occur (Figure 2.7A). Specimens did not adhere which resulted in their dislodgement during perfusion. Explants were then placed below a coverslip (Figure 2.7B), however, this prevented their perfusion and abolished visible peristalsis. As a result, explants were placed under a coverslip supported by foil trivets (Figure 2.7C). Reasonable stability was achieved, but again, some contractility was lost through compression of the principle airways. It became evident that lungs needed to be perfused without compression of the principle airways. Next, lungs were left in-situ upon their polytetrafluorethylene membrane culture-dish inserts and perfused from beneath (Figure 2.7D). Unfortunately, this resulted in them being dislodged from their membrane and uniform heating could not be guaranteed during experiments as only their undersurface was in contact with the solution.

In answer to the above problems, a custom made chamber was designed and built by myself, that utilised monofilament mesh to hold the lung around its periphery without compressing the principle airways (Figure 2.7E). Similar perfusion chambers have been built by others to secure brain slices or mouse lung slices (Bergner *et al.* 2002), however these tissues are much larger than embryonic lung (< 1 mm diameter). This chamber allowed submersion of the lung explants such that they were held securely during perfusion and provided good visibility and access to the airways such that confocal and photometric measurements of Ca^{2+}_i could be

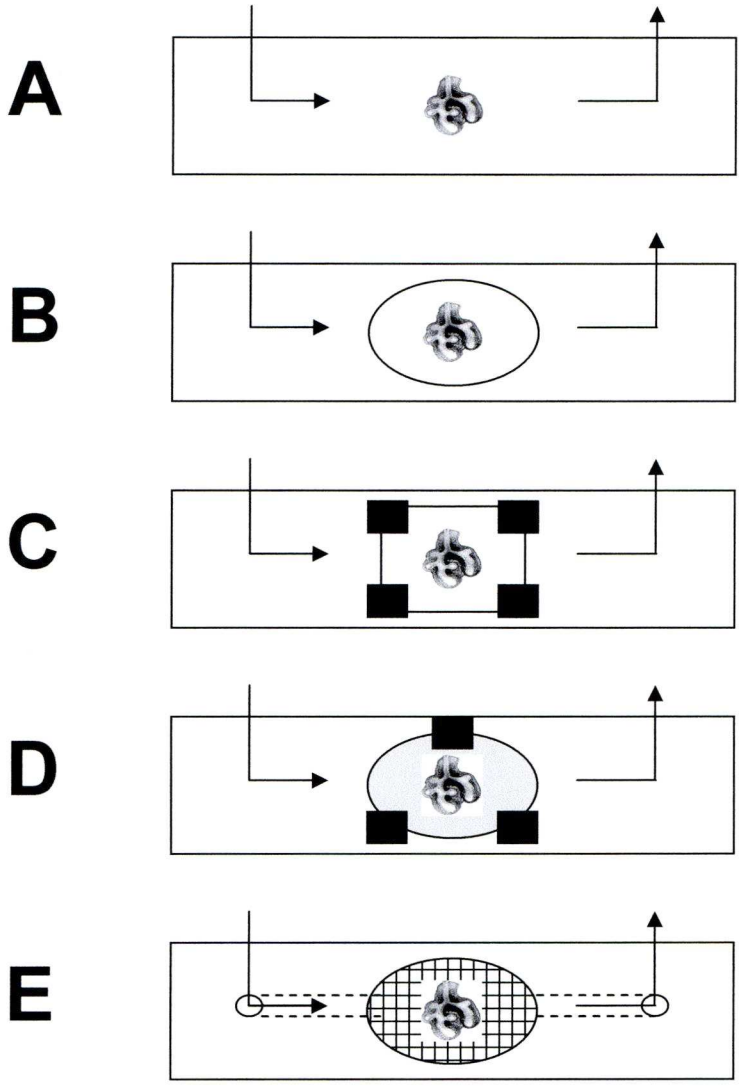

Figure 2.7. Development of the lung perfusion chamber. (A) Lung explants were placed upon glass coverslips. Adherence failed to occur and lungs were displaced when perfused (arrows). (B) Lung explants were placed beneath glass coverslips. This prevented perfusion and abolished visible peristalsis. (C) Lungs were placed beneath glass coverslips supported on foil trivets. Stability was achieved, perfusion could take place, but there was some loss of contractility through compression of the principle airways. (D) Lungs were left in-situ upon culture dish inserts. Explants lost their adherence during perfusion and uniform heating could not be guaranteed. (E) The prototype perfusion chamber used mesh to secure the periphery of explants, thereby, avoiding compression of the principle airways. There was minimal movement during perfusion and uniform heating was achieved.

undertaken (Figure 2.8 and Figure 2.9). A variety of sizes of monofilament mesh were trialled within the chamber assembly; 1000 μm mesh provided the best in terms of support and visibility.

2.2.4 Confocal measurements of Ca^{2+}_i

Confocal imaging was used to determine the spatiotemporal characteristics of intercellular Ca^{2+}_i waves (Figure 2.10). Confocal microscopy provides the ability to see inside relatively bulky specimens; as a result it can be used to optically section the explants permitting visualisation of the ASM surrounding the principle airways. It can focus on one specific tissue plane rejecting out of focus light, resulting in high quality images, and it can be used on living tissues and cells as well as fixed tissues.

Image acquisition was possible from a large area (2.1 x 1.6 mm with the 4x objective to 160 x 110 μm with the 60x objective). This was beneficial as the whole explant could be studied at low power to image intercellular Ca^{2+}_i waves (see chapter 3 and 4) and at high power to search for the origin of these waves. The imaging software permitted specific region(s) of interest to be defined within the lung and the fluorescence at this point(s) to be determined over the time; this was particularly useful for interrogating apparent initiation sites.

There are a number of disadvantages to confocal microscopy. Depth of optical sectioning is limited by the light scattering properties of the tissue itself, the amount of fluorescence quenched by overlying tissue and the

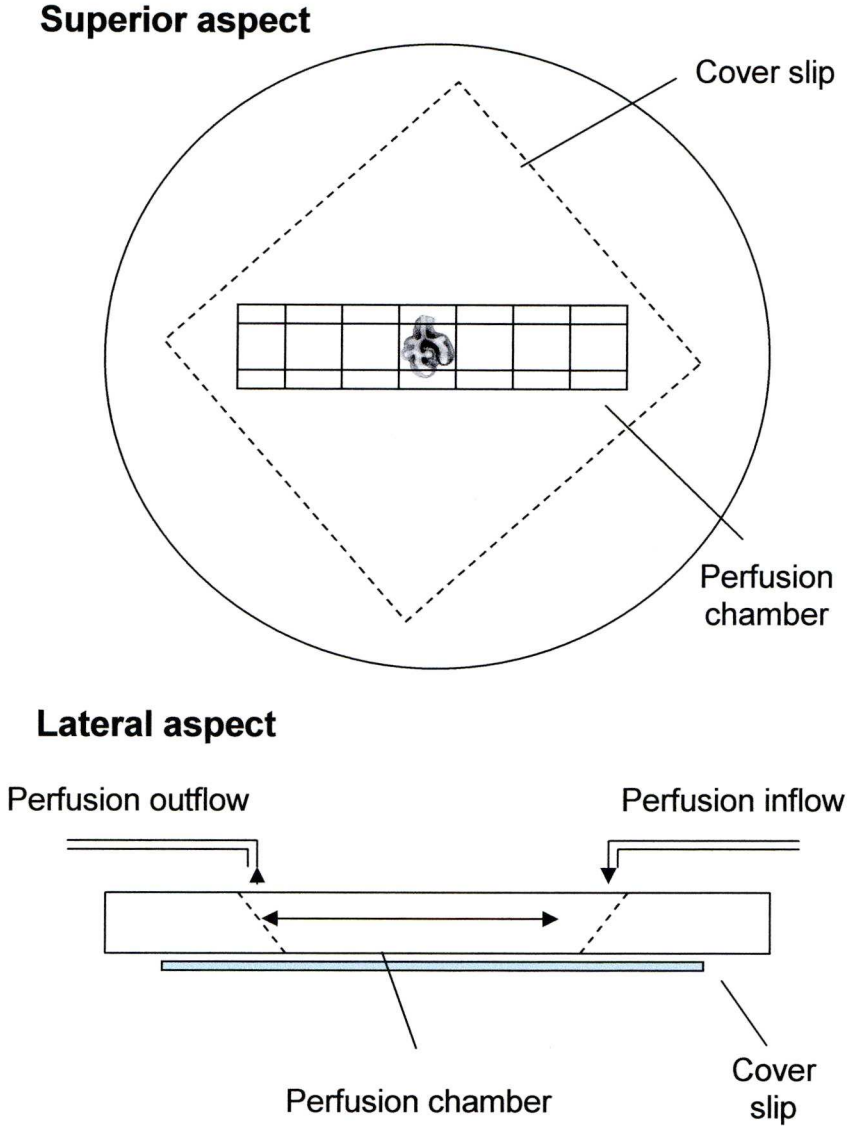

Figure 2.8. Schematic illustration of the final perfusion chamber assembly. The explant is secured by the mesh around its periphery such that compression of the principle airways is avoided. A glass coverslip forms the base of the chamber; it is held in position by vacumn gel. The lung is perfused by a system that ensures constant flow, temperature and rapid exchange of solutions.

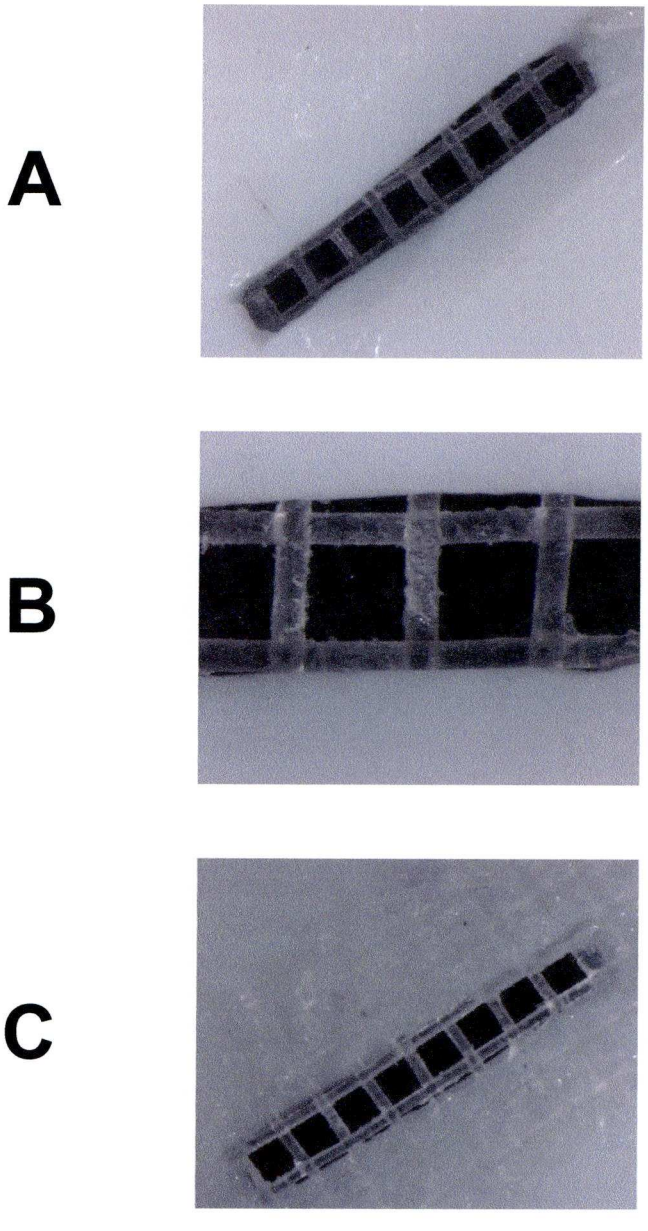

Figure 2.9. Photographs of the final perfusion chamber assembly. (A) Superior aspect of the chamber. (B) Close-up of monofilament that holds the lung around its periphery against the coverslip that forms the base of the chamber. (C) Undersurface of the perfusion chamber. The monofilament mesh is secured to the undersurface of the chamber using superglue allowing regular replacement.

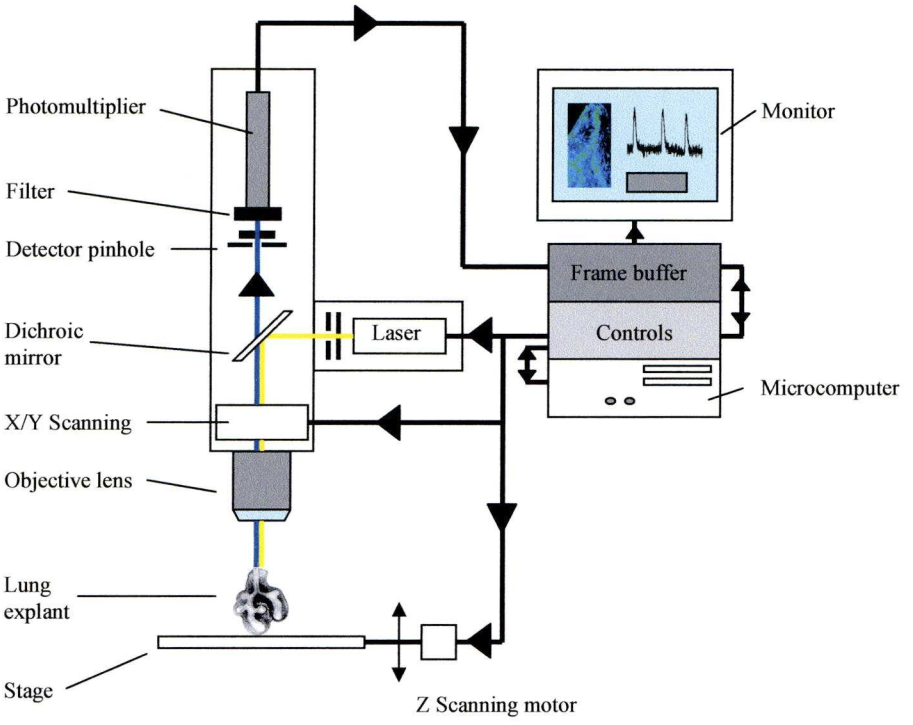

Figure 2.10. Confocal imaging of intercellular Ca^{2+}_i waves was performed on an Ultraview LCI spinning Nipkow disc, widefield Olympus IX70 inverted microscope (Perkin-Elmer Confocal Microscope System, Cambridge, UK) with an ORCA ER cooled CCD camera (Hamamatsu Photonics, Hamamatsu, Japan). Fluo-4 loaded explants were viewed at low power (4x objective, numerical aperture (NA) 0.13; 10x objective, NA 0.17) or high power magnification (60x water immersion objective, NA 0.9) and excited by argon / krypton laser at 488 nm. Resulting fluorescence was measured at 510 nm and was expressed as a function of maximum compared to basal values (F/F0).

working distance of the objective lens. Tissue must be loaded with fluorescent dyes to permit measurement of Ca^{2+}_i; cells must remain viable during imaging and dyes may load unevenly. The tissue is excited by an argon / krypton laser at 488 nm and the resulting fluorescence measured at 510 nm; relative Ca^{2+}_i is expressed as a function of maximum fluorescence compared to basal values (F/F_0). Laser illumination results in photobleaching and thus there is limited longevity to experimental protocols; Ca^{2+}_i transients from each lung were observed for not more than 90 seconds. Lastly, movement artefact is a problem especially when working at high magnification as the area under study may move out of the focal plane (x, y or z plane). Movement artefact is an inherent problem of investigating spontaneously contractile tissue and attempts were made to minimise it through use of the perfusion chamber.

2.2.5 Photometric measurements of Ca^{2+}_i

To study Ca^{2+}_i waves and effects of their modulation by temperature and pharmacological agents, Ca^{2+}_i signalling was also measured photometrically using two ratiometric Ca^{2+}_i sensitive indicators, Indo-1 or Fura-2. Dual channel ratioing techniques are used to measure Ca^{2+}_i when using these dyes. Briefly, when Indo-1 was used, the photometric system consisted of an Olympus IX50 inverted microscope (Olympus UK Ltd., London, UK) and Xenon lamp with an excitation wavelength of 340 nm (Figure 2.11). Light emitted by Indo-1 loaded explants at 400 nm and 500

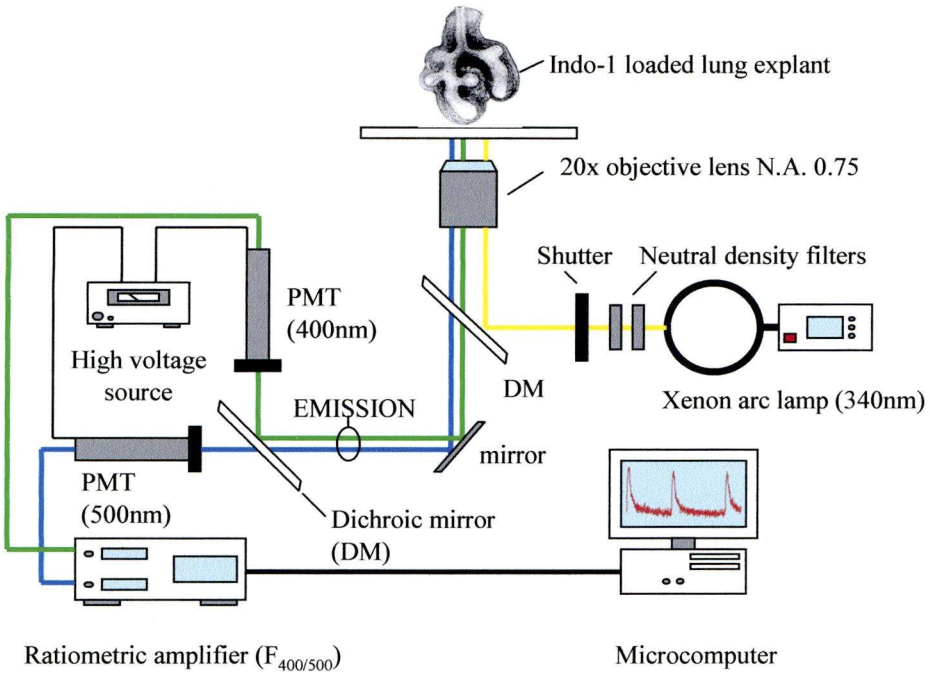

Figure 2.11. Photometric measurement of $Ca^{2+}{}_i$ signalling using Indo-1. The photometric system consisted of an Olympus IX50 inverted microscope and Xenon lamp with an excitation wavelength of 340 nm. Light emitted by Indo-1 loaded explants at 400 nm and 500 nm was detected via photo-multiplier tubes (PMT) and digitally recorded. The ratio of the fluorescence signal (F400/500; 400 nm: 500 nm emission) was used as an indicator of $[Ca^{2+}]_i$. $Ca^{2+}{}_i$ signals were recorded using a 20x objective (N.A. 0.75) from the second bronchial division of the right lung.

nm was detected via photo-multiplier tubes and digitally recorded. The ratio of the fluorescence signal ($F_{400/500}$; 400 nm: 500 nm emission) was used as an indicator of Ca^{2+}_i. Photometric measurements of Fura-2 loaded explants employed a Cairn (Cairn Research Ltd., Faversham, UK) monochromator with dual excitation (340 and 380 nm) and the fluorescent signals were measured at 510 nm ($F_{340/380}$) (Figure 2.12).

Dual channel ratioing provides more reliable quantification (than single channel measurement) as it is less susceptible to problems with dye loading or movement artifact. As such, they became a useful tool in our investigations as the embryonic lungs are spontaneously contracting and movement artifacts can occur. Additionally, perfusion and exchange of perfusion solutions can result in a certain amount of movement. Photometric measurements of Ca^{2+}_i are able to accommodate this whereas confocal imaging is not. Additionally, photobleaching is less of a problem with dual channel ratioing methods such that prolonged experimental protocols could be undertaken.

2.3 Conclusions

a) Organ culture upon translucent polytetrafluorethylene membrane culture-dish inserts permitted reproducible branching morphogenesis, growth in a pseudo 2-dimensional manner and easy

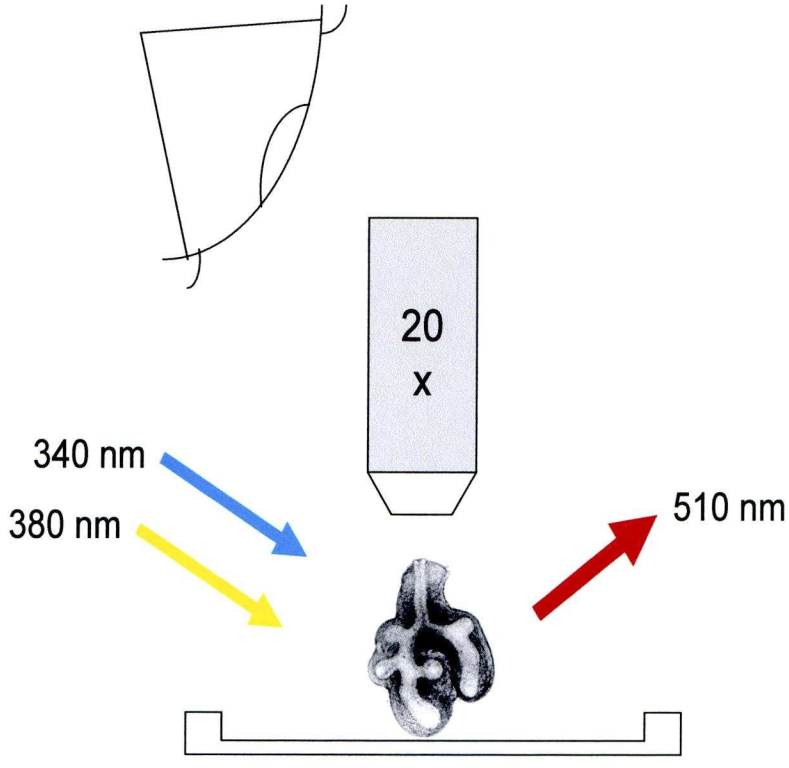

Figure 2.12. Photometric measurement of Ca^{2+}_i signalling using Fura-2. Photometric measurements of Fura-2 loaded explants employed dual excitation (340 and 380 nm) and the fluorescent signals were measured at 510 nm (F340/380). Ca^{2+}_i signals were recorded using a 20x objective (N.A. 0.75) from the second bronchial division of the right lung.

loading with calcium sensitive indicators. Organ culture is well-established in our laboratory permitting plentiful supply of embryonic lung explants on which to perform measurements of Ca^{2+}_i.

b) Ca^{2+}_i sensitive indicators (Indo-1 AM, Fura-2 AM and Fluo-4 AM) were chosen for these studies as their use is well-established, require no specific technology to load the tissues, and have been previously reported to be effective in most cell or tissue types with minimal side effects.

c) Development of a novel perfusion chamber that secured the embryonic lung without compressing the principle airways permitted application of confocal and photometric techniques to image and measure Ca^{2+}_i for the first time in whole embryonic lung organ cultures.

d) Confocal microscopy permitted investigation of the spatiotemporal characteristics of intercellular Ca^{2+}_i transients within whole lung explants. Experimental protocols were limited due to photobleaching (imaging was limited to a maximum of 90 seconds to minimise this). Movement artefacts are problematic when using high power objectives as spontaneous contractility of the lung explants resulted in specimens moving out of the focal plane.

e) Photometric measurements of Ca^{2+}_i transients permitted experimental protocols of long duration to be undertaken as

photobleaching is less problematic. Additionally, these Ca^{2+} sensitive fluorescent dyes used dual channel ratioing techniques which were beneficial as they are less susceptible to uneven dye loading or movement artefact (compared to confocal measurements of Ca^{2+}_i).

Chapter 3

SPONTANEOUS PROPAGATING Ca^{2+}_i WAVES UNDERPIN AIRWAY PERISTALSIS IN EMBRYONIC RAT LUNG

3.1 Introduction

Every 24 – 48 hours in the United Kingdom, a child is born with CDH. Historically, mortality was in the order of 40-60%, mainly due to pulmonary hypoplasia and pulmonary hypertension (Smith *et al.* 2005). More recently, several institutions have reported survival in 80-90% of cases with the introduction of new ventilatory strategies and adjuncts (e.g. permissive hypercapnea, inhaled nitric oxide, high frequency oscillatory ventilation etc.) (Downard *et al.* 2003; Bagolan *et al.* 2004). However, if 'hidden mortality' (*in utero* deaths, terminations of pregnancy, postnatal deaths prior to transfer to the paediatric surgical unit) are taken into account, mortality remains persistently high (Beresford *et al.* 2000; Stege *et al.* 2003; The Ontario Congenital Anomalies Study Group 2004; Colvin *et al.* 2005; Dillon *et al.* 2000).

Classical thinking suggested that pulmonary hypoplasia was secondary to compression from the herniated abdominal contents. However, studies undertaken during the last two decades have prompted reappraisal of these concepts. Work undertaken in the nitrofen model of CDH suggests that lung hypoplasia precedes closure of the diaphragm (Jesudason 2000; Jesudason 2001; Jesudason 2002; Keijzer *et al.* 2000).

Given these contemporary views, many researchers have chosen to study embryonic lung development in order to gain insight into the factors that influence pulmonary growth. It is now well established that lung growth not only requires a variety of growth factors, but also a number of

mechanical factors (Hogan 1999; Harding *et al.* 1996). Spontaneous contractility of the embryonic airways (airway peristalsis) is one such mechanical factor that may be linked with pulmonary development (Jesudason *et al.* 2005). Previous research suggests that Ca^{2+} influx in ASM may be involved in its generation (McCray 1993; Roman 1995; Sparrow *et al.* 1994).

We demonstrate that spontaneous propagating Ca^{2+}_i waves underpin or drive airway peristalsis. Given that airway peristalsis appears linked to pulmonary growth and Ca^{2+}_i waves drive airway peristalsis, this indicates Ca^{2+}_i waves drive lung growth.

3.2 Materials and methods

3.2.1 Retrieval of embryonic lung primordia

In accordance with UK legislation, embryos from Sprague-Dawley rats (Charles River Ltd, Margate, UK) were harvested on day 13.5 of gestation (vaginal plug = day 0, term = day 22.5) as previously described (Jesudason *et al.* 2000). This is 24 hours after the lung anlage forms as a diverticulum from the foregut. Upon retrieval, embryos were transferred to an isotonic saline bath cooled on ice. Microdissected from their extra-embryonic membranes, embryos were secured in a lateral position using cranial and caudal entomology pins. Using a Leica (Leica Microsystems (UK) Ltd., Milton Keynes, UK) MZ6 stereomicroscope and microsurgical instruments, a thoracic incision was performed to expose the embryonic

heart and lungs. The heart was teased from the lung rudiments before the oesophagus was freed carefully from the primitive carina. The trachea was then sectioned and the pulmonary complex transferred by pipette into serum-free culture medium (DMEM/F12 1:1, Gibco; Invitrogen Life Technologies, Paisley, UK). Lung rudiments were positioned on translucent polytetrafluorethylene membrane culture-dish inserts (Millicell, Millipore Corp, Bedford, MA) with serum-free culture medium incorporating penicillin (100 IU/ml) and streptomycin (100 μg/ml; GibcoBRL, Life Technologies, Paisley, UK). Lung primordia were incubated at 37°C in 5% CO_2 for periods up to 78 hours.

3.2.2 Assessment of viability

Using bright field microscopy, specimens were inspected daily for histological integrity, viability, and the periodic motion of luminal lung fluid. Culture media were changed every 48 hours. Spontaneous airway contractions were seen in 100% of explants by 48 hours *in vitro* using this established culture technique (Jesudason *et al.* 2005).

3.2.3 Loading lung explants with Ca^{2+}_i sensitive fluophores

Lungs were cultured for 54 or 78 hours before 4 hour incubation at 37°C with the membrane-permeant form of Fluo-4 AM (15 μM, Molecular Probes, Invitrogen Life Technologies, Paisley, UK) with Pluronic F (for confocal imaging), or 2 hour incubation at 37°C with the membrane-

permeant forms of Indo-1 AM or Fura-2 AM (15 μM, Molecular Probes) with Pluronic F (for ratiometric imaging of Ca^{2+}_i). Explants were then allowed to equilibrate for 30 minutes in physiological saline at 37°C.

3.2.4 Confocal and photometric measurements

For confocal and photometric studies, lung primordia were secured in a 200 μl custom-made perfusion chamber by nylon mesh (Plastok, Birkenhead, UK) that holds the lung periphery against the coverslip without compressing principal airways.

Confocal imaging was used to determine spatiotemporal characteristics of intercellular Ca^{2+}_i waves and performed on an Ultraview LCI spinning Nipkow disc, widefield Olympus IX70 inverted microscope (Perkin-Elmer Confocal Microscope System, Cambridge, UK) with an ORCA ER cooled CCD camera (Hamamatsu Photonics, Hamamatsu, Japan). This permits image acquisition from a large area (from 2.1 x 1.6 mm with 4x objective to 160 x 110 μm with 60x objective) at 20-30 frames per second with relatively low intensity laser illumination and at good signal to noise ratio. Fluo-4 loaded explants were viewed at low power (4x objective, numerical aperture (NA) 0.13; 10x objective, NA 0.17) or high power magnification (60x water immersion objective, NA 0.9) and excited by argon / krypton laser at 488 nm. Resulting fluorescence was measured at 510 nm and is expressed as a function of maximum compared to basal values (F/F_0). To reduce photobleaching, Ca^{2+}_i transients from each lung were observed for

not more than 90 seconds. Propagation speeds of the Ca^{2+}_i and contractile waves were measured using the Perkin-Elmer Microscope System. Regions of interest were defined in the airways. Pixel counts between regions of interest were then converted to distance (μm) using calibration measurements for each objective and pixel binning option. Measurement of the interval (sec) between initiation of the Ca^{2+}_i transient (or ASM contraction) at one region of interest and the next allowed the propagation speed to be quantified.

To study intracellular Ca^{2+}_i waves and effects of their modulation by temperature and pharmacological agents, Ca^{2+}_i signalling was also measured photometrically using two ratiometric Ca^{2+}_i sensitive indicators, Indo-1 or Fura-2. The optical system has been described previously (Burdyga *et al.* 1999). Briefly, when Indo-1 was used, the photometric system consisted of an Olympus IX50 inverted microscope (Olympus UK Ltd., London, UK) and xenon lamp with an excitation wavelength of 340 nm. Light emitted by Indo-1 loaded explants at 400 nm and 500 nm was detected via photo-multiplier tubes and digitally recorded. The ratio of the fluorescence signal ($F_{400/500}$; 400 nm: 500 nm emission) was used as an indicator of Ca^{2+}_i. Photometric measurements of Fura-2 loaded explants employed a Cairn (Cairn Research Ltd., Faversham, UK) monochromator with dual excitation (340 and 380 nm) and the fluorescent signals were measured at 510 nm ($F_{340/380}$). With both indicators, Ca^{2+}_i signals were recorded using a 20x objective (N.A. 0.75) from the second bronchial

division of the right lung (previously reported origin for most mechanical contractions) (Jesudason *et al.* 2005). For each lung primordia $Ca^{2+}{}_i$ transients were observed for at least 10 minutes. Temporal characteristics of the $Ca^{2+}{}_i$ waves (duration of fast and slow phases, time to achieve 50% of peak amplitude, amplitude, plateau duration, relaxation half-time (T_{50}) and duration at 50% relaxation) were determined from at least three representative transients per lung.

3.2.5 Solutions

Unless otherwise stated, lung explants were superfused at 37°C with buffered physiological saline (pH 7.4) containing (mM): 120 NaCl, 5.6 KCl, 0.12 $MgSO_4$, 2 $CaCl_2$, 11.7 glucose, 10.9 HEPES. 'Zero Ca^{2+}' solution used in certain experiments consists of physiological saline with $CaCl_2$ omitted and 2 mM EGTA added. Other additions to standard superfusate that were investigated include: nifedipine (10 μM), Bay-K 8644 (1 μM), 18-β glycyrrhetinic acid (18-βGA, 40 μM), tetraethylammonium (TEA, 10 mM), cyclopiazonic acid (CPA, 20 μM), caffeine (1 mM - 10 mM), ryanodine (20 μM), carbachol (10 μM -100 μM), 2-aminoethoxy-diphenylborate (2-APB, 50 μM) and high K^+ solution (120 mM). Carbachol and ryanodine were dissolved in distilled water; CPA, 2-APB and 18-βGA were dissolved in dimethylsulfoxide (DMSO), whilst nifedipine and Bay-K 8644 were dissolved in ethanol (EtOH). $Ca^{2+}{}_i$ wave generation and airway contractility were unaffected by applications

of vehicle alone (DMSO or ETOH). Ryanodine was obtained from Calbiochem (Merck Biosciences Ltd., Nottingham, UK). Sigma (Poole, Dorset, UK) supplied all other chemicals.

3.2.6 Immunohistochemistry

Cultured lungs were preserved after 78 hours in 4% paraformaldehyde (0.1 M phosphate-buffered saline [PBS], pH 7.4), rinsed in PBS, cryoprotected with 20% (w/v) sucrose, gelatine-embedded (7.5% [w/v] gelatin, 15% [w/v] sucrose in PBS) before being covered in Cryo-M-Bed (Bright, Huntingdon, UK) and snap-frozen at -40°C. Lung sections were taken at 7μm and mounted on chrome alum gel slides for storage at -40°C.

Slides were rinsed in PBS and incubated with α-smooth actin antibody (monoclonal anti- α-SMA Clone No.1A4, mouse; Sigma, Gillingham, UK) at 1:500 dilution with 0.1% BSA in PBS overnight at 4°C. They were then rinsed in PBS and the primary antibody labelled with FITC-labelled goat anti-mouse IgG (Sigma, Gillingham, UK) at 1:100 dilution. Slides were then mounted with fluorescent mounting medium (S3023; Dako, Ely, UK).

3.2.7 Statistical analysis

Data processing was performed using Origin 6.0 software (OriginLab Corporation, Northampton, MA, USA). The SPSS v12.0 package (SPSS UK Ltd., Woking, UK) was utilised for statistical analysis. Parametric data are reported as mean ± SEM and compared using Student's t-test. Non-

parametric data are reported as medians (interquartile ranges) and compared with Mann Whitney U test. Statistical significance was taken at $p < 0.05$.

3.3 Results

3.3.1 Spontaneous Ca^{2+}_i waves propagate via smooth muscle cells prior to contraction

Confocal imaging of Fluo-4 loaded embryonic lungs (n = 16) with low power magnification (4x or 10x) at 37^0C, revealed intercellular Ca^{2+}_i waves propagating longitudinally through principal airways (Figure 3.1A). The propagating Ca^{2+}_i waves originated from the trachea (Region 1, red box; Figures 3.1A, B, and D) or the second bronchial division of the right lung rudiment (Region 2, black box; Figures 3.1A, C, and D). Infrequently separate intercellular Ca^{2+}_i waves emanated simultaneously from two foci (data not shown). The initial phase of the Ca^{2+}_i transient differed between sites of Ca^{2+}_i wave initiation and sites of propagation (Figure 3.1D). Irrespective of the site of origin and direction of travel, Ca^{2+}_i waves propagated with an average speed of 219 ± 14 μm/s (n = 4 lung explants, 10 individual Ca^{2+}_i waves), and after a short delay (349 ± 30 ms, n = 4 lung explants), were followed by the mechanical contractile wave (recorded as the decrease in the airway luminal diameter)(Figure 3.2). Contractile ASM waves invariably propagated from the Ca^{2+}_i wave origin at a similar speed:

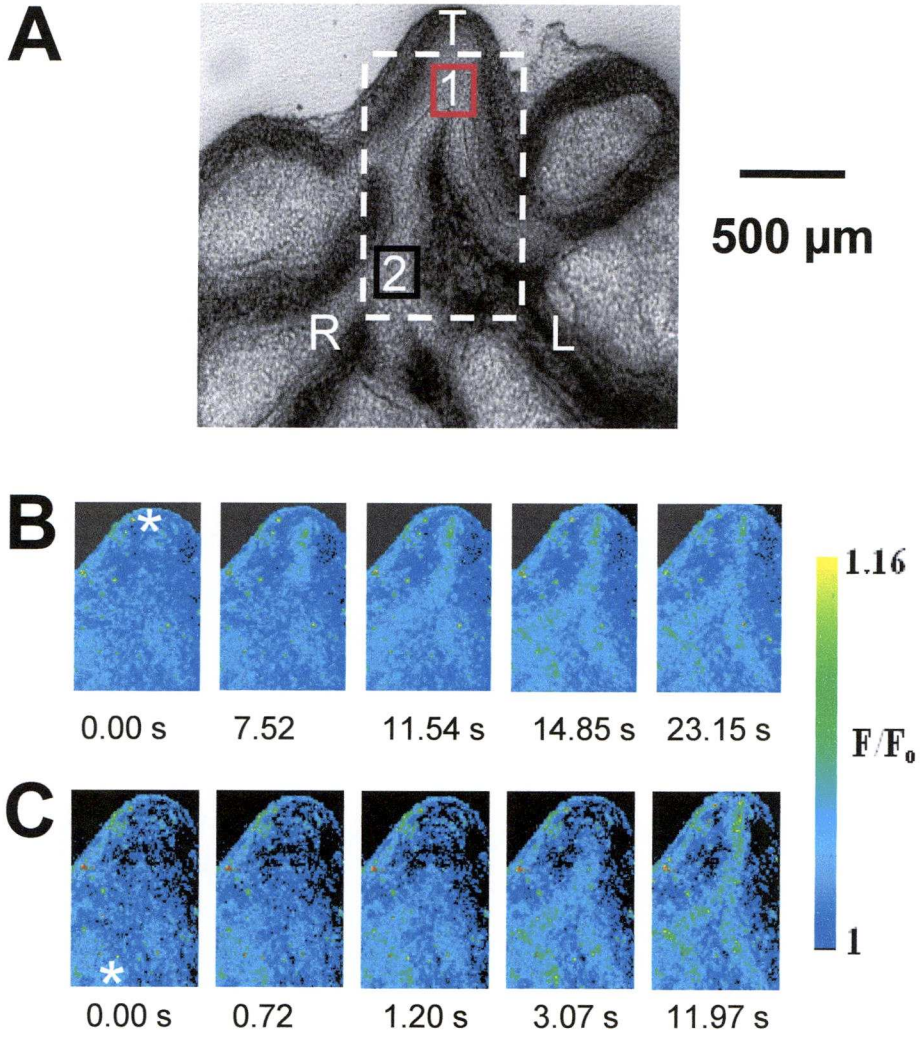

Figure 3.1. Intercellular Ca^{2+}_i waves in embryonic lungASM. (*A*) Transmitted light photomicrograph of a whole lung explant after 54 h *in vitro*: the *dashed box* contains the proximal airways shown in *B* and *C* (T = Trachea; R = Right and L = Left lung rudiments; Marked regions 1 and 2 are the sites of recording of the Ca^{2+}_i transients in D). (*B* and *C*) Stacks of pseudo-color confocal images of Fluo-4–loaded airways showing propagating Ca^{2+}_i waves with the initiation site (marked by an *asterisk*) in the trachea (*B*) and right lung rudiment (*C*).

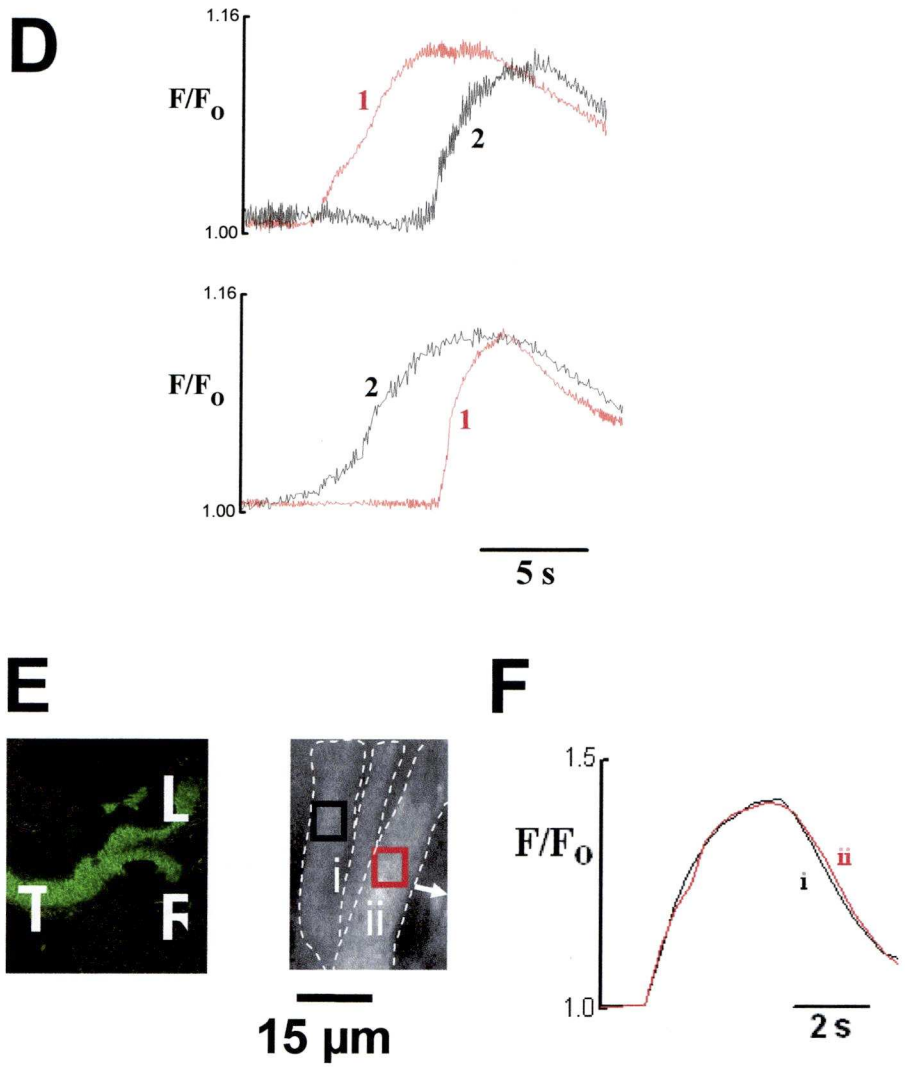

Figure 3.1. Intercellular Ca^{2+}_i waves in embryonic lung ASM. (*D*) Ca^{2+}_i transients measured in regions 1 and 2 (*see A*). The Ca^{2+}_i wave originates in the trachea (region 1; *top*) or the right lung (region 2; *bottom*). (*E*) *Left-hand panel* shows immunohistochemistry for α-smooth actin on a 7-µm section of a cultured lung explant. Smooth muscle cells expressing α-smooth actin are arranged perpendicular to the long axis of the airway (T = Trachea; R = Right and L = Left lung rudiments). *Right-hand panel* shows greyscale image of Fluo-4–loaded individual smooth muscle cells (outlined by *dashed line*) surrounding embryonic airway at 60x objective magnification. The *arrow* demonstrates the long axis of the airway. Marked regions i (*black*) and ii (*red*) are the sites of recording of the Ca^{2+}_i transients in *F*. (*F*) Ca^{2+}_i transients recorded in areas 1 and 2 (marked on cells at 60x objective magnification in *E*).

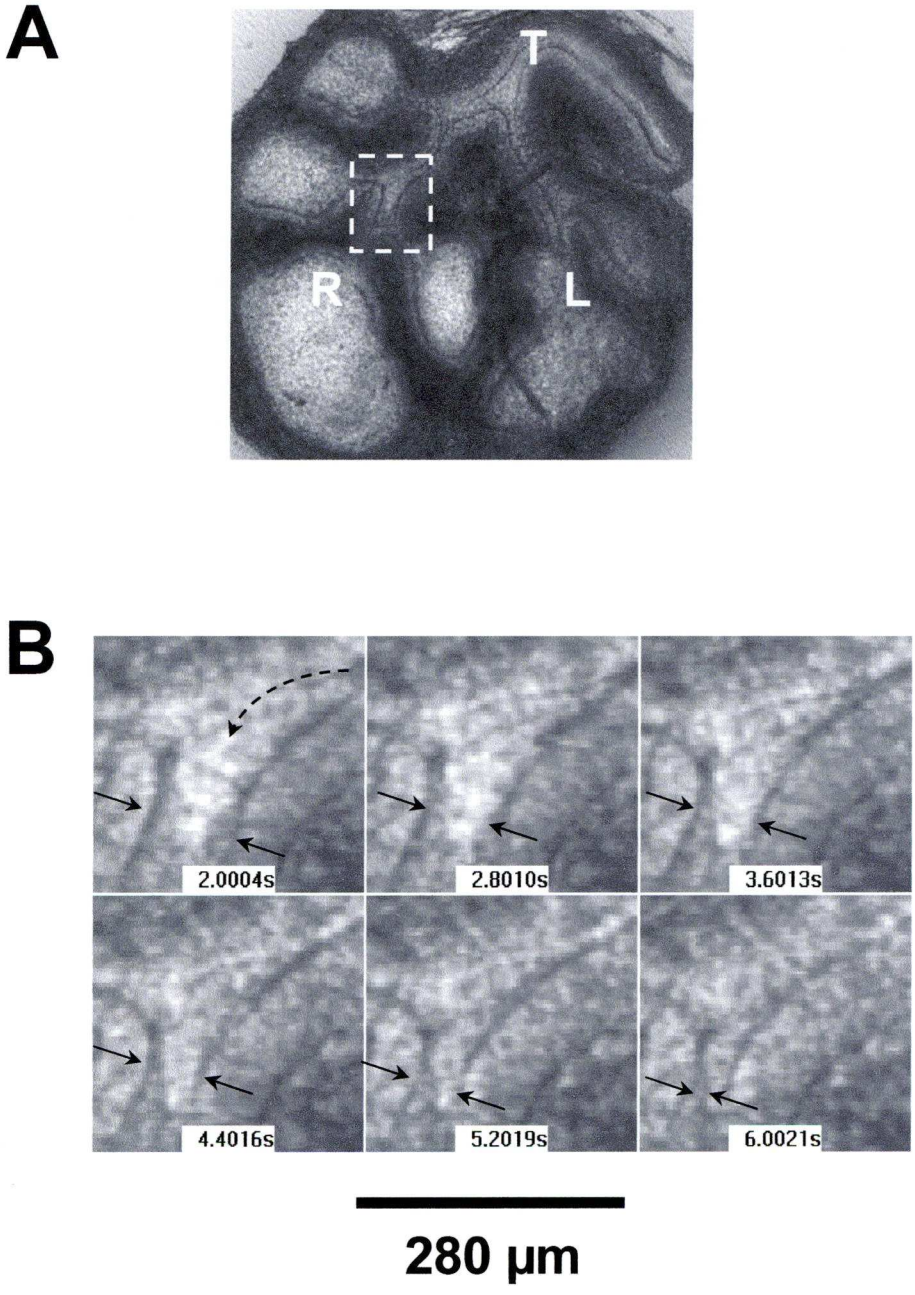

Figure 3.2. Relationship between $Ca^{2+}{}_i$ waves and ASM mechanical contractility. (*A*) Transmitted light image of a cultured lung (the *dashed box* contains the region shown at high magnification in *B*). T = Trachea; R = Right and L = Left lung rudiments. (*B*) Stack of grayscale transmitted light images showing airway contractility. The *dashed arrow* gives the direction of the contractile wave. The *small arrows* demonstrate the airway lumen.

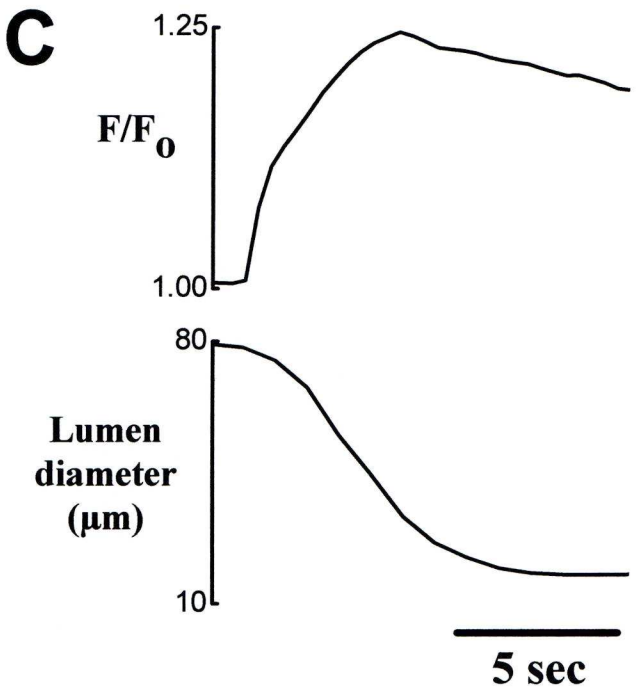

Figure 3.2. Relationship between Ca^{2+}_i waves and ASM mechanical contractility. (C) Change in Ca^{2+}_i as shown by F/F_0 (*top*) and lumen diameter in μm (*bottom*) with time. Fluorescence was measured at 510 nm and is expressed as a function of maximum compared to basal values (F/F_0).

177 ± 32 μm/s (n = 4 lungs, 8 contractile waves). Using high power magnification (60x objective), Ca^{2+}_i waves were also recorded in individual smooth muscle cells (Figure 3.1E, F). Ca^{2+}_i transients recorded photometrically or confocally exhibited similar time courses and 4 distinct phases (i) fast upstroke, (ii) slow attainment of peak, (iii) plateau and (iv) relaxation (Figures 3.3A and 3B). Using a 60x objective, developing ASM cells were observed lying circumferentially around the developing airway with their long axes perpendicular to that of the bronchi (Figure 3.1E). The diameters of these cells were approximately 8-14 μm. Histology and α-actin immunohistochemistry (n = 10) confirmed this typical ASM orientation (Figure 3.1E) (Sparrow *et al.* 2003).

3.3.2 Role of gap junctions

The propagation speed (Yamazawa *et al.* 2002; Stevens *et al.* 1999; Hashitani *et al.* 2001) and temporal phases (Burdyga *et al.* 2002) (above) of ASM intercellular Ca^{2+}_i waves are consistent with an action potential-mediated mechanism. Propagation of the action potential in smooth muscle tissue is mediated by gap junctions (Hashitani *et al.* 2001; Hashitani *et al.* 2004), To test whether propagating Ca^{2+}_i waves in the present experiments required gap junction integrity, we studied the effects of the gap junction uncoupler 18-β glycyrrhetinic acid (40 μM) on the Ca^{2+}_i waves. 18-β glycyrrhetinic acid abolished both propagating Ca^{2+}_i waves and coordinated peristalsis after an initial brief excitatory phase (n = 4)(Figure

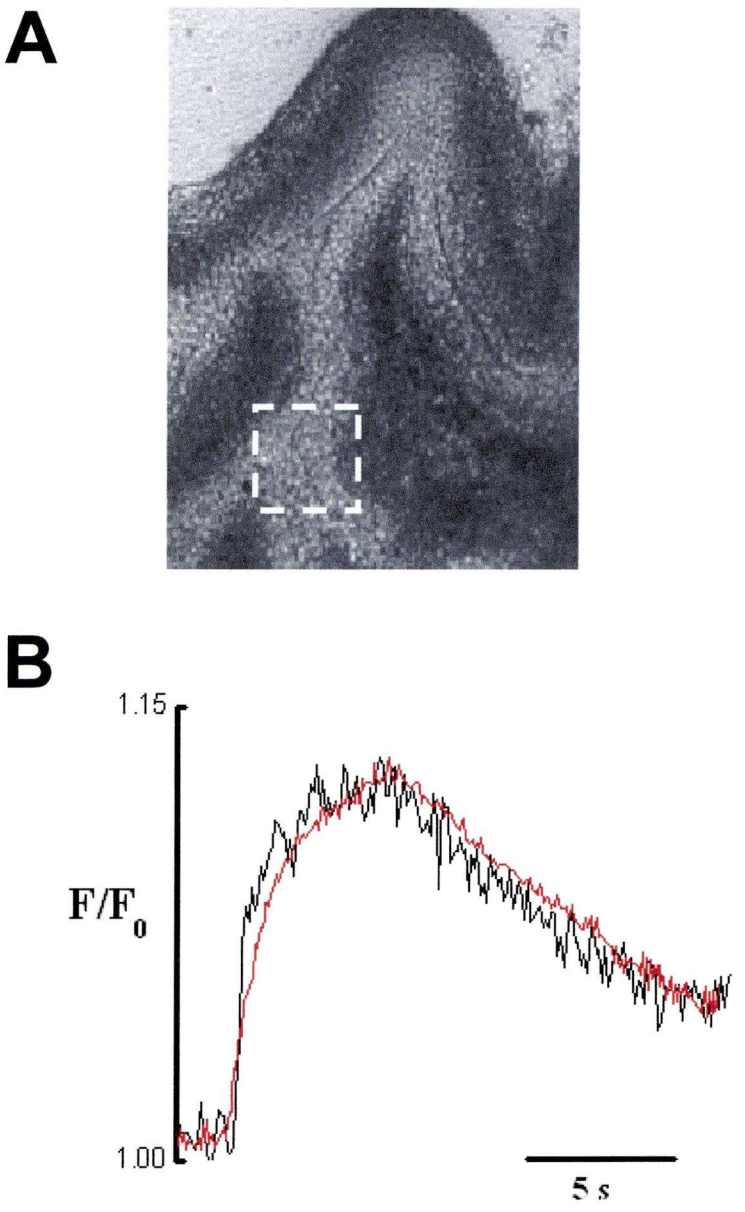

Figure 3.3. Effects of gap junction blockade and cooling on lung Ca^{2+}_i oscillations. (*A*) Transmitted light image of the proximal airways of an embryonic lung. The *dashed box* shows the region where Ca^{2+}_i transients were recorded. (*B*) Superimposed normalized traces of a typical Ca^{2+}_i transient recorded photometrically (*black trace*) and confocally (*red trace*) from the region in *A*. Fluorescence was measured at 510 nm and is expressed as a function of maximum compared to basal values (F/F_0).

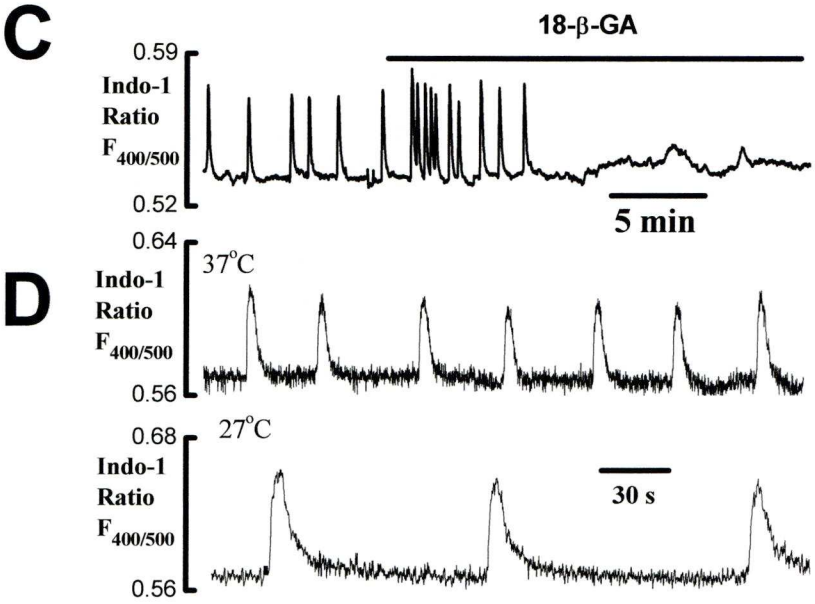

Figure 3.3. Effects of gap junction blockade and cooling on lung $Ca^{2+}{}_i$ oscillations. (*C*) Inhibition of $Ca^{2+}{}_i$ oscillations by 18-ß-glycyrrhetinic acid (40 μM). (*D*) Airway $Ca^{2+}{}_i$ oscillations at 37°C and 27°C. The ratio of the fluorescence signal ($F_{400/500}$) was used as an indicator of $Ca^{2+}{}_i$.

3.3C).

3.3.3 Effects of moderate cooling

Airway peristalsis and excitation-contraction coupling are temperature dependent (Lewis 1924; Burdyga *et al.* 2002). We therefore compared the temporal characteristics and frequency of ASM Ca^{2+}_i transients at 37°C and 27°C. Amplitude of the spontaneous Ca^{2+}_i transients is conventionally expressed as a percentage of peaks obtained with depolarising 120mM K^+ solution or 100 μM carbachol. Amplitude of spontaneous Ca^{2+}_i transients (% of high K^+ peak) was 27 ± 2% (n = 17 lungs) at 37°C and 22 ± 2% (n = 11 lungs) at 27°C (p = NS). In contrast, as a percentage of carbachol peak, amplitude of spontaneous Ca^{2+}_i transients was 28 ± 4% (n = 5 lungs) at 37°C and 15 ± 2% (n = 7 lungs) at 27°C (p = 0.01). Cooling to 27°C had no effect on time to 50% of peak amplitude of the Ca^{2+}_i transient whilst plateau phase, relaxation half-time (T_{50}) and duration at 50% amplitude were significantly prolonged (Table 3.1). There was a trend toward higher frequency Ca^{2+}_i oscillations at 37°C (0.81 ± 0.06 per minute, n = 23) compared to 27°C (0.7 ± 0.06 per minute, n = 22). Figure 3.3D highlights this trend.

3.3.4 Effects of Ca^{2+} and K^+ channel modulators

'Zero Ca^{2+}' solution (with 2 mM EGTA) decreased baseline Ca^{2+}_i and rapidly abolished both Ca^{2+}_i transients and peristalsis (n=4)(Figure 3.4A).

	37^0C (n = 5)	27^0C (n = 5)	p values
Fast phase duration (s)	0.68 ± 0.05	0.92 ± 0.08	0.027
Fast phase amplitude (% of peak)	73.06 ± 1.49	75.83 ± 2.33	NS
Time to 50% amplitude (s)	0.45 ± 0.03	0.57 ± 0.06	NS
Slow phase duration (s)	1.06 ± 0.12	1.18 ± 0.17	NS
Plateau duration (s)	1.94 ± 0.15	3.32 ± 0.27	0.002
Relaxation half time, T_{50} (s)	2.76 ± 0.44	4.57 ± 0.33	0.01
Width at 50% amplitude (s)	5.99 ± 0.56	9.44 ± 0.54	0.002

TABLE 3.1. Temporal characteristics of $Ca^{2+}{}_i$ oscillations recorded at 37°C and 27°C

Readmission of Ca^{2+} quickly restored Ca^{2+}_i oscillations and mechanical activity. These data indicate that Ca^{2+}_o entry is required for the generation of propagating Ca^{2+}_i waves. Blockade of L-type Ca^{2+} channels with nifedipine (10 μM) rapidly abolished spontaneous Ca^{2+}_i transients and peristalsis whilst reducing baseline Ca^{2+}_i (n = 4)(Figure 3.4B). In contrast, the L-type Ca^{2+} channel agonist, Bay-K 8644 (1 μM; n = 4) raised Ca^{2+}_i, increased Ca^{2+}_i wave amplitude (from 27 ± 5% to 46 ± 5% of peak obtained with depolarising 120mM K^+ solution; p = 0.045) and frequency (from 0.53 ± 0.14 to 2.57 ± 0.61 per minute; p = 0.017)(Figure 3.4C). The K^+ channel blocker TEA (10 mM; n = 4) produced a trend toward increased Ca^{2+}_i wave amplitude (from 13 ± 4% to 23 ± 7% of peak with high K^+ solution; p = NS) and frequency (from 0.65 ± 0.23 to 1.63 ± 0.46 per minute; p = NS)(Figure 3.4D). These data suggest that amplitude, duration and frequency of the Ca^{2+}_i transients are controlled by L-type Ca^{2+} channels and potentially by TEA-sensitive K^+ channels (voltage gated (K_V) or large conductance (BK) channels or both).

3.3.5 Role of the sarcoplasmic reticulum

Ca^{2+} handling by the sarcoplasmic reticulum is vital in smooth muscle excitation-contraction coupling. Ca^{2+}_i release is mediated by SR channels, ryanodine receptors (RyR) and inositol triphosphate receptors ($InsP_3R$); removal of released Ca^{2+}_i from the cytoplasm occurs primarily via the SR Ca^{2+}-ATPase (SERCA pump) (Sanders 2001; Taylor *et al.* 2002).

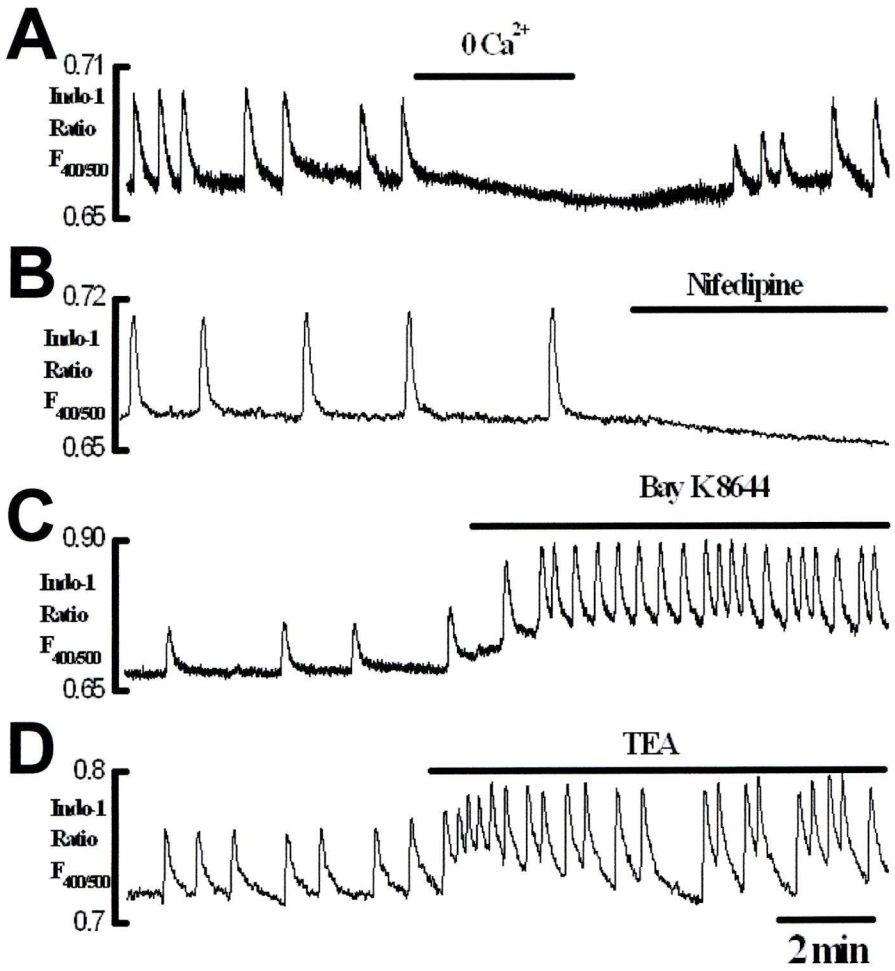

Figure 3.4. Effects of Ca^{2+} channel and K^+ channel modulators on Ca^{2+}_i oscillations in embryonic lung ASM. (*A*) Reversible inhibition of Ca^{2+}_i oscillations by removal of external Ca^{2+} (0 Ca^{2+} solution with 2 mM EGTA). (*B*) Abolition of Ca^{2+}_i oscillations by L-type Ca^{2+} channel blocker (nifedipine (10 μM). (*C*) Increased frequency of Ca^{2+}_i oscillations with L-type Ca^{2+} channel agonist Bay-K 8644 (1 μM). (*D*) K^+ channel blocker (TEA, 10 mM) increases Ca^{2+}_i oscillation frequency. The Y-axis shows the Indo-1 ratio ($F_{400/500}$) which was used as an indicator of Ca^{2+}_i.

Caffeine facilitates Ca^{2+}_i -induced Ca^{2+} release (CICR) properties of RyR (Endo 1977). Carbachol activates $InsP_3R$-mediated SR Ca^{2+}_i release through inositol triphosphate (IP_3) production (Sanders 2001; Taylor *et al.* 2002). Their effects were studied after initial application of high K^+ solution (to generate a 100% reference for Ca^{2+}_i) and then, to eliminate plasmalemmal Ca^{2+} entry, 2 minutes superfusion with Ca^{2+}-free solution (which decreased Ca^{2+}_i). Application of 20 mM caffeine then transiently increased Ca^{2+}_i (15% ± 7% of high K^+ response; n = 4)(Figure 3.5A) with brief tonic airway contraction. Subsequent application of carbachol (100 μM) for 1 minute generated high amplitude Ca^{2+}_i transients (120 ± 27% of high K^+ response; n = 4)(Figure 3.5A) and sustained tonic contraction. Therefore embryonic ASM cells appear to possess a sarcoplasmic Ca^{2+}_i store that is releasable via both RyR and $InsP_3R$ channels.

To examine the role of the SR in regulation of Ca^{2+}_i waves in embryonic airway smooth muscle we studied the effects on the Ca^{2+}_i transients of (a) blocking the SERCA pump with CPA (Kosterin *et al.* 1996), (b) activating CICR via RyRs with caffeine (Endo 1977), (c) blocking RyR channels with ryanodine (Fill *et al.* 2002) or (d) blocking $InsP_3Rs$ with 2-APB (Maruyama *et al.* 1997).

CPA (20μM) (n = 4) markedly increased baseline cytosolic Ca^{2+}_i and gradually abolished Ca^{2+}_i transients (Figure 3.5B). Similarly phasic mechanical contractions were progressively replaced by tonic airway contraction. Removal of CPA from the bathing solution reversed its

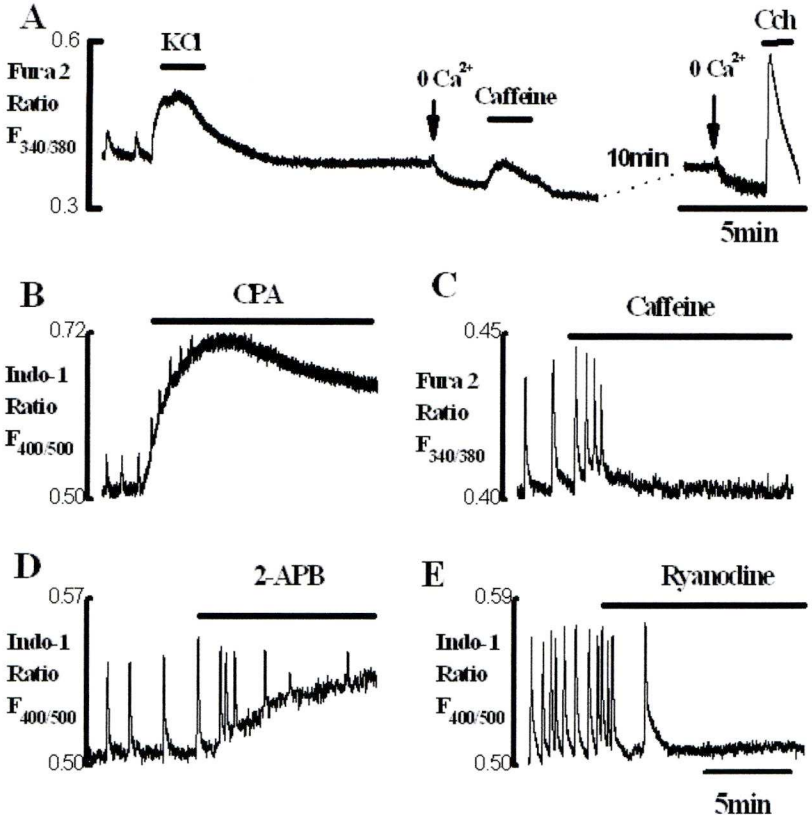

Figure 3.5. Sarcoplasmic calcium regulates $Ca^{2+}{}_i$ oscillations in embryonic ASM. (*A*) Agonist-induced SR Ca^{2+} release: $Ca^{2+}{}_i$ recording showing the effects of high K^+, caffeine (20 mM), and carbachol (100 μM). Caffeine and carbachol were applied after 2 min exposure to a 0 Ca^{2+} solution. Abolition of $Ca^{2+}{}_i$ oscillations by (*B*) CPA (20 μM), (*C*) caffeine (1 mM), (*D*) 2-APB (50 μM), and (*E*) Ryanodine (20 μM). The Y-axis shows either the Fura-2 ratio ($F_{340/380}$) or Indo-1 ratio ($F_{400/500}$) which was used as an indicator of $Ca^{2+}{}_i$.

effects. Caffeine's effects on Ca^{2+}_i were dose-dependent: caffeine (1 mM) initially stimulated and then abolished Ca^{2+}_i waves and contractility (n = 4)(Figure 3.5C). Caffeine (10 mM) increased baseline Ca^{2+}_i and basal tone with abolition of Ca^{2+}_i waves (n = 4) (data not shown). Variation in caffeine's effects may be due to complex sequelae of CICR that may include activation of depolarizing chloride channels and / or hyperpolarizing K^+ channels (Wellman *et al.* 2003; Kotlikoff *et al.* 1998). Blockade of the latter by TEA (10 mM) prevented caffeine's action and suggests that caffeine-induced CICR does mediate K^+ channel opening (n = 4; data not shown). Ryanodine (20 μM) also abolished spontaneous Ca^{2+}_i waves and contractility (n = 4) (Figure 3.5E). $InsP_3R$ blockade by 20-minute application of 2-aminoethoxy-diphenylborate (2-APB; 50 μM) increased baseline Ca^{2+}_i and gradually abolished both Ca^{2+}_i waves and contractility (n = 4) (Figure 3.5D) (Bilmen *et al.* 2002; Missiaen *et al.* 2001). Collectively these data demonstrate that sarcoplasmic calcium uptake via the SERCA pump and release via RyR and $InsP_3R$ channels are required for spontaneous propagating ASM Ca^{2+}_i waves and consequent peristalsis.

3.4 Discussion

Postnatal ASM function is under study due to its contribution to the morbidity of asthma. Now prenatal ASM activity is subject to increasing

scrutiny because of accumulating evidence that prenatal airway peristalsis (AP) regulates early lung growth (Jesudason *et al.* 2005). Altering either AP frequency or lung growth yields parallel changes in the other (Jesudason *et al.* 2005). Taking a specific example, nifedipine (L-type Ca^{2+} antagonist) not only abolishes AP (McCray 1993; Sparrow *et al.* 1994) but also inhibits lung morphogenesis and pulmonary cell proliferation *in vitro* (Roman 1995; Jesudason *et al.* 2005). Moreover, transgenic pulmonary epithelial expression of an inhibitor of the Ca^{2+}-binding protein calmodulin disrupts lung morphogenesis *in vivo* (Wang *et al.* 1996). Given these observations, we postulated that $Ca^{2+}{}_i$ signalling represents a promising mechanistic link between AP and lung growth.

3.4.1 Novel in-situ measurement of $Ca^{2+}{}_i$ in whole lung explants

We report the first demonstration of prenatal pulmonary $Ca^{2+}{}_i$ waves, determination of their spatiotemporal characteristics, and their relationship to consequent peristaltic airway contraction. We achieved this technically exacting task by Ca^{2+}-sensitive indicator loading of whole embryonic lung (rather than single cell preparations). Given that AP involves the entire airway, whole organ $Ca^{2+}{}_i$ imaging has been invaluable. We examined $Ca^{2+}{}_i$ waves with confocal imaging to measure spatiotemporal propagation, and photometric techniques for extended measurements and pharmacologic manipulation. Finding both techniques

yielded similar Ca^{2+}_i wave morphology reinforces the validity of our approach.

3.4.2 Airway peristalsis is underpinned by spontaneous Ca^{2+}_i waves

Using high-power magnification, we provide the first evidence that prenatal pulmonary Ca^{2+}_i waves propagate through typically arranged ASM cells rather than epithelium. Our data show that Ca^{2+}_i waves are transmitted via cells whose longitudinal axis is perpendicular to the airway. Furthermore the recordings demonstrate that these same cells then rapidly and invariably contract. Smooth muscle α-actin immunohistochemistry confirms that these cells are arranged in a typical circular fashion around the airway and are indeed ASM (Sparrow *et al.* 2003). Together this strongly indicates that ASM Ca^{2+}_i wave propagation causes AP.

3.4.3 Ca^{2+}_i waves are probably action potential-mediated

Calcium-dependent action potentials have been documented in a wide variety of smooth muscle (Duthie 1974; Weiss *et al.* 2006; Young 2007; Huizinga *et al.* 2009). Their unequivocal demonstration requires micro-electrode recording. However, small preparations such as embryonic lung present considerable difficulties: contractile activity readily dislodges micro-electrodes. Addressing this problem by pharmacologic abolition of contractility may simultaneously extinguish Ca^{2+}_i waves. Instead, we can

contend that ASM Ca^{2+}_i waves are likely to be action potential–mediated after demonstrating their following typical features: (*1*) high wave speed (Yamazawa *et al.* 2002; Stevens *et al.* 1999; Hashitani *et al.* 2001), (*2*) capacity for multidirectional propagation, (*3*) characteristic four-phase morphology of transients (Burdyga *et al.* 2002), (*4*) gap junction–dependent propagation (Hashitani *et al.* 2001; Hashitani *et al.* 2004), and (*5*) apparent regulation by membrane potential. Observations that support the latter point include: delaying repolarization with 10 mM TEA increases Ca^{2+}_i wave frequency and amplitude; depolarization with high-K^+ solution entrains a Ca^{2+}_i wave and contractility (data not shown); voltage-gated Ca^{2+} channel activity is required for and regulates ASM Ca^{2+}_i waves.

3.4.4 Ca^{2+}_i wave generation requires extracellular calcium entry

We have also demonstrated key mechanisms for generation and regulation of spontaneous ASM Ca^{2+}_i waves. Initially, we compared the temporal characteristics of ASM Ca^{2+}_i transients at 37°C and 27°C. Consistent with *passive* influx of Ca^{2+}_o, temperature reduction affected neither the early sharp rise in Ca^{2+}_i nor response to high K^+ (Burdyga *et al.* 2002). In contrast, plateau phase, T_{50} and duration at 50% amplitude were significantly prolonged, consistent with a requirement for *active* removal of cytosolic Ca^{2+} (Burdyga *et al.* 2002). These data implicate a plurality of Ca^{2+} transport processes in the generation of airway Ca^{2+}_i transients.

We established that Ca^{2+}_o entry via L-type channels is necessary for, and regulates, spontaneous regenerative ASM Ca^{2+}_i waves. Ca^{2+}_i waves were abolished by removal, and then reinstated by reintroduction of external Ca^{2+}. Abolition of AP by nifedipine was accompanied by cessation of periodic Ca^{2+}_i oscillations. The L-type Ca^{2+} channel agonist Bay-K 8644 increased Ca^{2+}_i wave frequency and baseline Ca^{2+}_i, whereas 'zero Ca^{2+}' solution or nifedipine prevented this.

3.4.5 Ca^{2+}_i wave generation requires intracellular calcium release

However, Ca^{2+}_o influx alone is insufficient for generation of ASM Ca^{2+}_i waves; Ca^{2+} uptake/release from the sarcoplasmic reticulum is required for, and regulates, ASM Ca^{2+}_i waves. Thus, cyclopiazonic acid, which empties the SR (Kosterin *et al.* 1996), abolished spontaneous Ca^{2+}_i waves and peristaltic activity while increasing basal tone. Similar effects have been reported in gravid rat myometria (Taggart *et al.* 1998). Second, inhibiting SR Ca^{2+} release via RyR channels, or $InsP_3R$ channels abolished Ca^{2+}_i wave generation and peristalsis (Hashitani *et al.* 2004; Liu *et al.* 2005a; Liu *et al.* 2005b). Third, we observed initial stimulation and subsequent abolition of Ca^{2+}_i waves when facilitating Ca^{2+}-induced Ca^{2+}_i release with caffeine. This biphasic response may result from activation of not only depolarizing Ca^{2+}-activated chloride channels (with positive feedback and increased contractile frequency), but also large-conductance (BK) Ca^{2+}-

activated K^+ channels (which produce hyperpolarization and cessation of periodic mechanical activity) (Wellman *et al.* 2003; Kotlikoff *et al.* 1998). Because TEA blockade of K_v and BK channels prevented the effects of 1 mM caffeine, the latter mechanism is suggested.

3.4.6 $Ca^{2+}{}_i$ waves may drive lung development

In this first study to demonstrate prenatal pulmonary $Ca^{2+}{}_i$ oscillations, we have provided clear evidence that peristaltic contractions of the prenatal airway are produced by spontaneous, regenerative, temperature-dependent $Ca^{2+}{}_i$ oscillations of myogenic origin that require $Ca^{2+}{}_o$ influx, sarcoplasmic Ca^{2+} uptake, $Ca^{2+}{}_i$ release via RyR and $InsP_3R$ channels, and propagate via ASM cells in a gap junction–dependent manner that is likely to be action potential–mediated. Two striking consequences of these novel findings deserve immediate discussion. First, if as recent data suggest, AP regulates prenatal lung growth (Jesudason *et al.* 2005), then from the present study we can assert that intercellular $Ca^{2+}{}_i$ oscillations in turn regulate antenatal lung development. Ca^{2+} signalling certainly participates in diverse roles ranging from transcriptional regulation and cell cycle kinetics (Berridge 1997) to modulation of cellular tension and contractility. Based on the present findings, we now propose that propagation of intercellular $Ca^{2+}{}_i$ oscillations throughout a complex developing organ may be integral to, and help coordinate, morphogenesis.

Second, our demonstration of regular spontaneous Ca^{2+}_i waves and phasic contractility in embryonic ASM contrasts sharply with infrequent spontaneous Ca^{2+}_i oscillations and tonic contractility in adult ASM (Boyle *et al.* 1992; Bergner *et al.* 2002). The stimulus for transition between ASM phenotypes is unknown. Indeed, although birth may be assumed to mark the phenotypic change, this has not been unequivocally demonstrated. ASM phenotype may be transformed by the same influences that modulate uterine contractility at the onset of labour (Shmygol *et al.* 2007; Young 2007; Wray *et al.* 2008). Alternatively descending neural control may change ASM behaviour: while AP persists beyond structural development of the pulmonary nervous system, our studies show how muscarinic activation and $InsP_3R$-mediated Ca^{2+}_i release could induce tonic contractility. Perhaps muscarinic activation of $InsP_3R$-mediated Ca^{2+}_i release is incomplete prenatally. Developmental maturation of this pathway might then explain the transition between ASM phenotypes. Clearly further investigation of both pre- and postnatal ASM will be required to test these possibilities.

3.5 Conclusions

a) Prenatal airway peristalsis is driven by temperature-sensitive spontaneous regenerative myogenic Ca^{2+}_i oscillations.

b) Ca^{2+}_i waves propagate between individual airway smooth muscle cells coupled via gap junctions.

c) Ca^{2+}_i waves are likely to be action potential–mediated (high wave speed, capacity for multidirectional propagation, characteristic four-phase morphology, gap junction-dependent propagation and apparent regulation by membrane potential).

d) Ca^{2+}_i waves are dependent on not only Ca^{2+}_o entry via L-type voltage-gated channels but also dependent on Ca^{2+}_i stores.

e) If AP regulates lung growth, these findings suggest that ASM Ca^{2+}_i waves may in turn regulate prenatal lung morphogenesis.

f) Future studies are directed to exploring the relationship of Ca^{2+}_i oscillations to lung growth and understanding the differences between pre- and postnatal ASM activity.

Chapter 4

AIRWAY SMOOTH MUSCLE DYSFUNCTION PRECEDES TERATOGENIC CONGENITAL DIAPHRAGMATIC HERNIA AND MAY CONTRIBUTE TO HYPOPLASTIC LUNG MORPHOGENESIS

4.1 Introduction

Fetal interventions are under trial to improve hypoplastic lung function and growth in CDH (Harrison *et al.* 2003; Deprest *et al.* 2005). Despite promising experimental and preliminary clinical data, conclusive evidence to back these interventions is awaited. To optimize such prenatal therapy, a better understanding of the determinants of lung growth is required (Warburton *et al.* 2000).

Normal lung growth is governed by a combination of biochemical and mechanical factors (Hogan 1999; Harding *et al.* 1996). For example, fibroblast growth factor-10 (FGF10) is required for branching morphogenesis and proximodistal pulmonary differentiation, whilst fetal breathing movements, lung liquid-induced stretch and ASM peristalsis appear to modulate pulmonary growth (Harding *et al.* 1996; Jesudason *et al.* 2005; Shannon *et al.* 2004; Bellusci *et al.* 1997). Evidence that FGF-10 is produced by ASM progenitors provides a putative link between biochemical and mechanical stimuli to lung growth and underlines the importance of ASM in lung development (Mailleux *et al.* 2005). ASM undergoes spontaneous peristaltic contractions prenatally in a variety of species including humans (McCray 1993; Schittny *et al.* 2000). This activity is coupled to, and appears to regulate, normal lung growth (Jesudason *et al.* 2005); these peristaltic waves are underpinned by temperature sensitive, gap-junction dependent propagating ASM $Ca^{2+}{}_i$ waves (Featherstone *et al.* 2005). Notably, transgenic pulmonary epithelial

expression of an inhibitor of the Ca^{2+}-binding protein, calmodulin, disrupts lung morphogenesis *in vivo* (Wang *et al.* 1996). If ASM function is important to normal lung growth, one might expect evidence of ASM abnormalities when lung growth is defective. Indeed, in both human and experimental lung hypoplasia ASM-related dysfunction is apparent near term. Human hypoplastic lung exhibits abnormalities of serum response factor (SRF) isoforms (SRFs regulate ASM gene expression) (Yang *et al.* 2000). In the nitrofen model of CDH, ASM hypercontractility is apparent near term (Belik *et al.* 2003). Moreover, survivors of CDH suffer with long-term bronchial hyperreactivity (Boas *et al.* 1996).

We have hypothesized that rather than being the 'appendix of the lung' (Mitzner 2004), ASM helps regulate early lung morphogenesis, e.g., via its interrelationship with FGF-10 production, and also modulates later fetal lung growth, via effects on lung compliance. Certainly when normal neonatal lung is exposed experimentally to chronic positive pressure ventilation, ASM dysfunction (airway hyper-reactivity) emerges in tandem with significant airway remodelling, again linking ASM activity and morphogenesis (Jobe *et al.* 2001). If, therefore ASM plays a key role in regulation of fetal lung compliance and hence growth, it seems likely that abnormal ASM function in hypoplastic fetal lung may not only impair late prenatal growth, but also increase susceptibility to postnatal barotrauma and remodeling.

In the present study we have tested the hypothesis that near term ASM dysfunction seen in hypoplastic CDH lung has its origins not simply in compression of the fetal lung by a visceral hernia, but is apparent from the embryonic stages of hypoplastic lung development (Jesudason 2006; Jesudason *et al.* 2006).

We have used $Ca^{2+}{}_i$ imaging of hypoplastic lung primordia to demonstrate early ASM dysfunction: $Ca^{2+}{}_i$ transients in hypoplastic lung feature prolonged plateau phase, reduced frequency (at certain temperatures) and increased amplitude. Given that we have also shown that hypoplastic lung ASM $Ca^{2+}{}_i$ transients have normal dependence on $Ca^{2+}{}_i$ and $Ca^{2+}{}_o$ and gap-junction mediated propagation, the anomalous temporal characteristics of these $Ca^{2+}{}_i$ transients suggest a key problem in the ASM ion channels / action potential generation.

4.2 Materials and methods

4.2.1 Generation of experimental lung hypoplasia and controls

Nitrofen (2,4-dichloro-4'-nitrodiphenylether) 100mg (Zheijang Chemicals, Hangzhou, China) dissolved in olive oil was gavage fed to timed-pregnant Sprague-Dawley rats (Charles River Ltd, Margate, UK) on day 9.5 of gestation (vaginal plug = day 0, term = day 22.5) to induce embryonic lung hypoplasia by day 13.5 of gestation and left-sided CDH and pulmonary hypoplasia in newborn pups (Kluth *et al.* 1990).

4.2.2 Retrieval of embryonic lung primordia

See section 3.2.1.

4.2.3 Embryonic lung culture

See section 3.2.1

4.2.4 Assessment of viability

See section 3.2.2

4.2.5 Loading lung explants with Ca^{2+}_i sensitive fluophores

See section 3.2.3

4.2.6 Confocal and photometric measurements

See section 3.2.4

4.2.7 Solutions

Unless otherwise stated, lung explants were superfused at 37°C with buffered physiological saline (pH 7.4) containing (mM): 120 NaCl, 5.6 KCl, 0.12 $MgSO_4$, 2 $CaCl_2$, 11.7 glucose, 10.9 HEPES. 'Zero Ca^{2+}' solution used in certain experiments consists of physiological saline with $CaCl_2$ omitted and 2 mM EGTA added. Other additions to standard superfusate that were investigated include: the L-type Ca^{2+} channel antagonist, nifedipine (10 μM); the L-type Ca^{2+} channel agonist, Bay-K 8644 (1 μM); the gap junction uncoupler, 18-β glycyrrhetinic acid (18-

βGA, 40 μM); the K^+ channel antagonist, tetraethylammonium (TEA, 10 mM); the sarcoplasmic reticulum (SR) Ca^{2+}ATPase inhibitor, cyclopiazonic acid (CPA, 20 μM); caffeine (1 mM - 20 mM), to facilitate calcium induced calcium release (CICR) via ryanodine receptors (RyR); ryanodine (20 μM), to inhibit ryanodine receptors; the muscarinic agonist, carbachol (1 μM - 100 μM); 2-aminoethoxy-diphenylborate (2-APB, 50 μM), a putative inhibitor of inositol triphosphate channels ($InsP_3R$); and depolarising high K^+ solution (10 mM - 140 mM). Carbachol and ryanodine were dissolved in distilled water; CPA, 2-APB and 18-βGA were dissolved in dimethylsulfoxide (DMSO), whilst nifedipine and Bay-K 8644 were dissolved in ethanol (EtOH). $Ca^{2+}{}_i$ wave generation and airway contractility were unaffected by applications of vehicle alone (DMSO or ETOH). Ryanodine was obtained from Calbiochem (Merck Biosciences Ltd., Nottingham, UK). Sigma (Poole, Dorset, UK) supplied all other chemicals.

4.2.8 Immunohistochemistry

See section 3.2.6

4.2.9 Statistical analysis

Data processing was performed using Origin 6.0 software (OriginLab Corporation, Northampton, MA, USA). The SPSS v12.0 package (SPSS UK Ltd., Woking, UK) was utilised for statistical analysis. Parametric data

are reported as mean ± SEM and compared using Student's t-test. Non-parametric data are reported as medians (interquartile ranges) and compared with Mann Whitney U test. Statistical significance was taken at $p < 0.05$. Dose response curves were created using Origin Microcal sigmoidal fitting to the experimental points presented as means ± SEM.

4.3 Results

4.3.1 Temporal characteristics of ASM Ca^{2+}_i waves are abnormal in experimental lung hypoplasia

Hypoplastic lung primordia exhibited spontaneous regenerative intercellular Ca^{2+}_i waves similar to those previously demonstrated in control embryonic lungs (Featherstone *et al.* 2005). Confocal imaging of Fluo-4 loaded hypoplastic lungs with low power magnification (4x or 10x) at 37°C, revealed intercellular Ca^{2+}_i waves propagating longitudinally through the principal airways. Similar to control lungs (Featherstone *et al.* 2005), hypoplastic ASM Ca^{2+}_i waves initiated from regions within the trachea, the left or right main airway, or occasionally from two foci simultaneously. High power magnification (60x) revealed the Ca^{2+}_i waves propagated via individual ASM cells, rather than undifferentiated mesenchyme or airway epithelium. Developing ASM cells were identified by their characteristic spindle-shape, immediate sub-epithelial location, the orientation of the cell's long axis perpendicular to the adjacent airway long axis and their smooth muscle actin immunopositivity (data not shown) as

previously described (Featherstone *et al.* 2005). Hypoplastic lung intercellular Ca^{2+}_i waves propagated with an average speed of 241 ± 14 μm/s (n=4, 24 individual Ca^{2+}_i waves); a similar speed to Ca^{2+}_i waves in control lung (219 ± 14 μm/s; n=4, 10 individual Ca^{2+}_i waves) (p = NS). Despite these similarities, the temporal characteristics of hypoplastic lung ASM Ca^{2+}_i transients were altered compared to control ASM Ca^{2+}_i transients at both 37°C and 27°C (Figure 4.1). Hypoplastic lung ASM Ca^{2+}_i transients show characteristic 4-phase morphology: (1) fast phase; (2) slow phase to plateau; (3) plateau phase and (4) relaxation phase. Hypoplastic lungs had an elongation of the plateau phase alone compared to normal control lung (2.45 ± 0.13 sec vs. 1.94 ± 0.15 sec, p = 0.028); this prolongation was accentuated by cooling to 27°C (4.83 ± 0.29 sec vs. 3.32 ± 0.27 sec, p = 0.005) (Table 4.1) and accompanied by a significant reduction in the frequency of Ca^{2+}_i oscillations (0.49 ± 0.04 vs. 0.7 ± 0.06 per minute, p = 0.003) (Table 4.1). The frequency of Ca^{2+}_i oscillations at 37°C did not differ significantly between hypoplastic and normal lungs (0.67 ± 0.06 vs. 0.81 ± 0.06 per minute, p = NS) (Figure 4.1).

4.3.2 Hypoplastic lung ASM Ca^{2+}_i transients require Ca^{2+}_o entry, Ca^{2+}_i release and gap junction mediated propagation

Normal ASM Ca^{2+}_i transients in control lung require (i) extracellular Ca^{2+} (Ca^{2+}_o) entry, (ii) intracellular Ca^{2+} (Ca^{2+}_i) release from the sarcoplasmic (SR) and (iii) propagation (at a speed characteristic of an action potential-

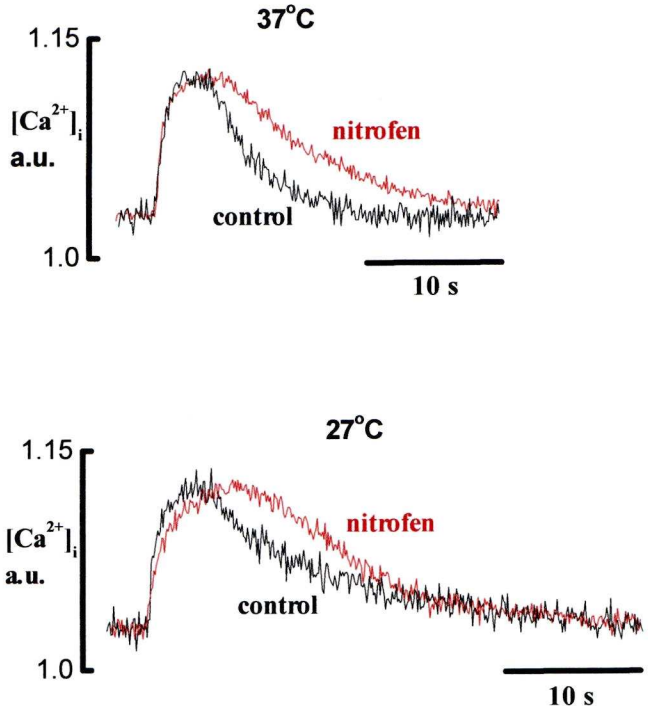

Figure 4.1. $Ca^{2+}{}_i$ transients within hypoplastic lung primordia have altered temporal characteristics. Superimposed normalized traces of typical $Ca^{2+}{}_i$ transients recorded photometrically at 37°C and 27°C in nitrofen hypoplastic lungs (red traces) and control lungs (black traces). Intracellular Ca^{2+} ($Ca^{2+}{}_i$)is shown on the y-axis (arbitrary units).

A

	37°C			27°C		
	Nitrofen (n = 9)	Control (n = 5)	p value	Nitrofen (n = 8)	Control (n = 5)	p value
Fast phase duration (s)	0.55 ± 0.08	0.68 ± 0.05	NS	1.07 ± 0.16	0.92 ± 0.08	NS
Time to 50% amplitude (s)	0.38 ± 0.05	0.45 ± 0.03	NS	0.75 ± 0.12	0.57 ± 0.06	NS
Slow phase duration (s)	1.00 ± 0.12	1.06 ± 0.12	NS	1.62 ± 0.20	1.18 ± 0.17	NS
Plateau duration (s)	2.45 ± 0.13	1.94 ± 0.15	0.028	4.83 ± 0.29	3.32 ± 0.27	0.005
Relaxation half time, T_{50} (s)	2.77 ± 0.31	2.76 ± 0.44	NS	4.52 ±0.38	4.57 ± 0.33	NS
Width at 50% amplitude (s)	6.19 ± 0.33	5.99 ± 0.56	NS	11.31 ± 0.79	9.44 ± 0.54	NS

B

	37°C			27°C		
	Nitrofen (n = 26)	Control (n = 23)	p value	Nitrofen (n = 28)	Control (n = 22)	p value
Frequency per minute	0.67 ± 0.06	0.81 ± 0.06	NS	0.49 ± 0.04	0.7 ± 0.06	0.003

Table 4.1. Ca^{2+}_i transients within hypoplastic lung primordia have altered temporal characteristics. (B) Temporal characteristics of Ca^{2+}_i transients recorded at 37°C and 27°C in hypoplastic and control lung primordia. Data are presented as mean ± SEM. (C) Frequency of Ca^{2+}_i transients recorded at 37°C and 27°C in hypoplastic and control lung primordia. Data are presented as mean ± SEM.

potential-mediated event) via gap junctions (Featherstone *et al.* 2005). Given the observed differences in the temporal characteristics of hypoplastic ASM $Ca^{2+}{}_i$ oscillations, we tested whether hypoplastic lung ASM had different requirements for $Ca^{2+}{}_o$ entry (using 'zero Ca^{2+}' solution, nifedipine, Bay-K 8644 and TEA), $Ca^{2+}{}_i$ release (using caffeine, carbachol, CPA, TEA, ryanodine and 2-APB) and / or gap junction mediated transmission (using 18-β-GA).

There were no gross differences between hypoplastic and normal lungs in the requirements of these three elements of Ca^{2+} signaling for the initiation or regulation of $Ca^{2+}{}_i$ oscillations (Figures 4.2 and 4.3). Thus, in hypoplastic lung, propagating ASM $Ca^{2+}{}_i$ transients (and consequent peristaltic contraction) require (i) external entry of Ca^{2+} via L-type Ca^{2+} channels, (ii) sarcoplasmic reticulum (SR) Ca^{2+} uptake via the SR Ca^{2+}ATPase (SERCA pump), (iii) Ca^{2+} release via ryanodine (RyR) and inositol triphosphate ($InsP_3R$) channels and (iv) functioning gap junctions.

4.3.3 Relative amplitudes of ASM $Ca^{2+}{}_i$ transients in hypoplastic lungs are increased

Observed differences in the morphology and frequency of hypoplastic lung ASM $Ca^{2+}{}_i$ transients are not readily attributable to abnormality of extra- or intracellular Ca^{2+} signalling examined thus far. To further elucidate the observed abnormality of ASM $Ca^{2+}{}_i$ transients in lung hypoplasia, the amplitudes of spontaneous $Ca^{2+}{}_i$ transients were analysed in normal and

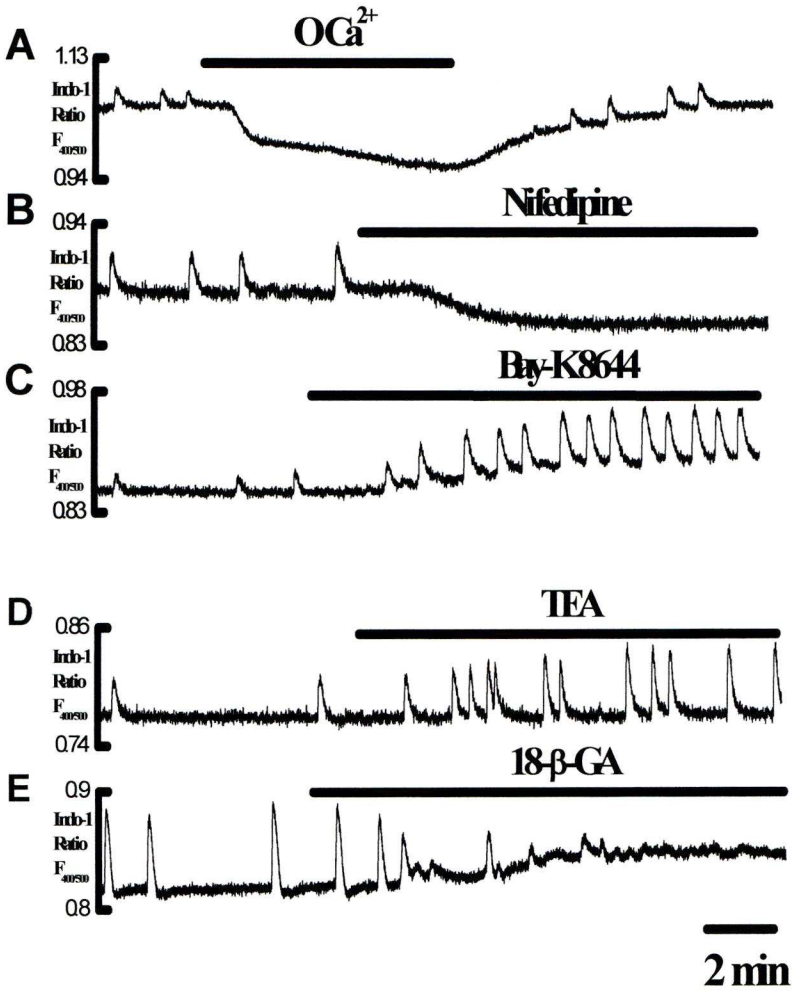

Figure 4.2. Ca^{2+}_i transients within hypoplastic lung primordia are dependent on extracellular Ca^{2+} and gap junction integrity. (A) Exposure of lungs to a Ca^{2+}-free solution decreased baseline Ca^{2+}_i and rapidly abolished both Ca^{2+}_i transients and peristalsis in hypoplastic lung explants. Readmission of Ca^{2+} quickly restored Ca^{2+}_i oscillations and mechanical activity. (B) Nifedipine (L-type Ca^{2+} channel blocker) rapidly abolished spontaneous Ca^{2+}_i transients and peristalsis whilst reducing baseline Ca^{2+}_i. (C) Bay-K 8644 (L-type Ca^{2+} channel agonist) raised Ca^{2+}_i, increased Ca^{2+}_i wave amplitude and frequency. (D) TEA (K^+ channel blocker) increased Ca^{2+}_i wave amplitude and frequency (E) The gap junction uncoupler 18-β-glycyrrhetinic acid abolished both propagating Ca^{2+}_i waves and coordinated peristalsis after an initial brief excitatory phase. Data were obtained at 27^0C.

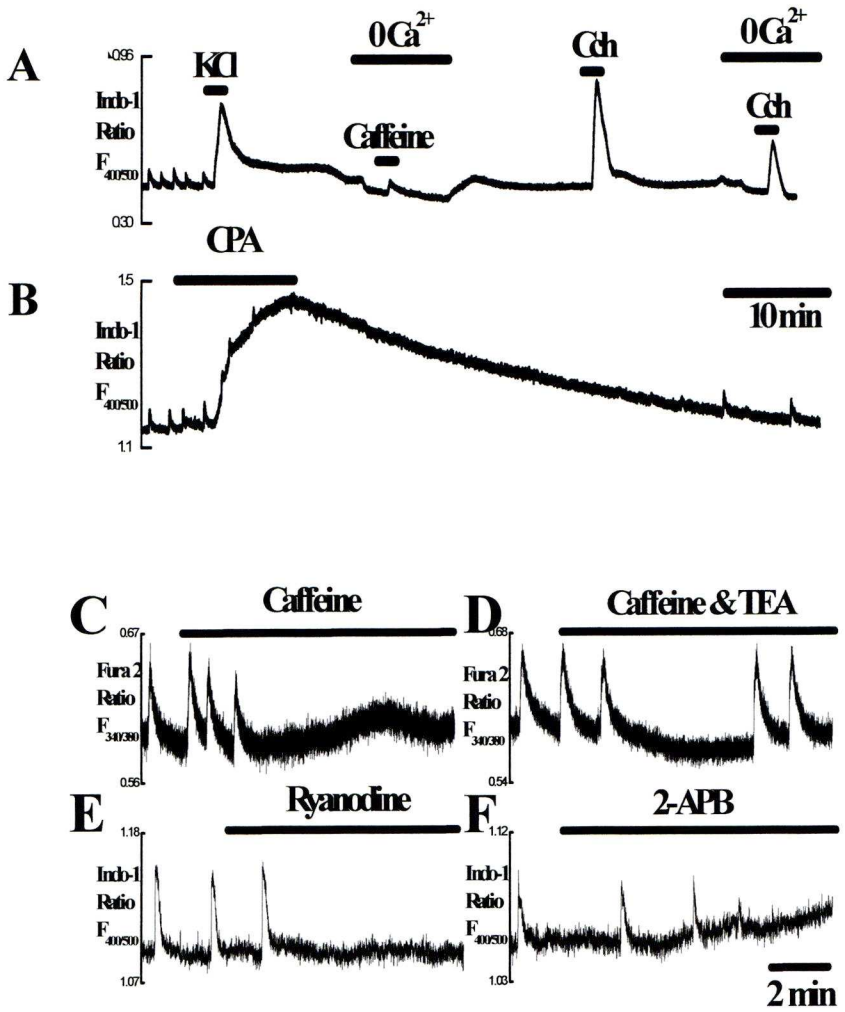

Figure 4.3. Sarcoplasmic Ca^{2+} regulates $Ca^{2+}{}_i$ oscillations in embryonic hypoplastic ASM (A) Caffeine was used to facilitate the Ca^{2+}-induced Ca^{2+} release (CICR) properties of RyR & carbachol was used to activate $InsP_3R$-mediated SR Ca^{2+} release via inositol triphosphate (IP_3) production. Ca^{2+}-free solution was used to eliminate $Ca^{2+}{}_o$ entry. Caffeine (20 mM) transiently increased $Ca^{2+}{}_i$, accompanied by brief tonic airway contraction. Carbachol (100 μM) generated high amplitude $Ca^{2+}{}_i$ transients and sustained tonic contraction. (B) SERCA pump blockade with CPA markedly increased baseline $Ca^{2+}{}_i$ and abolished $Ca^{2+}{}_i$ transients. Phasic mechanical contractions were replaced by tonic airway contraction. (C) Facilitating CICR via caffeine resulted in a biphasic response, which may be due to activation of depolarizing Cl^- channels and/or hyperpolarizing K^+ channels. (D) Blockade of K^+ channels by TEA prevented caffeine's inhibitory action, suggesting that caffeine-induced CICR mediates K^+ channel opening. (E) Inhibiting SR Ca^{2+} release via RyR using ryanodine abolished spontaneous $Ca^{2+}{}_i$ waves and contractility. **(F)** Inhibition of $InsP_3R$ mediated SR Ca^{2+} release using 2-aminoethoxy-diphenylborate (2-APB) increased baseline $Ca^{2+}{}_i$ and gradually abolished both $Ca^{2+}{}_i$ waves and contractility.

hypoplastic lung. When expressed as a % of high K^+ peak (120 mM) or as a % of carbachol peak, Ca^{2+} transient relative amplitudes were significantly increased in hypoplastic lungs at 37°C and at 27°C compared to normal controls (Figure 4.4).

4.3.4 Hypoplastic lung ASM exhibits an enhanced sensitivity to depolarising KCl solution

To investigate potential causes for the abnormal relative amplitude (and frequency) of ASM $Ca^{2+}{}_i$ transients in hypoplastic lung, the dose-response relationship was established for depolarising KCl solutions (10 – 140 mM) and the resulting change of $Ca^{2+}{}_i$ in hypoplastic and control lung primordia. ASM $Ca^{2+}{}_i$ increased in response to one-minute applications of depolarising KCl solution. This dose-response relationship approximated a sigmoidal curve. Hypoplastic lungs exhibited an enhanced sensitivity to depolarising KCl solution than controls (greater elevations of $Ca^{2+}{}_i$ expressed as % of peak Ca^{2+} transient obtained). These differences were significant at 40, 60 and 100 mM KCl (Figure 4.5).

4.3.5 Carbachol increases $Ca^{2+}{}_i$ in similar manner in both normal and hypoplastic lung ASM

The difference in the magnitude of the $Ca^{2+}{}_i$ response to depolarizing KCl suggests that normal and hypoplastic lung may differ in terms of voltage-gated Ca^{2+} channel functioning. To explore whether dysfunctional SR Ca^{2+}

A

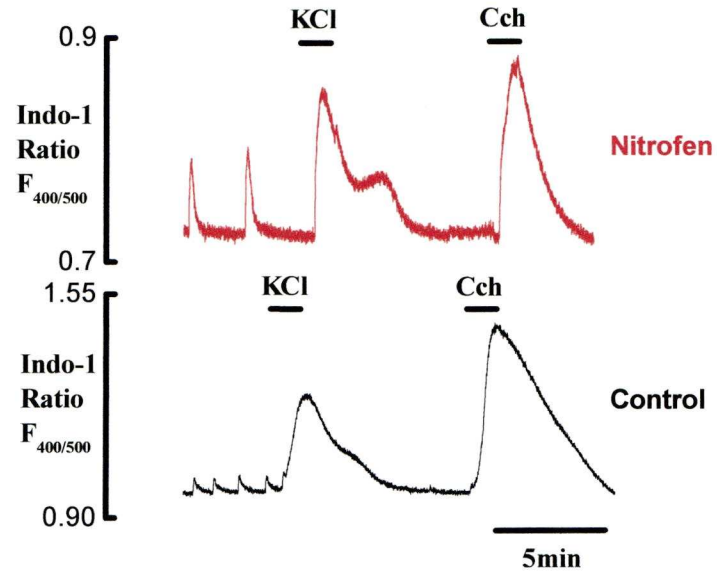

B

		Nitrofen	Control	p value
37^{0}C	KCl	55 ± 5% (n = 18)	27 ± 2% (n = 17)	<0.001
	CCh	49 ± 7% (n = 7)	28 ± 4% (n = 5)	0.043
27^{0}C	KCl	33 ± 4% (n = 16)	21 ± 2% (n = 11)	0.033
	CCh	24 ± 4% (n = 14)	15 ± 2% (n = 7)	NS

Figure 4.4. Amplitudes of Ca^{2+}_i transients in hypoplastic lung primordia are elevated compared with controls. (A) Experimental traces highlighting the amplitude of Ca^{2+}_i transients in nitrofen (upper trace) and control (lower trace) lungs compared to 1 minute control applications of depolarising high-K^+ solution or 100 μM carbachol. Data were obtained at 27°C. (B) Amplitudes of Ca^{2+}_i transients in hypoplastic and control lung primordia recorded at 37^{0}C and 27^{0}C. Data are presented as mean ± SEM.

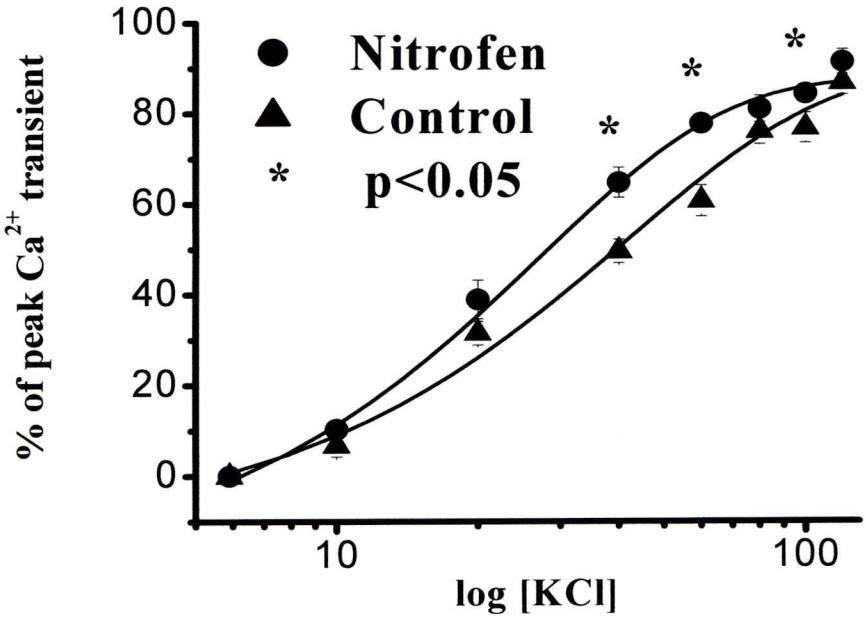

Figure 4.5. Dose-response curve illustrating the activation of the $Ca^{2+}{}_i$ transient by depolarising high-K^+ solution (10 – 140 μM) in hypoplastic lungs (circles) and control lungs (triangles). The dose-response curve was constructed from the phasic component only of the activated $Ca^{2+}{}_i$ transient. The tonic component was inconsistent in hypoplastic (n = 10) and control (n = 12) lungs. Data are presented as mean ± SEM.

release also contributes to increased amplitude of Ca^{2+}_i transients in hypoplastic lung, Ca^{2+}_i responses to carbachol (1, 10 and 100 μM) were compared in normal and in nitrofen-exposed lung. In contrast to applications of depolarising KCl solution, there were no significant differences between hypoplastic and control lung primordia (Figure 4.6).

4.3.6 SR Ca^{2+} release does not differ significantly between hypoplastic and control lung ASM

The role of SR Ca^{2+} release was further investigated in hypoplastic lung Ca^{2+}_i transients by studying the effects of caffeine (facilitating calcium induced calcium release via RyR) and carbachol (via inositol triphosphate receptors ($InsP_3R$)) on Ca^{2+}_i in Ca^{2+}-free solution to eliminate Ca^{2+}_o entry). First, high K^+ solution was applied (to generate a 100% reference for Ca^{2+}_i); then, 2 minutes superfusion with Ca^{2+}-free solution decreased Ca^{2+}_i. Application of 20 mM caffeine in Ca^{2+}-free solution, transiently increased Ca^{2+}_i and produced brief tonic airway contraction without significant difference from normal lung (Figure 4.7). Subsequent application of carbachol (100 μM) in Ca^{2+}-free solution for 1 minute generated high amplitude Ca^{2+}_i transients and sustained tonic contraction. The responses in hypoplastic lung did not differ significantly from normal lung.

Thus, in hypoplastic lung, increased plateau duration, reduced frequency and elevated amplitude of ASM Ca^{2+}_i transients may be due to dysfunction of plasmalemmal ion channels, affecting, e.g., membrane and / or action

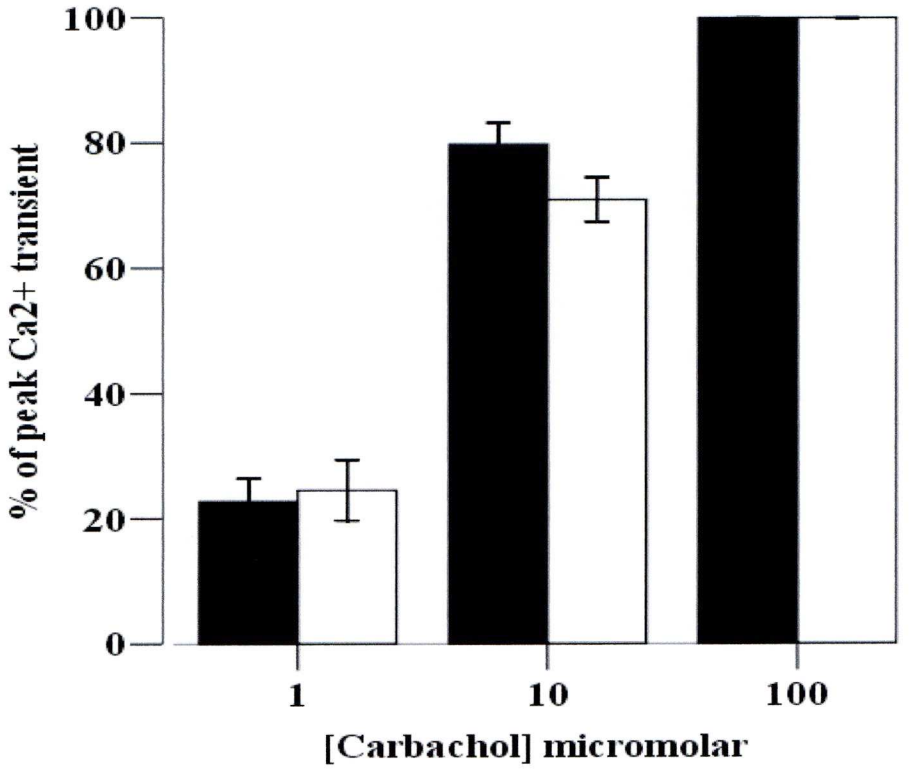

Figure 4.6. Bar chart illustrating the activation of the Ca^{2+} transient by the muscarinic agonist, carbachol (1 – 100 μM), in hypoplastic lungs (white bars; n = 9) and control lungs (black bars; n = 9). Data are presented as mean ± SEM.

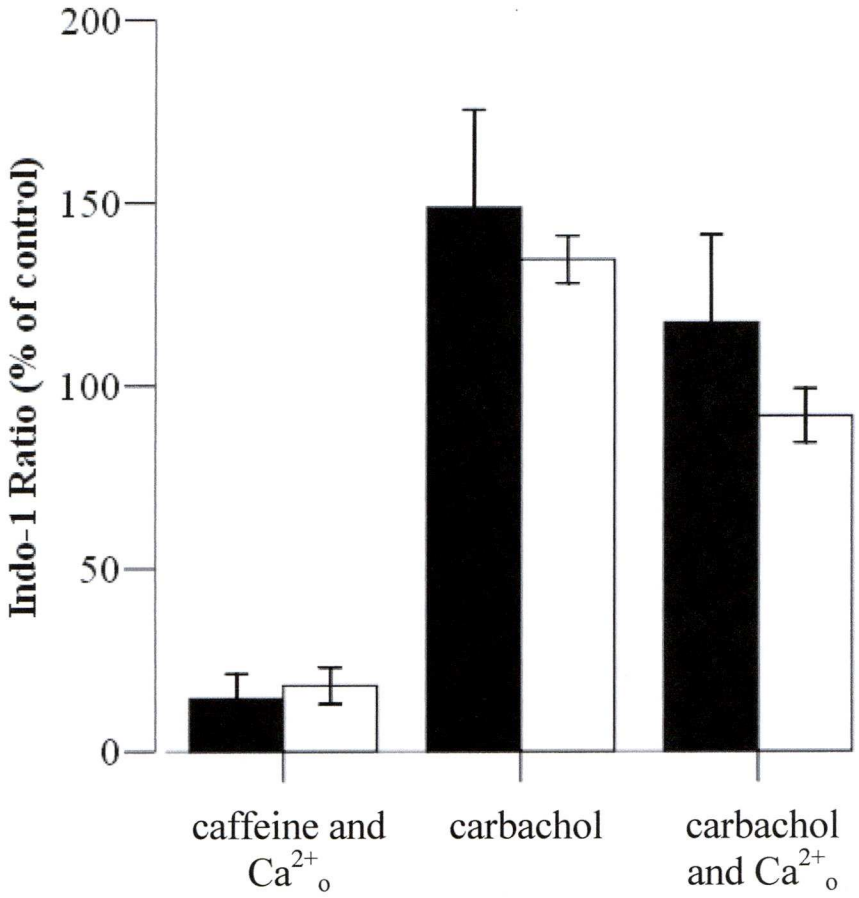

Figure 4.7. Bar chart illustrating the Ca^{2+}_i response to applications of caffeine (20 mM in zero Ca^{2+}_o solution and 2 mM EGTA), carbachol (100 μM) and carbachol (100 μM in zero Ca^{2+}_o solution and 2 mM EGTA). High K^+ application (1 minute) was applied to generate a 100% reference for $[Ca^{2+}]_i$. Hypoplastic lungs are represented by white bars (n = 8); control lungs are represented by black bars (n = 7). Data are resented as mean ± SEM.

potentials.

4.4 Discussion

4.4.1 When do airway smooth muscle abnormalities develop in CDH?

The hypoplastic lung and its susceptibility to barotrauma are key determinants of survival in congenital diaphragmatic hernia (Smith *et al.* 2005). We have postulated that ASM function is important not only in FGF-10 driven early lung morphogenesis but also in compliance-regulated late prenatal lung growth and potentially in regulating remodelling responses to ventilation. This overarching 'smooth muscle' hypothesis is based upon several observations including: (i) ASM progenitors produce FGF10 (Mailleux *et al.* 2005); (ii) ASM activity is coupled to embryonic lung growth *in vitro* (Jesudason *et al.* 2005); (iii) human and experimental lung hypoplasia is associated with perinatal ASM dysfunction together with decreased lung compliance (Yang *et al.* 2000; Belik *et al.* 2003); (iv) neonatal lung responds to chronic positive pressure ventilation with a combination of ASM dysfunction, impaired compliance and airway remodeling (Jobe *et al.* 2001). This study examines the hypothesis that ASM dysfunction observed near-term in human and experimental lung hypoplasia is not merely a late sequel of lung compression by a visceral hernia, but is instead an early indicator of (and perhaps contributor) to

embryonic failure of lung growth.

4.4.2 Lung hypoplasia can be modelled *in vitro*

To test this, we have utilized the nitrofen model of CDH: embryonic lungs exposed *in utero* to nitrofen display hypoplastic growth before the visceral hernia supervenes (Jesudason *et al.* 2000). In contrast to the surgically created lamb model of CDH, nitrofen-induced CDH permits investigation of early pre-CDH events in the developing hypoplastic lung (de Lorimier *et al.* 1967).

4.4.3 Novel in-situ measurement of Ca^{2+}_i in whole hypoplastic lung explants

In order to study early ASM dysfunction in embryonic lung explants, we have used confocal imaging and photometric measurements of Ca^{2+}_i for two reasons. Firstly, novel in-situ Ca^{2+}_i imaging is feasible in whole embryonic lung explants; Ca^{2+}_i transients are known to underpin ASM peristalsis in normal lung explants (Featherstone *et al.* 2005). Secondly, spontaneously contracting cultured lung explants of <0.5mm lengths do not readily lend themselves to measurement of force.

4.4.4 Ca^{2+}_i signalling is abnormal in hypoplastic lungs prior to development of CDH

Using these techniques we have shown that the Ca^{2+}_i transients in

hypoplastic lung exhibit significant abnormalities that together suggest a lesion of ASM plasmalemmal ion channels and /or action potential generation. Furthermore, we have shown that ASM peristalsis in hypoplastic lung is underpinned by spontaneous regenerative $Ca^{2+}{}_i$ waves propagating via gap-junctions that are dependent on not only $Ca^{2+}{}_o$ entry but also $Ca^{2+}{}_i$ release.

Normal and hypoplastic ASM $Ca^{2+}{}_i$ transients appear to be action potential mediated given their characteristic 4-phase morphology, propagation speed and transmission via gap junctions (Hashitani *et al.* 2001; Burdyga *et al.* 2002). Hence, prolongation of the plateau phase of $Ca^{2+}{}_i$ transients at 37^0C and 27^0C in hypoplastic lung ASM is likely to be due to alteration in the action potential (Burdyga *et al.* 2002). Further support for a prolongation of the action potential derives from the observed increase in relative amplitude of the $Ca^{2+}{}_i$ transients in hypoplastic lung (relative to KCl and carbachol induced maxima) (Burdyga *et al.* 2002). Underlying abnormalities of membrane potential and ion channel functioning are also suggested by the significant reduction observed in the frequency of $Ca^{2+}{}_i$ transients in hypoplastic lung at 27^0C (Burdyga *et al.* 2002). Again consistent with an alteration in membrane potential / ion channel functioning, hypoplastic lung exhibited an elevated sensitivity to depolarizing KCl solutions. However, mechanisms controlling initial entry and / or release of Ca^{2+} and its subsequent SR uptake or extrusion from the cell appear unaffected in hypoplastic lung: the rates of rise and relaxation

of the Ca^{2+}_i transients at 37^0C and 27^0C are comparable between normal and hypoplastic lung. Indeed, hypoplastic lung ASM appears to have normal SR activity: Ca^{2+}_i dose-response to carbachol showed no significant difference between hypoplastic lungs and controls, even when Ca^{2+}_o entry was eliminated. Similarly, there was no significant difference in the caffeine response in hypoplastic and control lung primordia. Unequivocal demonstration of the abnormalities of action and / or membrane potential necessitates micro-electrode recording (Burdyga *et al.* 2002). However, the embryonic lung presents considerable difficulties due to its small size and mechanical activity dislodging micro-electrodes. However, in the adult rat ureter preparation, prolongation of the plateau phase of the smooth muscle Ca^{2+}_i transient (by cooling) is similarly accompanied by increase in the amplitude of the Ca^{2+}_i transient and elongation of the action potential plateau phase (Burdyga *et al.* 2002).

4.4.5 Abnormalities of airway smooth muscle function may unify the observed lung hypoplasia and late sequelae (bronchial hyper-reactivity) in CDH

Embryonic nitrofen-exposed lung, therefore, features abnormal Ca^{2+}_i transients that accompany early hypoplasia and precede supervention of the visceral hernia. Since propagating Ca^{2+}_i waves underpin ASM peristalsis (Featherstone *et al.* 2005), this indicates that ASM function is already abnormal at the embryonic stages of hypoplastic lung development. The

latter conclusion is significant given that a) ASM progenitors furnish the FGF10 required for early branching morphogenesis; and b) nitrofen-exposed lung primordia exhibit branching abnormalities in tandem with FGF10-deficiency (Mailleux *et al.* 2005; Acosta *et al.* 2001). Together, this supports the thesis that ASM contributes to early FGF10-driven lung morphogenesis and that this relationship is disrupted prior to CDH supervening. ASM dysfunction also persists after CDH develops: nitrofen-exposed fetal lungs display increased ASM contractility and human CDH survivors manifest reactive airways disease (Belik *et al.* 2003; Boas *et al.* 1996). Therefore, the embryonic ASM dysfunction we have shown (increased duration and amplitude of embryonic ASM $Ca^{2+}{}_i$ transients) may underlie, in part, later post-CDH ASM abnormalities (airway hyper-reactivity).

Having shown that early ASM dysfunction accompanies embryonic growth failure and is consistent with late ASM lesions, it is worth considering the mechanisms whereby ASM dysfunction might contribute to impaired lung growth. The 'smooth muscle hypothesis' postulates that ASM abnormalities may impair not only embryonic lung growth (related to FGF10-producing ASM progenitors) but also fetal pulmonary growth (via dysregulated lung compliance) (Jesudason 2006). This latter role of ASM dysfunction in fetal and postnatal lung development merits review. ASM contractility generates tension in the airway wall (Schittny *et al.* 2000). It is reasonable to assume that such changes are accompanied by alterations in

intraluminal pressure. The latter is known to influence several aspects of lung cell and organ growth (Harding *et al.* 1996; Xu *et al.* 1998). Hence ASM activity can plausibly affect lung growth by virtue of its wider mechanical effects on lung compliance. Experimental support for this concept emerges from observation that *in vitro* inhibition / stimulation of Rho-associated kinase results in decreased / increased lung growth respectively (presumably via modulation of cytoskeletal tension) (Moore *et al.* 2005). Certainly if unrecognised ASM dysfunction impairs compliance of hypoplastic lung, one might expect more unpredictable results from prenatal tracheal occlusion (Heerema *et al.* 2003). Indeed the results of tracheal occlusion in previously normal fetal lung may be less easily extrapolated to effects in hypoplastic lung. Moreover the reported benefits of dynamic rather than static tracheal occlusion may arise in part due to simulation of the pressure waves generated by ASM peristalsis (Nelson *et al.* 2005). Finally, if ASM participates in the regulation of neonatal lung compliance, observed ASM dysfunction may help explain the increased susceptibility of the hypoplastic lung to barotrauma (Wung *et al.* 1995).

4.5 Conclusions

a) ASM $Ca^{2+}{}_i$ transients in hypoplastic lung primordia exhibit abnormal temporal characteristics compared to control embryonic lungs. These differences may be due to altered expression of membrane

ion channels and / or underlying action potentials.

b) ASM Ca^{2+}_i transients in hypoplastic lung primordia depend upon Ca^{2+}_o entry and Ca^{2+}_i release.

c) ASM Ca^{2+}_i transients in hypoplastic lung primordia propagate via smooth muscle cells coupled by gap junctions.

d) ASM Ca^{2+}_i transients in hypoplastic lung are likely to be action potential–mediated.

e) The observed abnormalities precede CDH and yet are congruent with ASM dysfunction observed perinatally. We have proposed that such early ASM lesions may be important to defective lung development not only in embryogenesis but also in late fetal life and following postnatal ventilation.

f) Testing this 'smooth muscle hypothesis' may therefore help us to explain the survival benefits of limiting postnatal ventilatory pressures and emphasise the need for similar consideration during tracheal occlusion in human fetuses with CDH.

Chapter 5

CYCLOPIAZONIC ACID REVERSIBLY ABOLISHES LUNG BRANCHING MORPHOGENESIS AND AIRWAY PERISTALSIS

5.1 Introduction

CDH retains high mortality due to pulmonary hypoplasia and pulmonary hypertension (Smith *et al.* 2005). Normal lung development requires a variety of growth factors and a number of mechanical factors. Airway peristalsis (AP) is one such mechanical factor; it has been recently reported to be coupled to lung growth *in vitro* (Jesudason *et al.* 2005).

We have already shown that spontaneous regenerative propagating $Ca^{2+}{}_i$ waves underpin mechanical airway contraction in developing lungs (Featherstone *et al.* 2005) and that these $Ca^{2+}{}_i$ waves were abnormal in an experimental model of CDH (Featherstone *et al.* 2006). ASM $Ca^{2+}{}_i$ waves underpinning spontaneous mechanical airway contraction (AP) therefore appear to influence and regulate normal lung development. Spontaneous ASM $Ca^{2+}{}_i$ waves require $Ca^{2+}{}_o$ entry and $Ca^{2+}{}_i$ release (Featherstone *et al.* 2005). Culturing lung explants in the presence of nifedipine (an L-type Ca^{2+} channel blocker that irreversibly inhibits $Ca^{2+}{}_o$ entry) results in lung hypoplasia but does not affect branching (Roman, 1995; Jesudason *et al.*, 2005).

Given that spontaneous $Ca^{2+}{}_i$ ASM waves require both $Ca^{2+}{}_o$ entry and $Ca^{2+}{}_i$ release, in these studies, we abolished sarcoplasmic $Ca^{2+}{}_i$ reuptake using cyclopiazonic acid (CPA), a compound isolated from the fungus *Penicillium cyclopium* (Holzapfel, 1968). We show CPA completely and reversibly abolished lung branching morphogenesis. Sarcoplasmic Ca^{2+}

appears essential to lung branching morphogenesis (whether due to release via ryanodine (RyR) or inositol triphosphate ($InsP_3R$) channels or re-uptake via the SR Ca^{2+}-ATPase (SERCA pump)).

5.2 Materials and methods

5.2.1 Retrieval of embryonic lung primordia

See section 3.2.1

5.2.2 Embryonic lung culture

Lung rudiments were positioned on translucent polytetrafluorethylene membrane culture-dish inserts (Millicell, Millipore Corp, Bedford, MA) with serum-free culture media incorporating penicillin (100 IU/ml) and streptomycin (100 μg/ml; GibcoBRL, Life Technologies, Paisley, UK). Lung primordia were incubated at 37°C in 5% CO_2 for periods up to 78 hours ± CPA (20 μM). Additionally, some explants were exposed to CPA after 30 or 54 hours *in vitro*; others were 'rescued' from CPA exposure after 30 or 54 hours.

5.2.3 Assessment of viability

See section 3.2.2

5.2.4 Morphometric analysis of *in vitro* lung development

Lung explants were photographed at 0, 30, 54 and 78 hours *in vitro* to track growth and branching morphogenesis. Photographs were scanned into a microcomputer and Scion Image Beta 4.03 software (Scion Corporation, Frederick, Maryland, USA) was used to trace the epithelial contour from each image in order to calculate the individual lung epithelial area and perimeter. The number of terminal buds was also recorded at each time point.

5.2.5 Immunohistochemistry

See section 3.2.6

5.2.6 Statistical analysis

See section 3.2.7

5.3 Results

5.3.1 CPA inhibits branching morphogenesis in embryonic lung explants

Embryonic rat (n=8) and mouse lungs (n=8) cultured in the presence of CPA exhibited inhibition of lung branching morphogenesis (Figures 5.1 and 5.2). Lung morphometry performed on rat lungs (Figure 5.3) showed similar areas at 0 h (0.34 ± 0.01 mm^2 vs. 0.35 ± 0.01 mm^2) but significantly reduced specimen area at 30 h (0.66 ± 0.03 mm^2 vs. 0.39 ± 0.01 mm^2), 54

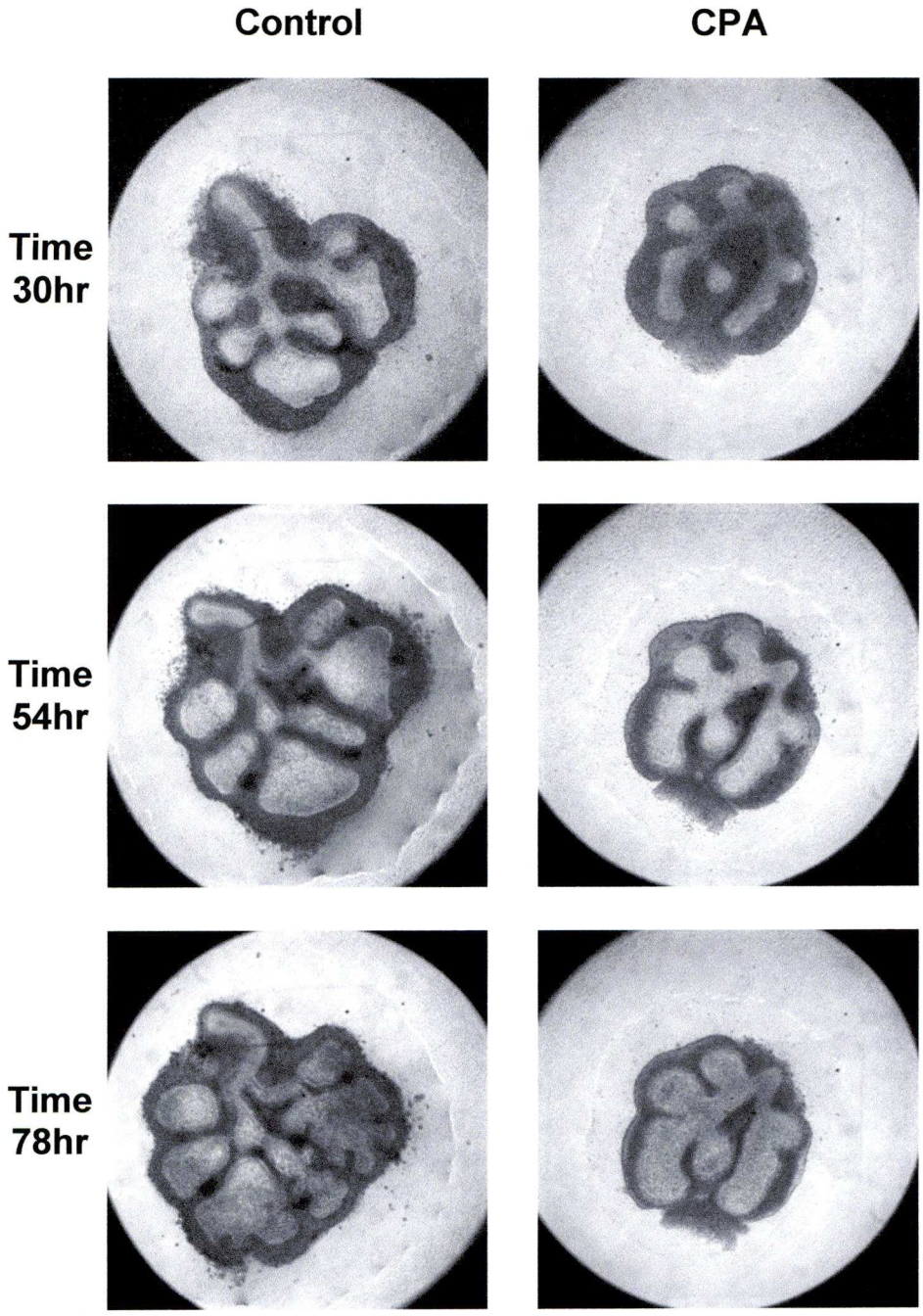

Figure 5.1. Effect of cyclopiazonic acid (CPA) on the morphological development of embryonic rat lung primordia *in vitro*. Photomicrographs were taken at 30, 54 and 78 hours. CPA abolished branching morphogenesis.

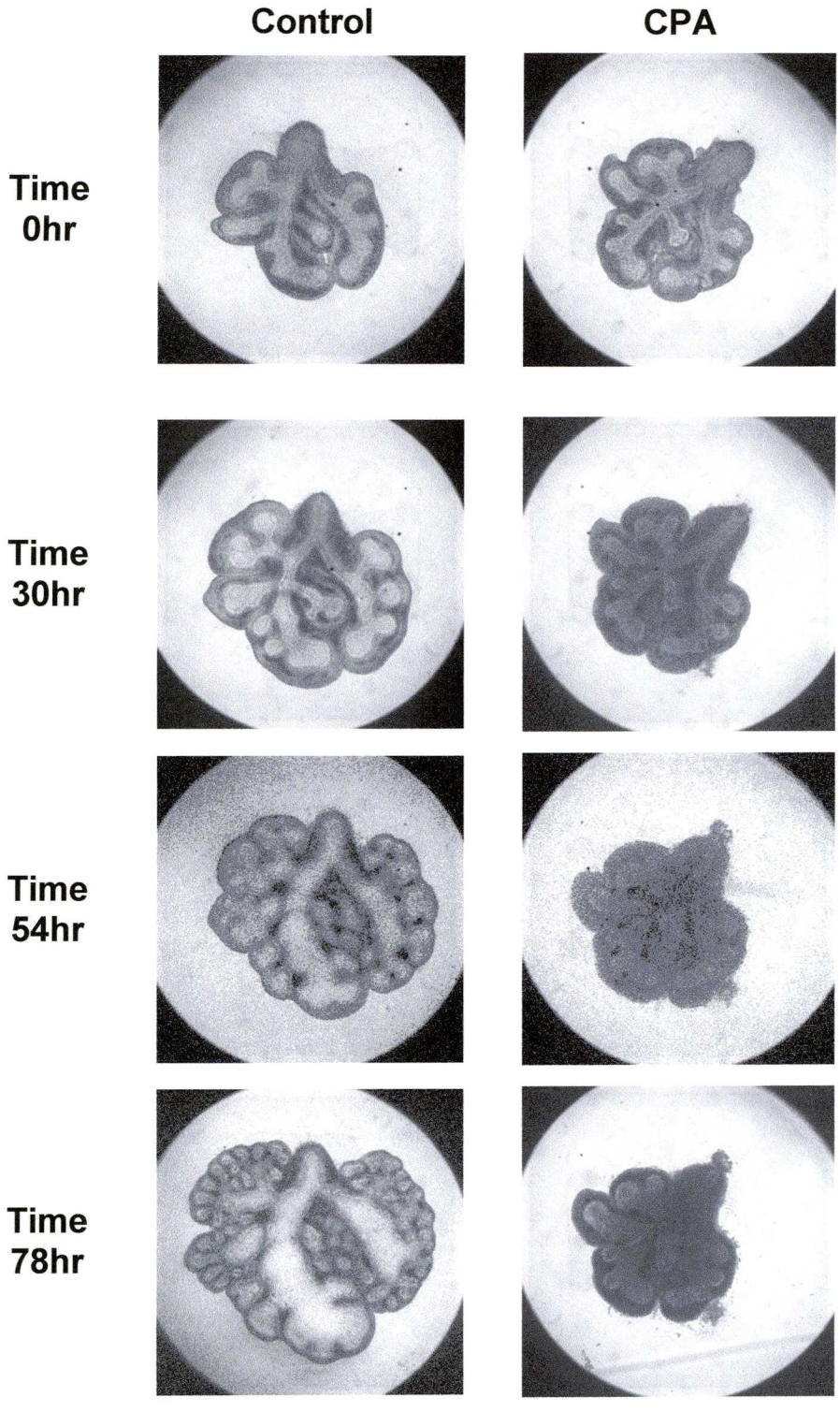

Figure 5.2. Effect of cyclopiazonic acid (CPA) on the morphological development of embryonic mouse lung primordia *in vitro*. Photomicrographs were taken at 0, 30, 54 and 78 hours. CPA abolished branching morphogenesis.

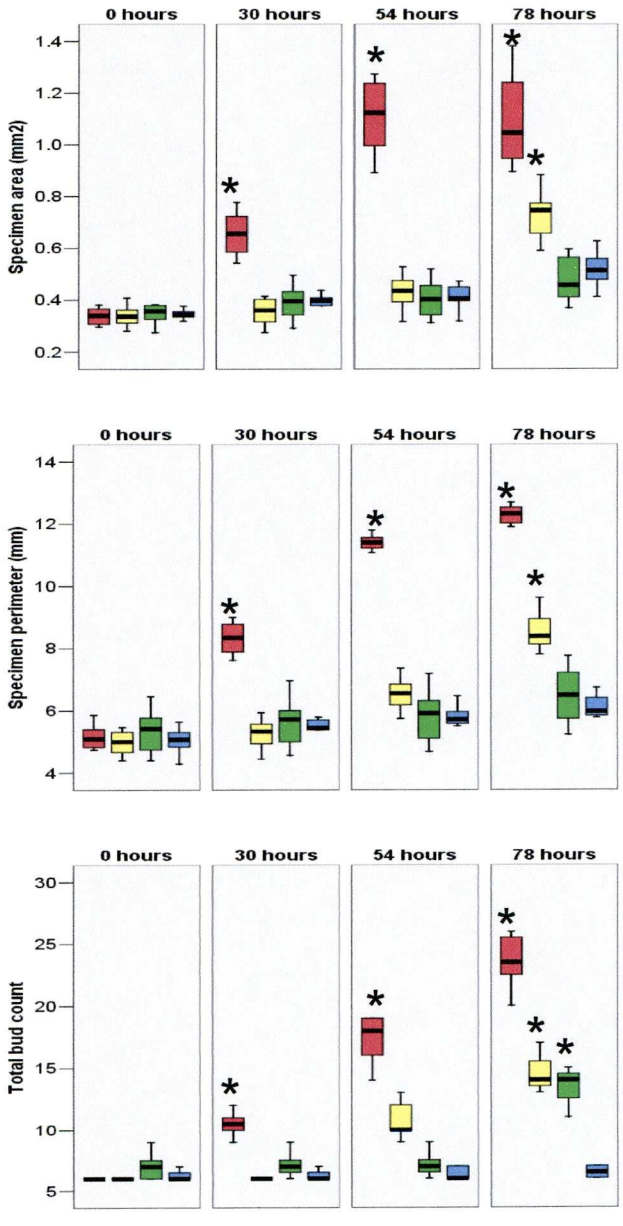

Figure 5.3. Box plots illustrating the morphometric data for control rat lungs cultured in serum-free medium (red); with rat lungs 'rescued' from CPA (20 μM) at 30 hours *in vitro* (yellow); with rat lungs 'rescued' from CPA (20 μM) at 54 hours *in vitro* (green); and rat lungs exposed to CPA (20 μM) for up to 78 hours (blue). Data are shown at 0, 30, 54 and 78 hours. Bars represent medians and boxes' interquartile range. * Significant increase compared to lungs cultured in the presence of CPA for 78 hours ($P < 0.001$).

h (1.11 ± 0.06 mm^2 vs. 0.41 ± 0.02 mm^2) and 78 h (1.09 ± 0.06 mm^2 vs. 0.52 ± 0.02 mm^2) ($p < 0.001$). Likewise, specimen perimeter whilst the same at 0 h (5.16 ± 0.14 mm vs. 5.05 ± 0.14 mm) was significantly reduced at 30 h (8.33 ± 0.18 mm vs. 5.47 ± 0.17 mm), 54 h (11.34 ± 0.15 mm vs. 5.69 ± 0.20 mm) and 78 h (12.04 ± 0.32 mm vs. 6.00 ± 0.20 mm) ($p < 0.001$). Total bud count was also abolished at 30 h (10.50 ± 0.33 vs. 6.25 ± 0.16), 54 h (17.29 ± 0.78 vs. 6.38 ± 0.18) and 78 h (24.25 ± 1.16 vs. 6.50 ± 0.19) ($p < 0.001$).

5.3.2 Lung explants removed from CPA resume branching

Embryonic rat lung explants were 'rescued' from CPA exposure at 30 and 54 hours *in vitro.* Return to normal culture medium resulted in a return of branching morphogenesis; there was an increase in the specimen areas, perimeters and total bud counts (Figures 5.3 and 5.4).

'Rescue' at 30 hours increased ($p < 0.001$) specimen area, perimeter and bud count at 78 hours compared to lungs cultured in the continued presence of CPA. Specimen area was 0.73 ± 0.03 mm^2 vs. 0.52 ± 0.02 mm^2; specimen perimeter was 8.54 ± 0.21 mm vs. 6.00 ± 0.2 mm; and total bud count was 14.50 ± 0.50 vs. 6.50 ± 0.19. In a similar manner, 'rescue' at 54 hours *in vitro*, resulted in a statistically significant increase ($p < 0.001$) in total bud count at 78 hours compared with lungs cultured in the continued presence of CPA. Total bud count was 8.78 ± 0.60 vs. 6.50 ± 0.19.

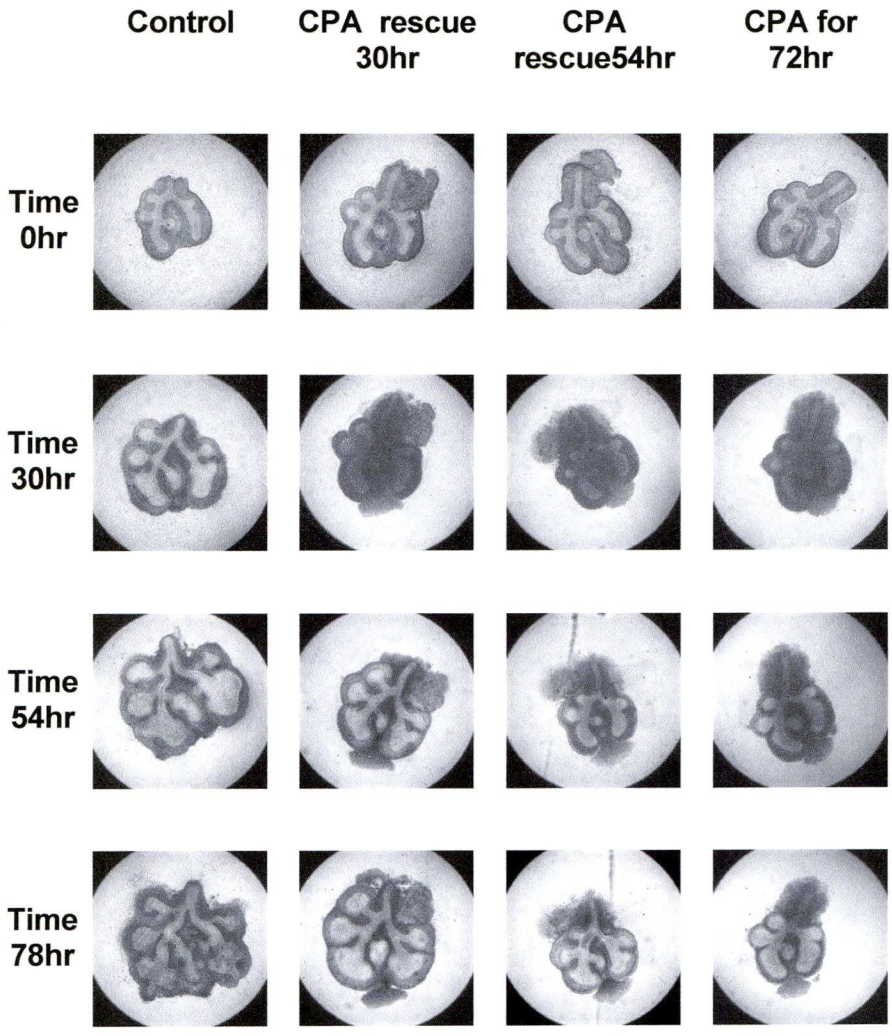

Figure 5.4. Effect of 'rescuing' rat lung explants from cyclopiazonic acid (CPA) on the morphological development of embryonic rat lung primordia *in vitro*. Explants were 'rescued' at 30 or 54 hours. 'Rescue' from CPA resulted in re-establishment of branching morphogenesis.

5.3.3 CPA inhibits branching morphogenesis if added to lung explants at later time points in culture

To determine whether CPA application would abolish or reduce branching morphogenesis at other time points in culture, we changed the culture medium to one containing CPA (20 μM) at 30 hours (n = 8) or 54 hours (n = 8) *in vitro*. As before, addition of CPA resulted in abolition of branching morphogenesis in embryonic rat lungs (Figure 5.5 and 5.6). When CPA was added at 30 hours, the total bud count did not increase significantly with subsequent culture (54 hours: 18.13 ± 0.91 buds; 78 hours: 20.25 ± 1.10 buds (p = NS)). When lung explants were cultured in standard medium, there was a significant increase in total bud count between 54 and 78 hours *in vitro* (54 hours: 17.29 ± 0.78 buds; 78 hours: 24.25 ± 1.16 buds ($P < 0.001$)). Similar data were obtained with the addition of CPA to the culture medium at 54 hours *in vitro*.

5.3.4 CPA may delay morphological development

Our provisional data appears to suggest that CPA exposure delayed morphological development; tracheal cartilage rings were clearly evident upon light transmitted images of lung explants cultured in standard medium for 78 hours, however, they failed to develop in lung explants cultured in the presence of CPA (Figure 5.7).

Given that CPA inhibited branching morphogenesis and delayed morphological development in lung cultures, we considered that its

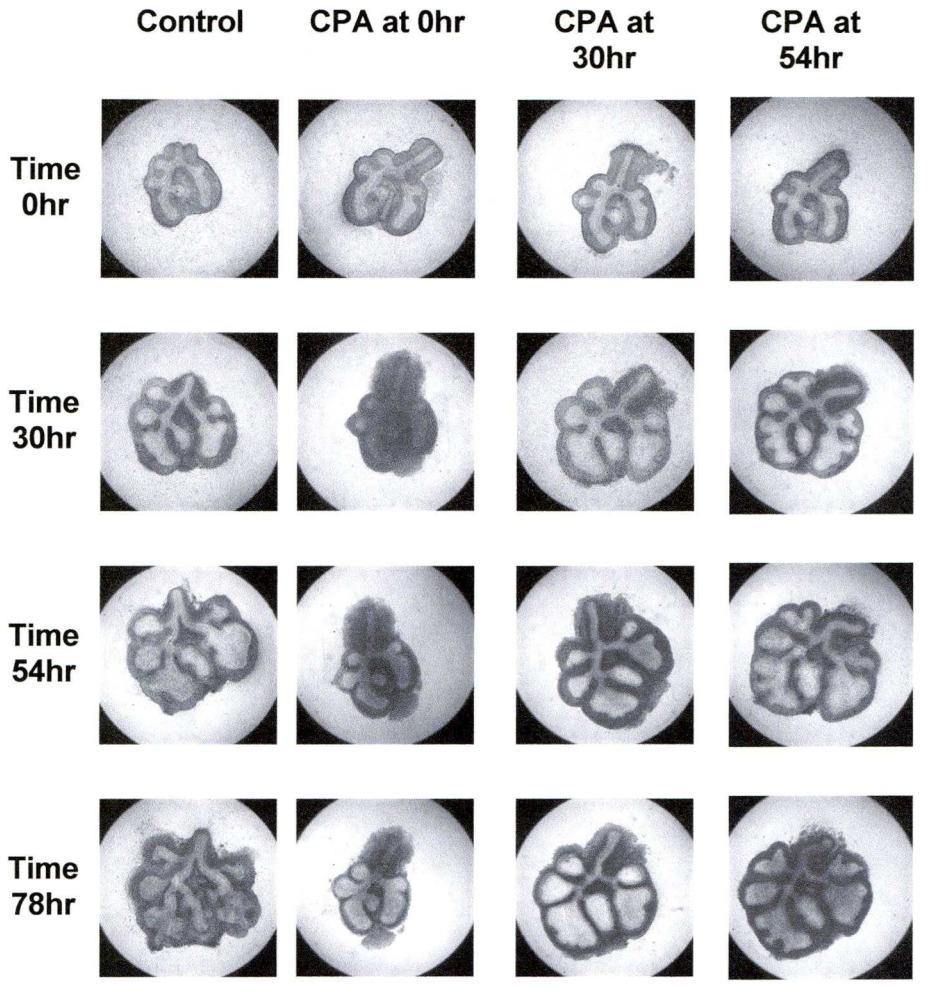

Figure 5.5. Effect of adding cyclopiazonic acid (CPA) at later stages of culture upon the morphological development of rat lung primordia *in vitro*. Explants were exposed to cyclopiazonic acid at 0, 30 or 54 hours. Addition of cyclopiazonic acid to the culture medium resulted in abolition of branching morphogenesis.

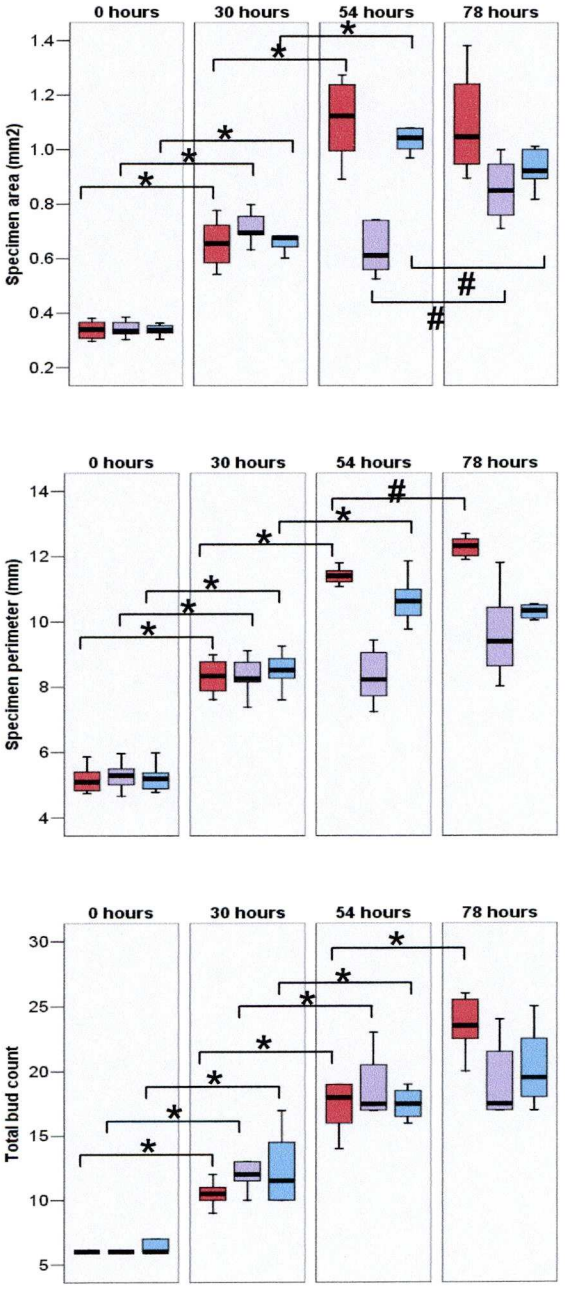

Figure 5.6. Box plots illustrating the morphometric data for control lungs cultured in serum-free medium (red); with cyclopiazonic acid (20 μM) added at 30 hours *in vitro* (cyan); and cyclopiazonic acid (20 μM) added at 54 hours *in vitro* (light blue). Data are shown at 0, 30, 54 and 78 hours. Bars represent medians and boxes' interquartile range. Significant increase (*$P < 0.001$, $^{\#}$ $P < 0.05$) compared with previous 24 hours.

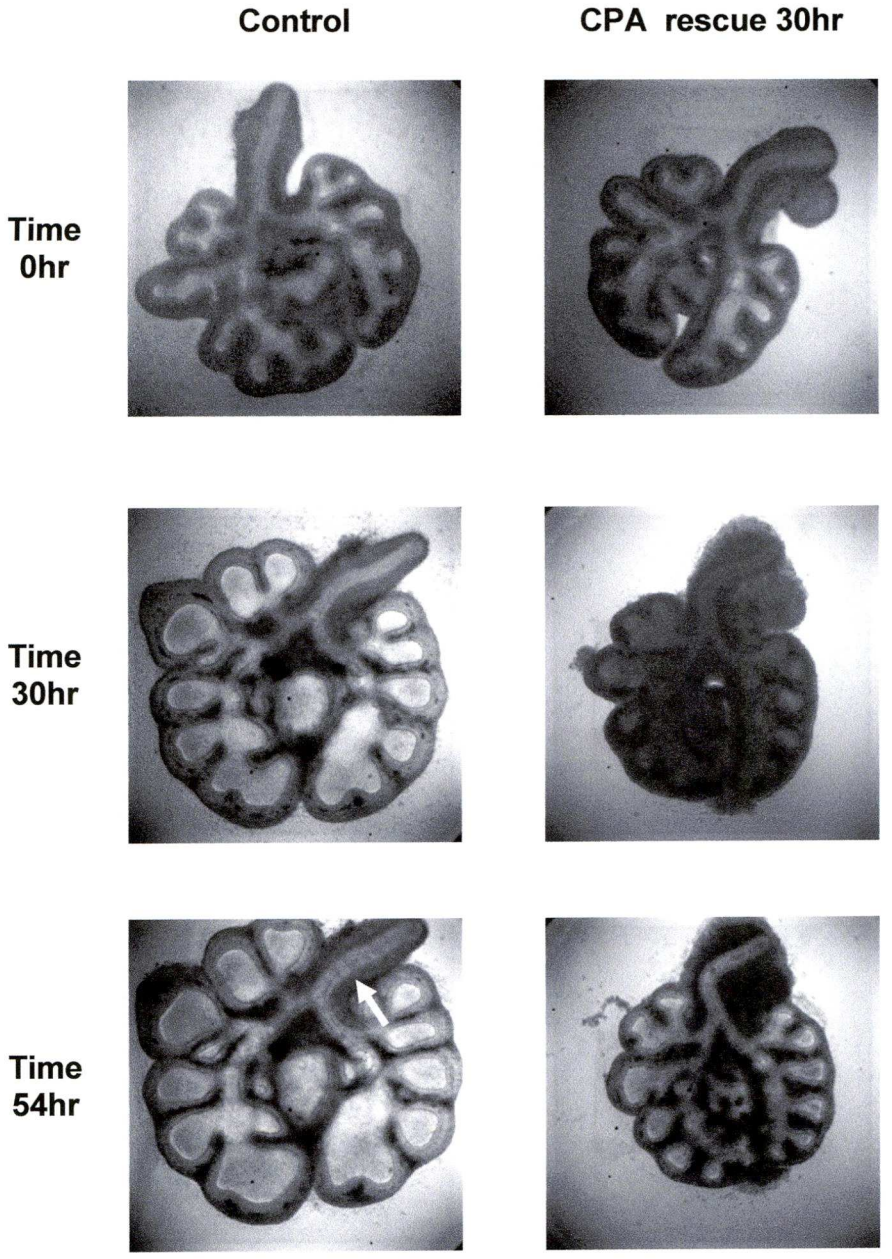

Figure 5.7. Effect of CPA acid (20 μM) on the ontological development of embryonic rat lungs *in vitro*. At 54 hours, control lungs display collagen rings orientated parallel to the long axis of the trachea (arrow). However, collagen rings are not apparent in those lungs exposed to CPA for 30 hours and then 'rescued'.

application *in vitro* may also result in delayed physiological maturation. ASM has been reported to be developmentally regulated (Jesudason *et al.* 2005, Jesudason *et al.* 2006). At 30 h, spontaneous contractions primarily originated from the second bronchial division of the right lung (R-waves) and outnumbered those from the left lung (L-waves), which in-turn outnumbered those from the trachea (T-waves). By 54 h and 72 h *in vitro*, T-waves peter out in normal lung i.e. proximal ASM (T-waves) become quiescent.

Consequently, quantification of the origin of contractile waves at 54 or 78 hours was undertaken in specimens cultured in the presence (n = 8) of CPA for 30 hours and then 'rescued' and in lungs cultured in standard media (n = 7). As previously reported (Jesudason *et al.* 2005, Jesudason et al. 2006), there was a decline in 'T-wave' activity in control specimens with time (Figure 5.8). However, there was a persistence of 'T-waves' in lungs cultured in the presence of CPA. This difference, however, did not reach statistical significance (P = NS).

5.3.5 α-SMA expression is reduced after CPA application

As CPA inhibited both peristalsis and morphological development of the embryonic lung, we wanted to determine its effect on airway smooth muscle ontogeny. We cultured rat lungs in standard culture solution with (n = 8) or without CPA (n = 8). After 72 h in culture, lungs were fixed in paraformaldehyde and processed for α-SMA immunohistochemistry. This

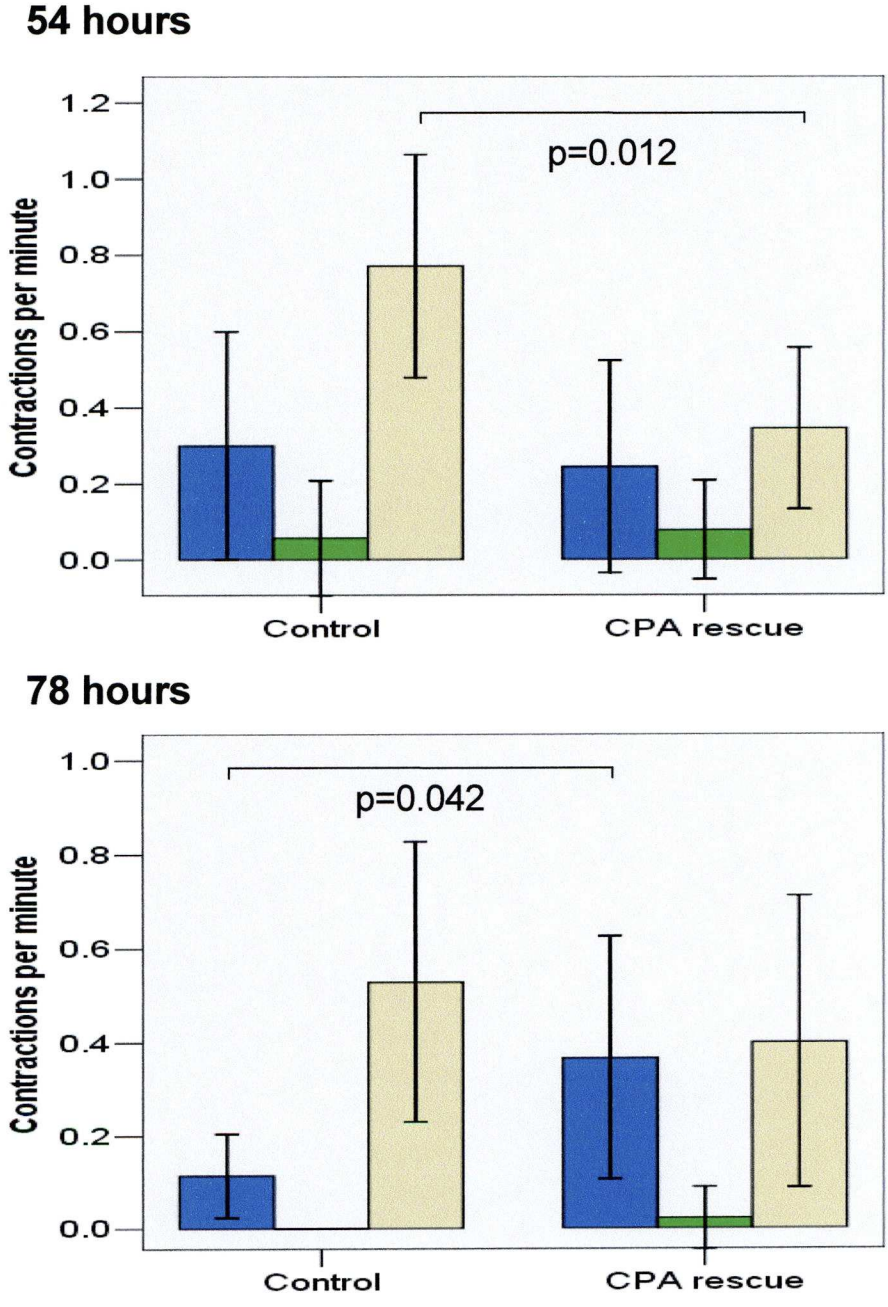

Figure 5.8. Changing distribution of the origin of spontaneous contractile waves with development. Data are shown for waves (rates of contraction per minute) originating in the left lung (blue), trachea (green, and right lung (light brown) at 54 hours (top) and 78 hours (bottom) *in vitro*. Control rat lungs were cultured for 78 hours in standard medium. 'CPA rescue' rat lungs were cultured in the presence of CPA until 30 hours and then returned to standard medium. Bars represent means ± SD.

showed that compared to normal lung explants, pulmonary α-SMA expression was reduced by culture in the presence of CPA (Figure 5.9).

5.3.6 CPA reduces cell proliferation in cultured lung

Since culturing lungs in the presence of CPA resulted in inhibition of branching morphogenesis, we were interested to determine whether its effects were in part due to inhibition of proliferation.

Brdu (5-bromo-2'-deoxyuridine) pulse labelling was performed to assess cellular proliferation. CPA application resulted in a statistically significant reduction in cells labelling positive for Brdu at 24 hours in the end buds ($p < 0.001$) and airway ($p = 0.009$). At 48 hours, although there was a reduction in the proportion of cells labelling positively for Brdu in CPA treated lungs, the differences observed were not statistically significant (p = NS). Figures 5.10 and 5.11 show the results. The results suggest that, *in vitro*, CPA suppresses cellular proliferation at 24 hours, but not at 48 hours.

5.4 Discussion

CDH retains high morbidity and mortality; lung hypoplasia and pulmonary hypertension are primarily responsible. To understand lung hypoplasia and potential therapies to 'rescue' the CDH lung, it is first necessary to appreciate the processes regulating normal lung development.

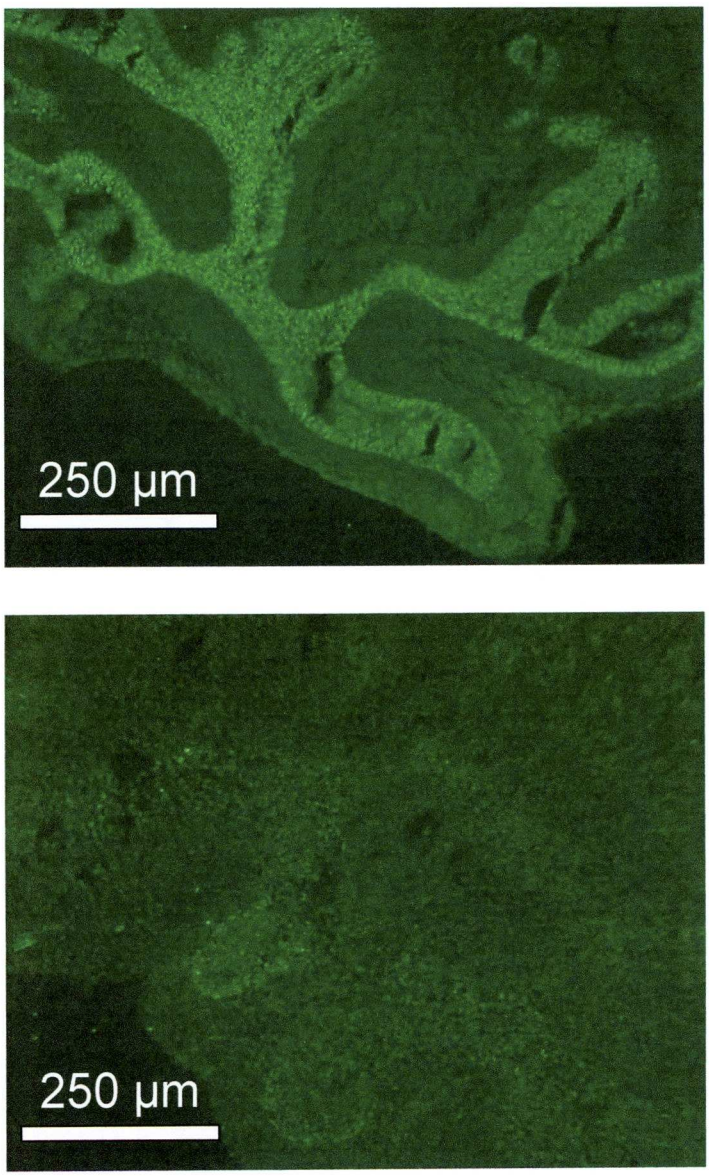

Figure 5.9. Immunohistochemistry for α-smooth muscle actin. After a period of 48 hours *in vitro* culture, control rat lung explants (top) show normal α-smooth muscle actin expression; however, in lungs exposed to CPA (bottom), the expression is abolished.

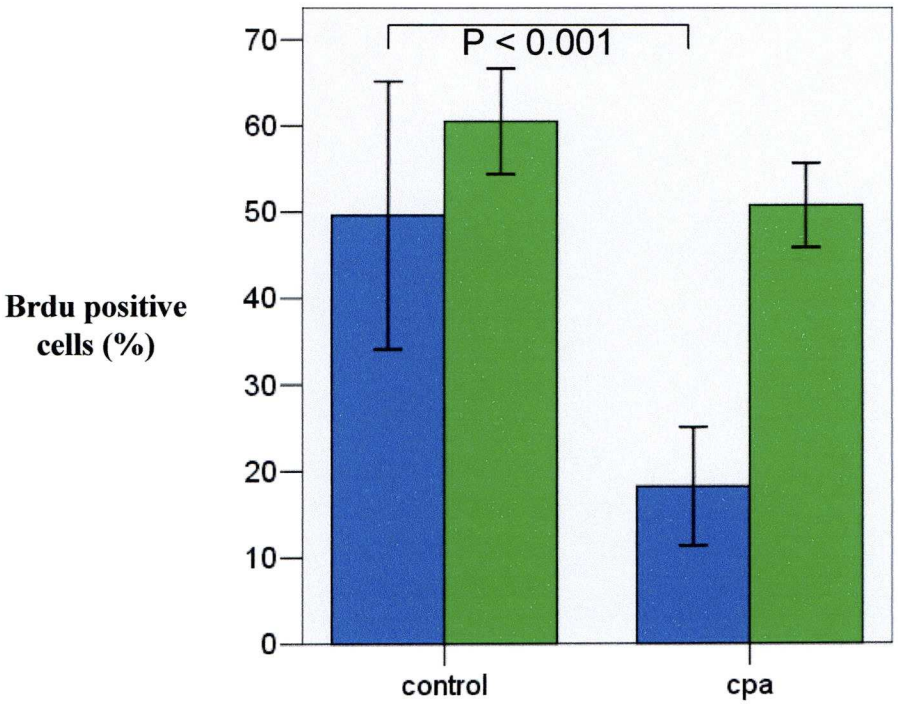

Figure 5.10. The effect of cyclopiazonic acid (CPA) on cellular proliferation as assessed by Brdu (5-bromo-2'-deoxyuridine) labelling within the end-buds of embryonic rat lung explants. Data are shown at 24 (blue bars) and 48 hours (green bars) for control lungs and explants cultured in the presence of CPA. CPA significantly reduced cells labelling positively for Brdu at 24 hours, but not at 48 hours. Bars represent means and SD.

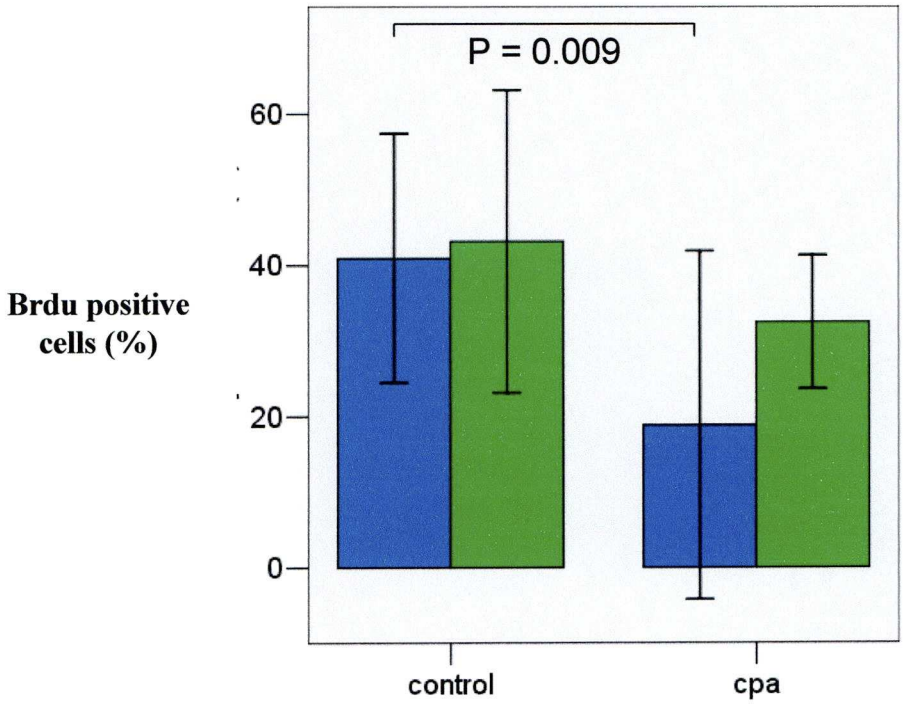

Figure 5.11. The effect of cyclopiazonic acid (CPA) on cellular proliferation as assessed by Brdu (5-bromo-2'-deoxyuridine) labelling within the airway of embryonic rat lung explants. Data are shown at 24 (blue bars) and 48 hours (green bars) for control lungs and explants cultured in the presence of CPA. CPA significantly reduced cells labelling positively for Brdu at 24 hours, but not at 48 hours. Bars represent means and SD.

Prenatal airway smooth muscle (ASM) peristalsis is a mechanical factor that has been reported to be coupled to lung growth (Jesudason *et al.*, 2005). ASM peristalsis is underpinned by spontaneous regenerative propagating Ca^{2+}_i waves, which in turn depend on Ca^{2+}_o entry and Ca^{2+}_i release (Featherstone *et al.*, 2005). Thus if AP regulates lung growth, airway smooth muscle Ca^{2+}_i waves regulate prenatal lung morphogenesis.

5.4.1 CPA inhibits branching morphogenesis in embryonic rat and mouse lung explants

CPA inhibits removal of Ca^{2+} from the cytoplasm of the cells by the sarcoplasmic reticulum (SR) Ca^{2+}-ATPase (SERCA pump); it is a compound isolated from the fungus *Penicillium cyclopium* (Holzapfel, 1968). We have previously shown CPA markedly increases baseline Ca^{2+}_i and gradually abolishes Ca^{2+}_i transients and associated mechanical activity; phasic airway activity being gradually replaced by tonic airway contraction (Featherstone *et al.*, 2005). CPA empties the SR and prevents Ca^{2+} release via ryanodine (RyR) channels or inositol triphosphate ($InsP_3R$) channels.

CPA abolished branching morphogenesis in both embryonic rat and mouse lung explants whether applied at the beginning of the culture period or at later time intervals. Our observations give further support to the thesis that ASM contractility and Ca^{2+}_i waves are a prerequisite for normal lung development.

Ca^{2+}_i pools have been previously shown to play a key role in controlling vascular smooth muscle cell (VSMC) proliferation *in vitro* (Shukla *et al.* 1997). Similarly, Ca^{2+}_i inhibitors are capable of arresting cell growth in DDT_1MF-2 smooth muscle cells (Short *et al.* 1993). They suggest that emptying the internal Ca^{2+} pool maintains cells in a G_0-like quiescent state. Once intracellular pools refill, the cell cycle resumes. CPA may act in a similar manner resulting in inhibition of the cell cycle.

We showed that CPA inhibited branching morphogenesis. Nifedipine, in contrast, does not inhibit branching (Roman, 1995; Jesudason *et al.*, 2005). These observations suggest that Ca^{2+}_i waves and consequent ASM peristalsis are perhaps necessary for lung growth, but not branching morphogenesis. Inhibiting Ca^{2+} release from the internal store abolished lung branching morphogenesis and produced lung hypoplasia. Therefore, Ca^{2+} release from the SR via RyR channels or $InsP_3R$ channels appears critical to lung branching morphogenesis. Inhibition of Ca^{2+} release from the SR may prevent dynamic temporo-spatial Ca^{2+}_i signalling (Berridge *et al.*, 2003; Lipskaia *et al.*, 2004). Furthermore, CPA produces an elevation in Ca^{2+}_i and tonic airway contraction (Featherstone *et al.*, 2005). Previous investigators have shown that modulating cytoskeletal force also plays an important role in epithelial branching morphogenesis (Moore *et al.*, 2005). CPA application may therefore increase cell tension; excess tension may result in contraction and cessation of organ development (Moore *et al.*, 2005).

5.4.2 'Rescue' of lung explants from CPA exposure results in a return of branching morphogenesis

Removal of CPA from the system results in a return of spontaneous contractile ASM activity and branching morphogenesis. These data indicate that the SR controls ASM contractile activity and provides further evidence that the SR appears to play a crucial role in the control of epithelial branching morphogenesis. In particular, the SR Ca^{2+}-ATPase (SERCA pump) plays a central role. It is required to remove Ca^{2+} from the cytoplasm and permit refilling of the SR (Sanders 2001; Taylor *et al.* 2002). These data also give further support to the thesis that spontaneous airway contractile activity is required for normal lung development.

The abolition of lung branching morphogenesis by CPA may be due to several mechanisms e.g. 1) abrogation of SR Ca^{2+} release; 2) marked elevation of $Ca^{2+}{}_i$; 3) increased ASM tone and / or 4) direct CPA-effects on the cell cycle.

5.4.3 CPA application results in morphological delays in development

CPA application appeared to delay morphological development; tracheal cartilage rings were clearly evident upon light transmitted images of rat lung explants cultured in standard medium for 78 hours, however, they failed to develop in explants cultured in the presence of CPA. CPA may

also delay physiological development; normally ASM peristalsis is developmentally regulated with early T-wave activity being gradually replaced by L- and R-waves (Jesudason *et al.* 2006). Hypoplastic lungs, deficient in FGF-10, exhibit retardation of this developmental regulation (Jesudason *et al.* 2006). We re-established that ASM peristalsis is developmentally regulated in control lungs. However, lungs exposed to CPA for 30 hours prior to rescue, continued to exhibit T-waves at 54 and 78 hours. These data did not reach statistical significance and further studies are required to determine the effects of CPA on the developmental regulation of AP.

5.4.4 α-SMA expression is reduced after CPA application

Smooth muscle actin expression in human lung and other animals is developmentally regulated throughout gestation (Jostarndt-Fögen *et al.*, 1998; Sparrow *et al.*, 1999; Tollet *et al.*, 2001; Yamada *et al.*, 2002). ASM cells develop from the mesenchyme directly underlying the epithelium at the base of the epithelial buds (Sparrow *et al.* 2003; Mailleux *et al.* 2005). In our experiments, α-SMA expression was reduced in lung explants exposed to CPA. This was associated with a loss of branching morphogenesis. This gives further support to the thesis that SM activity is required for prenatal lung development and not merely the 'appendix of the lung' (Mitzner 2004; Jesudason *et al.*, 2005; Jesudason, 2006).

5.4.5 CPA reduced cellular proliferation at 24 hours *in vitro*

$Ca^{2+}{}_i$ inhibitors, thapsigargin and di-tert-butylhydroquinone have been shown to inhibit cell proliferation *in vitro* (Short *et al.*, 1993). Likewise, CPA may have a similar effect. There was a significant reduction at 24 hours of proliferation in both end buds and airway, but not at 48 hours (the bioavailability of CPA may alter over time, cellular resistance may develop, metabolism may alter, or novel Ca^{2+} influx channels could appear and lead to a resurgence in proliferation). These data may in part explain the inhibition of branching morphogenesis. However, the control of branching morphogenesis is complex, CPA may also affect cytoskeletal tension which may itself inhibit branching (Moore *et al.*, 2005). Further work is needed to investigate further the relationship between CPA, proliferation / the cell cycle and branching morphogenesis.

5.5 Conclusions

a) SERCA pump inhibition with CPA reversibly abolished airway peristalsis, abrogated branching morphogenesis and inhibited αSMA expression; it also impaired development of cartilage tracheal rings and induced a transient reduction in pulmonary cell proliferation. Together these findings support a key role of prenatal sarcoplasmic Ca^{2+} signalling in lung morphogenesis, contractility

and cell fate. They also indicate that the 'growth arrest' induced by CPA is not simply due to inhibition of lung cell proliferation. Therefore, the SERCA pump appears to play a critical role in lung growth and epithelial branching morphogenesis.

b) Release of Ca^{2+} from the SR via RyR channels or $InsP_3R$ channels appears to be central to branching morphogenesis. CPA completely abolished branching morphogenesis (in contrast to nifedipine, which results in lung hypoplasia alone).

c) Inhibition of the SR Ca^{2+}-ATPase significantly reduced cellular proliferation at 24 hours *in vitro*. CPA may empty the $Ca^{2+}{}_i$ pool resulting in cells entering a quiescent state and reduced cellular proliferation. Re-establishment of branching morphogenesis upon 'rescue' from CPA exposure is consistent with this theory.

d) CPA results in an ontological delay in lung development, which is consistent with a reduction in cellular proliferation and delayed lung growth.

Chapter 6

EFFECTS OF SUCROSE AND NIFLUMIC ACID UPON AIRWAY PERISTALSIS, Ca^{2+}_i TRANSIENTS AND LUNG MORPHOLOGY

6.1 Introduction

Pulmonary hypoplasia and pulmonary hypertension account for the high mortality in newborns with congenital diaphragmatic hernia (Smith *et al.* 2005). Consequently, surgeons have attempted to improve the outcome for CDH newborns by improving lung growth through fetal tracheal occlusion (Harrison *et al.* 2003; Deprest *et al.* 2005; Kitano, 2007). However, this technique is not without problems; it expands the lung, but also results in abnormal differentiation (Lipsett *et al.* 1998), depletion of alveolar type II cells (De Paepe *et al.* 1998) and surfactant deficiency (O'Toole *et al.* 1996). Repeated cyclical occlusion and release appears to promote maturation and development of a saccular lung (Nelson *et al.* 2005).

Similarly, *in vitro*, it has been demonstrated that over-accumulation of lung fluid disrupts lung branching morphogenesis (Nogawa *et al.* 2002). However, mechanical drainage or osmotic manipulation of the lung culture medium using sucrose, NaCl, or lactose reduces luminal distension and stimulates branching morphogenesis (Nogawa *et al.* 2002). Since spontaneous contractile activities of the musculature of the embryonic airways (airway peristalsis) have been reported to be coupled to lung growth *in vitro* (Jesudason *et al.* 2005), we were interested to determine the effect of manipulation of luminal lung fluid (by changing osmotic conditions) upon airway peristalsis in our experimental model; the data obtained may have implications for therapies such as tracheal occlusion.

Throughout gestation, lung liquid is produced; it is central to pulmonary development and arises as a result of the continued secretion of chloride (Cl^-) (McCray *et al.* 1992). The Ca^{2+}-activated Cl^- channel is one of a number of Cl^- channels implicated as being involved (Clarke *et al.* 1994). We sought to determine the effect of niflumic acid, known to inhibit Cl^- conductances (White *et al.* 1990; Korn *et al.* 1991; McCarty *et al.* 1993), on lung branching morphogenesis and ASM $Ca^{2+}{}_i$ waves in our experimental model.

We show that the manipulation of osmotic pressure using sucrose improved branching morphogenesis, but decreased the frequency of spontaneous contractions. Niflumic acid stimulated branching morphogenesis, increased the frequency of spontaneous contractions and reduced the amplitude of ASM $Ca^{2+}{}_i$ waves.

6.2 Materials and methods

6.2.1 Retrieval of embryonic lung primordia

See section 3.2.1

6.2.2 Embryonic lung culture

Lung rudiments were positioned on translucent polytetrafluorethylene membrane culture-dish inserts (Millicell, Millipore Corp, Bedford, MA) with serum-free culture media incorporating penicillin (100 IU/ml) and streptomycin (100 μg/ml; GibcoBRL, Life Technologies, Paisley, UK).

Lung primordia were incubated at 37°C in 5% CO_2 for periods up to 78 hours ± sucrose (20, 30, 50 or 100 mM) or niflumic acid (10, 50 or 100 μM).

6.2.3 Assessment of viability

See section 3.2.2

6.2.4 Morphometric analysis of *in vitro* lung development

See section 5.2.4

6.2.5 Analysis of spontaneous airway contractility

The frequency of spontaneous airway contractions were recorded in individual lung explants for 10-minute periods at 37^0C as previously described (Jesudason *et al.* 2005). Inter-contraction intervals were calculated from the data obtained.

6.2.6 Loading lung explants with Ca^{2+}_i sensitive fluophores

See section 3.2.3

6.2.7 Photometric measurements

See section 3.2.4

6.2.8 Solutions

Unless otherwise stated, lung explants were superfused at 37°C with buffered physiological saline (pH 7.4) containing (mM): 120 NaCl, 5.6 KCl, 0.12 $MgSO_4$, 2 $CaCl_2$, 11.7 glucose, 10.9 HEPES. Other additions to standard superfusate that were investigated include: carbachol (100 μM) and high K^+ solution (120 mM). Carbachol was dissolved in distilled water. Sigma (Poole, Dorset, UK) supplied all chemicals.

6.2.9 Statistical analysis

See section 3.2.7

6.3 Results

6.3.1 Sucrose increases lung branching morphogenesis

Lung explants were cultured in either standard culture medium (n = 6) or in medium to which sucrose had been added to give a final concentration of 20, 30, 50 or 100 mM (n = 6 per group). In a similar manner to that reported by Nogawa *et al.* in 2002, the addition of sucrose to the standard culture medium stimulated branching morphogenesis (Figure 6.1) (Nogawa *et al.*, 2002). Figure 6.2 shows the morphometric results (specimen area, specimen perimeter and total bud count) for lungs cultured in standard media and sucrose media. Lungs cultured in the presence of 100 mM sucrose exhibited statistically significant increases ($p < 0.001$) in the specimen perimeter (17.27 ± 0.64 vs. 11.48 ± 0.55 mm) and total bud

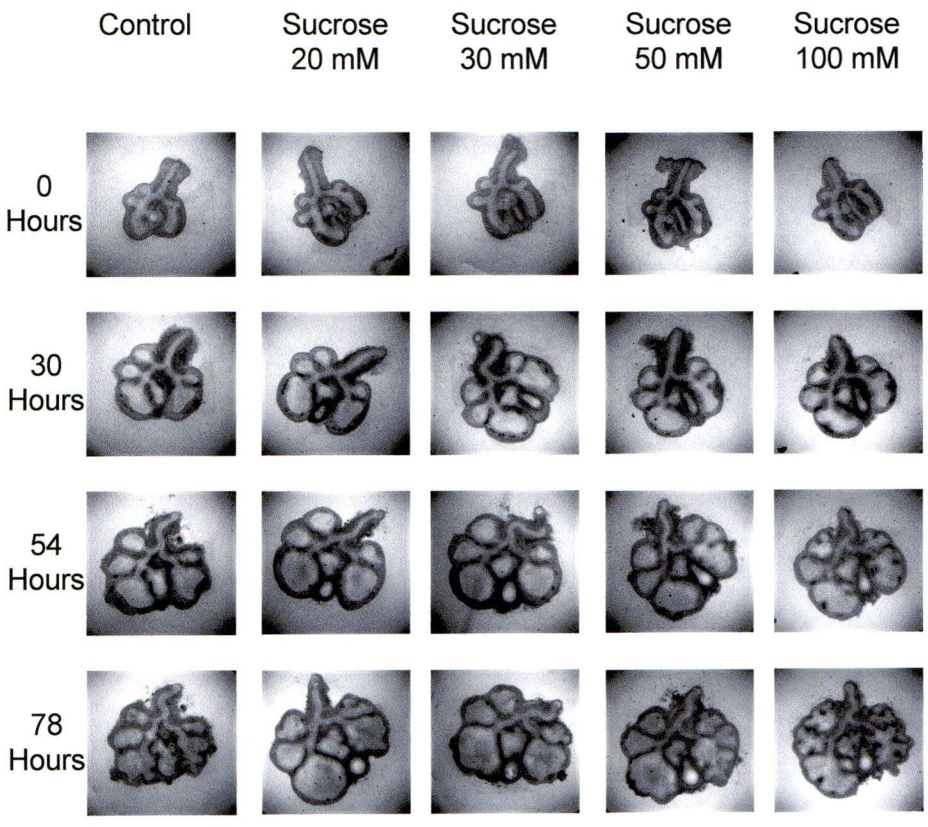

Figure 6.1. Effect of sucrose (20, 30, 50 and 100 mM) on the morphological development of embryonic rat lung primordia *in vitro*. Photomicrographs were taken at 0, 30, 54 and 78 hours. Sucrose stimulated branching morphogenesis.

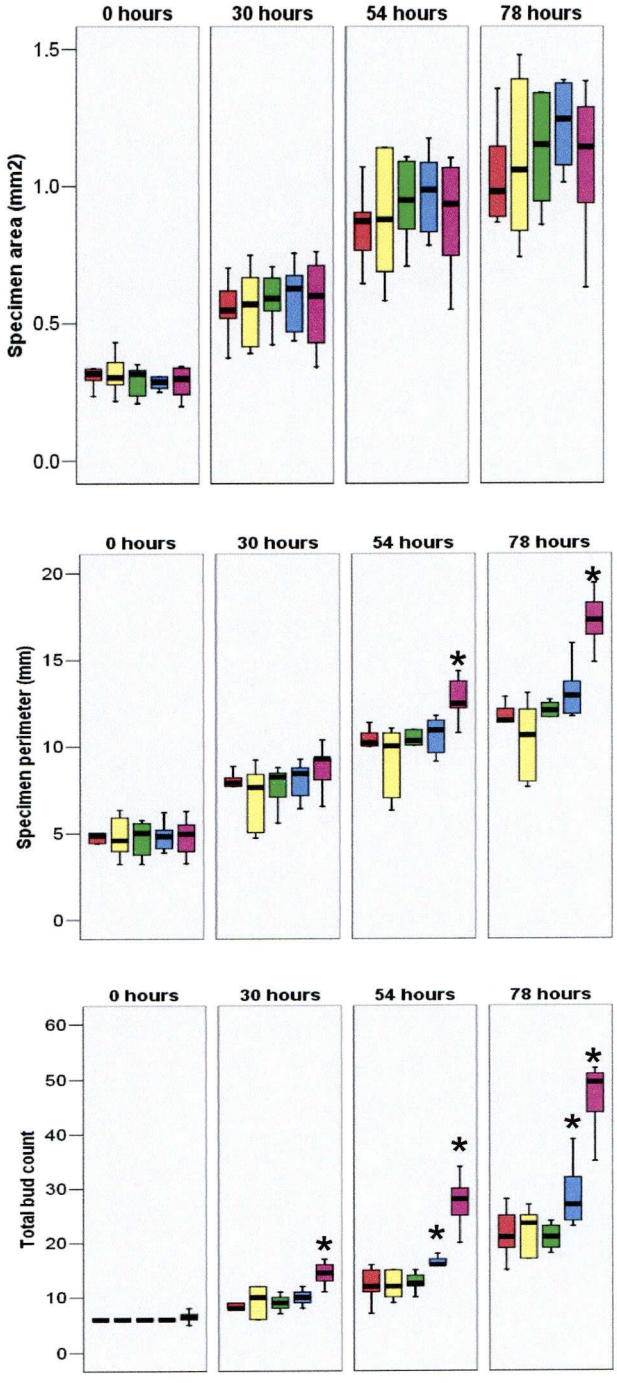

Figure 6.2. Box plots illustrating the morphometric data for control lungs cultured in serum-free medium (red); with sucrose 20 mM (yellow); with 30 mM sucrose (green); 50 m sucrose (blue); and 100 mM sucrose (purple) at the corresponding time points 0, 30, 54 and 78 hours *in vitro*. Bars represent medians and boxes' interquartile range. * Significant increase compared to control lungs ($p < 0.001$).

count (49.50 ± 2.63 vs. 21.00 ± 1.93) compared to control lungs after 78 hours of *in-vitro* culture.

6.3.2 Sucrose reduces airway peristaltic frequency

Inter-contraction intervals were calculated for control lungs and explants cultured in the presence of sucrose (20, 30, 50 and 100 mM) at time 30, 54 and 78 hours *in vitro*. The frequency of spontaneous airway contractions (airway peristalsis) was significantly decreased (compared to controls) in embryonic lung explants cultured in the presence of sucrose at the time points studied despite exhibiting increased branching morphogenesis (Figure 6.3).

6.3.3 Niflumic acid increases lung branching morphogenesis

Lungs were cultured in standard culture medium or in media to which niflumic acid had been added to give a final concentration of 10, 50 or 100 μM. Figure 6.4 shows that the addition of niflumic acid to the standard culture medium produced a dose-dependent increase in lung branching morphogenesis. Morphometric data obtained at time 0, 30, 54 and 78 hours *in vitro* is shown in Figure 6.5. Lungs cultured in the presence of niflumic acid showed a marked increase in branching morphogenesis (increased specimen perimeter, elevated total bud count and reduced specimen area). There were statistically significant differences between explants cultured in the presence of niflumic acid and controls (Figure 6.5).

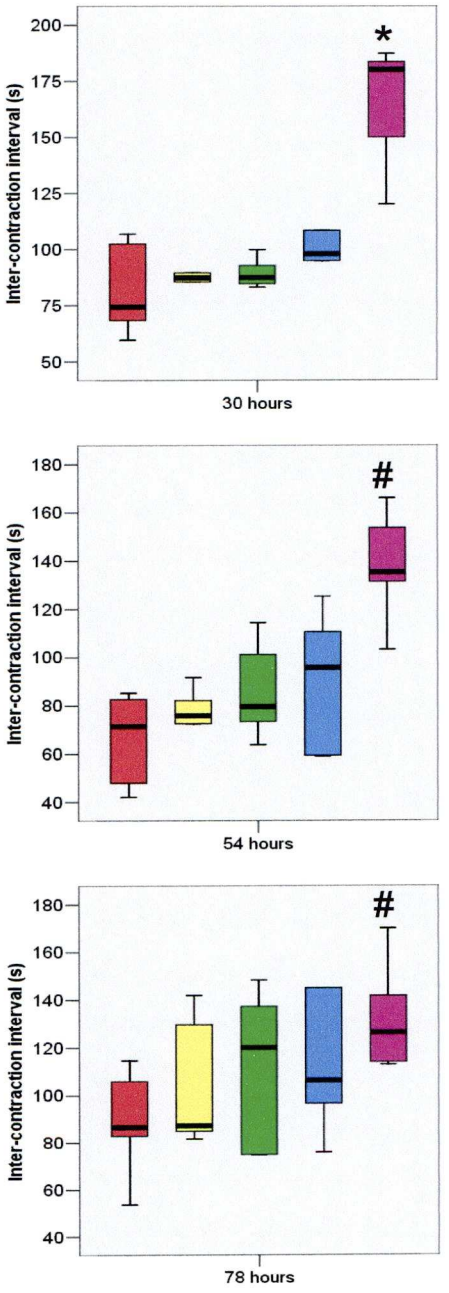

Figure 6.3. Box plots illustrating the intercontraction intervals (seconds) at 30, 54 and 78 hours *in vitro*. Data are shown for control lungs cultured in serum-free medium (red); with sucrose 20 mM (yellow); with 30 mM sucrose (green); 50 mM sucrose (blue); and 100 mM sucrose (purple). Bars represent medians and boxes' interquartile range. Sucrose 100 mM significantly increased inter-contractile intervals compared to control lungs at 30, 54 and 78 hours (*$p < 0.05$, #$p < 0.01$).

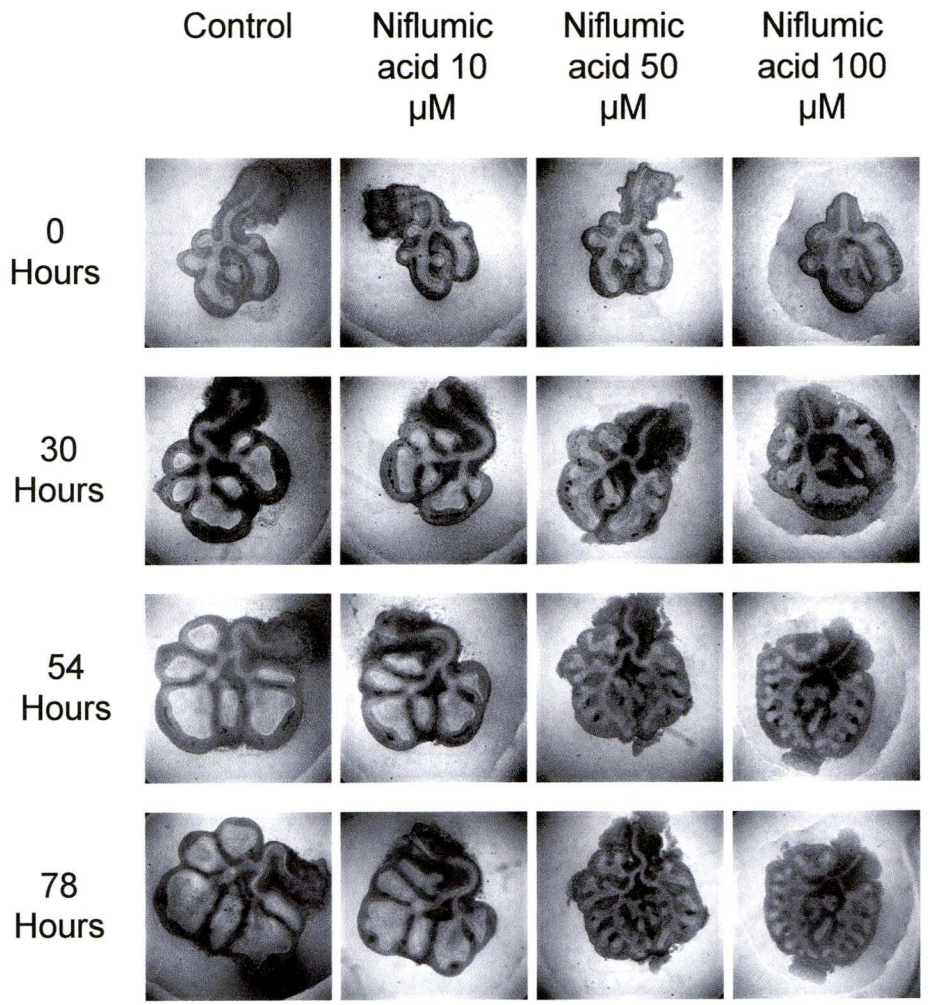

Figure 6.4. Effect of niflumic acid (10, 50 and 100 µM) on the morphological development of embryonic rat lung primordia *in vitro*. Photomicrographs were taken at 0, 30, 54 and 78 hours. Niflumic acid stimulated branching morphogenesis and reduced luminal distension.

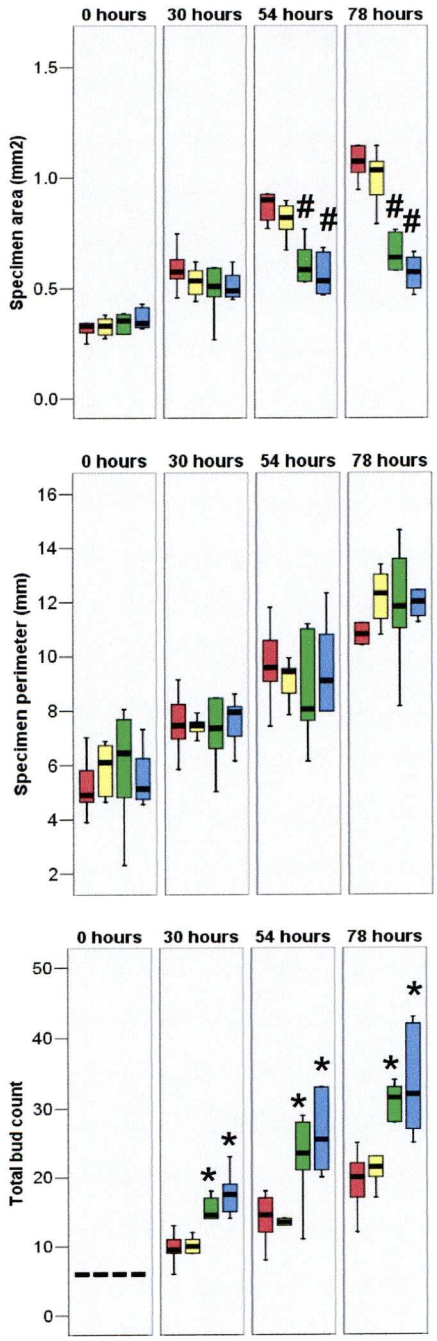

Figure 6.5. Box plots illustrating the morphometric data for control lungs cultured in serum-free medium (red); with niflumic acid 10 μM (yellow); with 50 μM niflumic acid (green); 100 μM niflumic acid (blue) at the corresponding time points 0, 30, 54 and 78 hours *in vitro*. Bars represent medians and boxes' interquartile range. * Significant increase compared to lungs cultured in serum free medium ($p < 0.05$). # Significant decrease compared to lungs cultured in serum free medium ($p < 0.05$).

6.3.4 Niflumic acid reduces airway peristalsis inter-contraction intervals

Given niflumic acid stimulated branching morphogenesis, and airway peristalsis has been reported to be correlated with lung growth, we were interested to determine whether it had an effect on airway peristalsis. The frequency of spontaneous airway contractility was statistically significantly increased ($p = 0.022$) in explants exposed to media containing 100 μM niflumic acid after 78 hours (Figure 6.6).

6.3.5 Niflumic acid reduces the amplitude of ASM $Ca^{2+}{}_i$ waves

We were also interested to determine the effect of niflumic acid exposure upon the amplitude of ASM $Ca^{2+}{}_i$ waves in lung explants. Although numbers were small (control = 2; niflumic acid 10 μM = 1; niflumic acid 50 μM = 2; and niflumic acid 100 μM = 2), there was a clear reduction in the relative amplitude of ASM $Ca^{2+}{}_i$ transients (Figure 6.7). These findings may have become statistically significant should sufficient experimental data been gathered. Consistent with this finding, video images of contractions in control lungs and explants exposed to niflumic acid show the relative amplitudes of contraction to be less in the treatment group.

6.4 Discussion

In order to develop new putative rescue therapies for congenital diaphragmatic hernia (CDH) or improve existing therapies e.g. tracheal

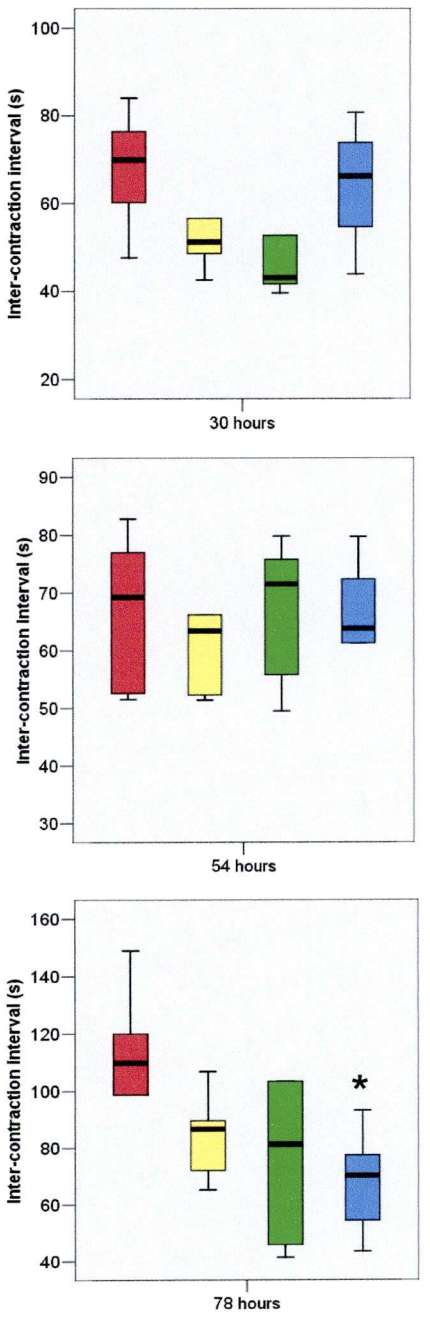

Figure 6.6. Box plots illustrating the intercontraction intervals (seconds) at 30, 54 and 78 hours *in vitro*. Data are shown for control lungs cultured in serum-free medium (red); with niflumic acid 10 μM (yellow); with 50 μM niflumic acid (green); and 100 μM niflumic acid (blue). Bars represent medians and boxes' interquartile range. Niflumic acid (100 μM) significantly decreased the inter-contractile interval at 78 hours compared to control lung (*$p < 0.05$).

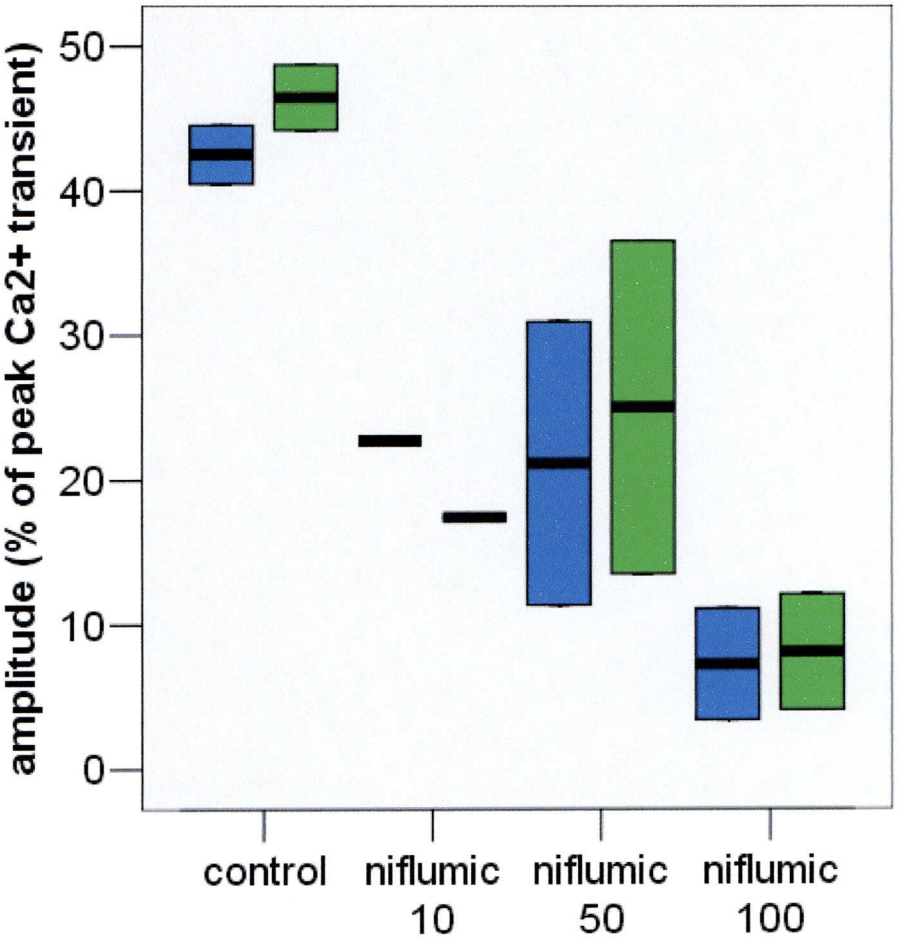

Figure 6.7. Effect of niflumic acid (10, 50 and 100 μM) on ASM $Ca^{2+}{}_i$ wave amplitude. The amplitude of the spontaneous $Ca^{2+}{}_i$ transients are expressed as a percentage of the peaks obtained with 120 mM K^+ solution (blue) or 100 μM carbachol (green). Bars represent medians and boxes' interquartile range.

occlusion, it is first necessary to appreciate the processes regulating normal lung development.

6.4.1 Sucrose increases lung branching morphogenesis

Nogawa *et al.* (2002) have previously shown that the addition of sucrose to culture medium stimulates branching morphogenesis and reduces luminal distension (Nogawa *et al.*, 2002). Our results were in-keeping with their published data. They postulated sucrose may either act as a nutrient or generate osmotic pressure such that water moves by osmosis from the luminal fluid to the culture medium. They provided further evidence for the latter by increasing osmotic pressure with lactose or sodium chloride. Draining lung liquid mechanically also stimulated branching morphogenesis in their experimental model. Together, their results suggested that over-accumulation of lung fluid disrupts lung branching morphogenesis. These findings may have important implications for tracheal occlusion. Over-distension of the airways may impair lung development. Indeed, tracheal occlusion expands the lung, but also results in abnormal differentiation (Lipsett *et al.* 1998), depletion of alveolar type II cells (De Paepe *et al.* 1998) and surfactant deficiency (O'Toole *et al.* 1996). Repeated cyclical occlusion and release promotes maturation and development of a saccular lung (Nelson *et al.* 2005).

6.4.2 Sucrose reduces airway peristaltic frequency

Airway peristalsis has previously been reported to be coupled to lung growth (Jesudason *et al.* 2005). Modulating lung growth resulted in parallel changes in airway peristalsis and vice versa. However, culturing lungs in the presence of sucrose resulted in a significant slowing of spontaneous ASM activity despite stimulation of branching morphogenesis. Why should this be the case? It is possible that the relationship between airway peristalsis and lung growth may not be as clear as previously reported. Some of the observed responses may be secondary to other effects on airway smooth muscle e.g. depolarisation of membrane potential / activation of ionic channels. In a similar manner, sucrose may reduce smooth muscle activity although branching morphogenesis is increased, as a consequence of the alteration in osmolality. Changing extracellular osmolality has been shown to lower the frequency of spontaneous contractions in detrusor smooth muscle strips (Proctor *et al.* 1999).

6.4.3 Niflumic acid increases lung branching morphogenesis and reduces airway peristalsis inter-contraction intervals

Lung liquid production throughout gestation is central to pulmonary development and arises as a result of the continued secretion of chloride (McCray *et al.* 1992). It remains unclear as to which Cl^- channels are involved. Although the CFTR channel is an essential Cl^- channel, patients

with cystic fibrosis (CF) have normal lung morphology at birth (Sturgess *et al.* 1982), suggesting other Cl^- channels may be involved in lung fluid production. Other candidate channels include Ca^{2+}-activated Cl^- channels (Clarke *et al.* 1994), outward rectifying Cl^- channels (Gabriel *et al.* 1993), or members of the voltage-gated CLC family of Cl^- channels (CLC-2, -3 and -5) (Murray *et al.* 1995; Lamb *et al.* 2001; Blaisdell *et al.* 2000; Edmonds *et al.* 2002; Blaisdell *et al.* 2004).

Niflumic acid, a non-steroidal anti-inflammatory aromatic compound (Hoffmann *et al.* 1966; Kohler *et al.* 1992) is a known inhibitor of Ca^{2+}-activated Cl^- channels (White *et al.* 1990; Korn *et al.* 1991; McCarty *et al.* 1993). Niflumic acid stimulated lung branching morphogenesis (total bud count, specimen perimeter and specimen area) and 'rescued' lungs from the development of cystic morphology. Lung explants in our culture system exhibit cystic morphology after 78 hours of *in vitro* culture (Jesudason *et al.* 2005). This may be related to the culture system in use and also in part to the system being 'closed'; the trachea spontaneously seals within the first 24 hours of culture replicating tracheal occlusion. As a consequence, secreted lung fluid accumulates within the principal airways and terminal buds. Over-distension may inhibit branching morphogenesis (Nogawa *et al.* 2002; Moore *et al.*, 2005). If Ca^{2+}-activated Cl^- channels are involved in lung fluid production as proposed by Clarke *et al.* (1994), niflumic acid blockade, should reduce lung fluid production via these channels and lung branching morphogenesis should increase as a

consequence (Clarke *et al.*, 1994). Certainly, our data appear to confirm that Ca^{2+}-activated Cl^- channels play a role in lung fluid production as niflumic acid exposure reduced luminal distension and augmented lung branching morphogenesis (Figures 6.4 and 6.5).

Niflumic acid exposure was also associated with an increase in the frequency of airway peristalsis in lung explants. These data correlate well with the observations of Jesudason *et al.* (2005) who reported that augmented lung growth is associated with an increase in peristaltic frequency (Jesudason *et al.*, 2005). However, the frequency of airway peristalsis (and ASM $Ca^{2+}{}_i$ waves) and the amplitude of ASM $Ca^{2+}{}_i$ waves may be closely interrelated. Analogous to bowel obstruction *in vivo*, over-distension of the airways may result in decreased peristaltic frequency (and increased ASM $Ca^{2+}{}_i$ wave amplitude). Following this thesis, reducing lung fluid production with niflumic acid and decreasing airway distension should result in an increased peristaltic frequency (and reduction in $Ca^{2+}{}_i$ wave amplitude). Our data are in-keeping with this theory. Likewise, co-culture of lung explants with FGF-10 reduced spontaneous airway contractility and increased ASM $Ca^{2+}{}_i$ amplitude (data not shown), which may be a response to stimulation of lung fluid production and airway distension.

Another possibility to consider is that niflumic acid may exhibit cross reactivity and/or alter ionic currents such that airway peristalsis is stimulated. There are important caveats associated when using Cl^- channel

blockers such as niflumic acid as they show low potency, low selectivity, tissue variability and can affect other ion channels (Greenwood *et al.* 2007). It is well established that niflumic acid can stimulate large conductance Ca^{2+}-activated K^+ channels (BK_{Ca}) at similar concentrations to those required to block Ca^{2+}- activated Cl^- channels (Greenwood *et al.* 1995; Toma *et al.* 1996). However, stimulation of BK_{Ca} channels would result in decreased frequency of ASM contraction as tetraethylammonium (TEA) blockade of K^+ channels is known to augment peristaltic frequency (Featherstone *et al.* 2005; Featherstone *et al.* 2006).

6.4.4 Niflumic acid reduces the amplitude of ASM $Ca^{2+}{}_i$ waves

Although overall numbers were small in our preliminary data set, we observed that the relative amplitude of ASM $Ca^{2+}{}_i$ waves decreased in lung explants cultured with niflumic acid. This coincided with increased branching morphogenesis and reduced distension of the embryonic airways. It was also evident that the relative amplitude of the visualised contractions became less. One hypothesis (as above) is that airway distension secondary to lung fluid production results in decreased frequency and increased amplitude of ASM $Ca^{2+}{}_i$ waves.

6.5 Conclusions

1) Sucrose increased lung branching morphogenesis but reduced the frequency of ASM contractility in our experimental model. Alteration of osmolality may be responsible for the decreased ASM contractility. These data illustrate that lung development and airway peristalsis are not always coupled *in vitro*.

2) Ca^{2+}-activated Cl^- channels appear to play a role in lung liquid production in the developing embryonic rat lung. Niflumic acid reduced luminal distension and stimulated lung branching morphogenesis.

3) Niflumic acid exposure stimulated lung branching morphogenesis and increased the frequency of ASM contractility, supporting the thesis that ASM activity may be coupled to lung growth *in vitro*.

4) Considering tracheal occlusion for CDH, these data suggest that it is necessary to determine the optimal pressure for normal lung development. If airway distension occurs through tracheal occlusion, deleterious effects on lung growth will occur.

Chapter 7

CLOSING REMARKS & FUTURE DIRECTIONS

7.1 Overview

Congenital diaphragmatic hernia (CDH) retains high mortality mainly because of pulmonary hypoplasia and pulmonary hypertension (Smith *et al.* 2005). As a consequence, many researchers have chosen to study pulmonary development in order to gain greater insights into the factors that control / influence lung development.

This thesis was based upon the knowledge that pulmonary hypoplasia is one of the major determinants of mortality in CDH. Recently, spontaneous airway contractility (airway peristalsis) has been shown to be coupled in lung growth *in vitro* (Jesudason *et al.* 2005). Ca^{2+} appears to play an important role in airway peristalsis (McCray 1993; Sparrow *et al.* 1994; Roman 1995). Thus if airway peristalsis controls lung growth and Ca^{2+} underpins airway peristalsis, then ultimately, $Ca^{2+}{}_i$ waves drive lung growth.

7.1.1 $Ca^{2+}{}_i$ waves may drive lung development

Peristaltic contractions of the prenatal airway are produced by spontaneous, regenerative, temperature-dependent $Ca^{2+}{}_i$ oscillations of myogenic origin that require extracellular Ca^{2+} influx, sarcoplasmic $Ca^{2+}{}_i$ uptake, $Ca^{2+}{}_i$ release via RyR and $InsP_3R$ channels, and propagate via ASM cells in a gap junction–dependent manner that is likely to be action potential–mediated (Featherstone *et al.* 2005). Therefore, if as recent data suggest, AP regulates prenatal lung growth (Jesudason *et al.* 2005), then from the

present study we can assert that intercellular Ca^{2+}_i oscillations in turn regulate antenatal lung development (Featherstone *et al.* 2005; Featherstone *et al.* 2006; Jesudason 2006); propagation of intercellular Ca^{2+}_i oscillations throughout a complex developing organ may be integral to, and help coordinate, morphogenesis.

7.1.2 Ca^{2+}_i signalling is abnormal in hypoplastic lungs prior to development of CDH

Ca^{2+}_i transients in hypoplastic lung ASM exhibit significant abnormalities during embryogenesis (Featherstone *et al.* 2006); the temporal characteristics of hypoplastic lung ASM Ca^{2+}_i transients were altered compared to control ASM Ca^{2+}_i transients at both 37°C and 27°C. Hypoplastic lung ASM Ca^{2+}_i transients showed an elongation of the plateau phase compared to normal control lung which was accentuated by cooling to 27°C and accompanied by a significant reduction in the frequency of Ca^{2+}_i oscillations. Additionally, the relative amplitudes of Ca^{2+}_i transients were significantly increased in hypoplastic lungs at 37°C and at 27°C compared to normal controls. Hypoplastic ASM also exhibited enhanced sensitivity to depolarising KCl solution.

7.1.3 Abnormalities of airway smooth muscle function may unify the observed lung hypoplasia and late sequelae (bronchial hyper-reactivity) in CDH

Embryonic nitrofen-exposed lung, therefore, features abnormal $Ca^{2+}{}_i$ transients that accompany early hypoplasia and precede supervention of the visceral hernia (Featherstone *et al.* 2006). Since propagating $Ca^{2+}{}_i$ waves underpin ASM peristalsis (Featherstone *et al.* 2005), this indicates that ASM function is already abnormal at the embryonic stages of hypoplastic lung development. This is significant given that a) ASM progenitors furnish the FGF10 required for early branching morphogenesis; and b) nitrofen-exposed lung primordia exhibit branching abnormalities in tandem with FGF10-deficiency (Mailleux *et al.* 2005; Acosta *et al.* 2001). Together, this supports the thesis that ASM contributes to early FGF10-driven lung morphogenesis and that this relationship is disrupted prior to CDH supervening (Featherstone *et al.* 2006; Jesudason 2006; Jesudason *et al.* 2006). ASM dysfunction also persists after CDH develops: nitrofen-exposed fetal lungs display increased ASM contractility and human CDH survivors manifest reactive airways disease (Belik *et al.* 2003; Boas *et al.* 1996). Therefore, the embryonic ASM dysfunction we have shown (increased duration and amplitude of embryonic ASM Ca^{2+} transients) may underlie, in part, later post-CDH ASM abnormalities (airway hyper-reactivity).

7.1.4 Blockade of Ca^{2+}_i release using CPA abolishes AP and branching morphogenesis

CPA abolished branching morphogenesis in both embryonic rat and mouse lung explants whether applied at the beginning of the culture period or at later time intervals. It was associated with decreased expression of α-ASM and delays in morphological and physiological development. These observations give further support to the thesis that ASM, airway peristalsis and Ca^{2+}_i waves are a prerequisite for normal lung development.

7.1.5 Reduction of lung fluid production via alteration of Cl^- secretion (niflumic acid) results in '*coupled growth*'

Niflumic acid application resulted in 'coupled growth'; there was an increase in both lung branching morphogenesis and airway peristalsis. Given that niflumic acid decreased luminal distension within lung explants, Ca^{2+}-activated Cl^- channels appear to play a role in lung liquid production in the developing embryonic rat lung.

7.1.6 Reduction of lung fluid production through osmotic modulation (sucrose) results in '*uncoupled growth*'

Osmotic modulation (sucrose) resulted in 'uncoupled growth'; there was an increase in lung branching morphogenesis but reduction in the frequency of ASM contractility. These contrasting findings (section 7.1.5 and 7.1.6) suggest that further investigation is warranted into the

relationship between lung liquid production, airway peristalsis and pulmonary development. However, considering tracheal occlusion for CDH, these data suggest that it is necessary to determine the optimal pressure for normal lung development. If airway over-distension occurs through tracheal occlusion, deleterious effects on lung growth will occur (Silver *et al.* 1988; Heerema *et al.* 2003).

7.2 Future Work

1. Ca^{2+}_i imaging is a fast moving subject and it is hard to predict technological advances that will occur in the future. However, there have been many advances in the construction of genetically encoded probes that permit optical imaging of activity in excitable cells (Rizzuto *et al.* 1992; Rizzuto *et al.* 1994). This is possible through the fusion of fluorescent proteins to proteins involved in physiological signalling, such as those that monitor Ca^{2+}_i, pH and membrane potential. Through the use of specific promoters and targeting signals, the probes are introduced into an intact organism and may be directed to specific tissues, cell types or sub-cellular locations. This permits specific signals to be studied more efficiently and relevantly than previously. In this manner, Ca^{2+}_i signalling and its controlling factors could be further investigated in a complex organ such as the lung.
2. We have demonstrated that airway peristalsis relies in part upon Ca^{2+}_i release (Featherstone *et al.* 2005; Featherstone *et al.* 2006). Blockade

of the SERCA pump (SR Ca^{2+}-ATPase) using cyclopiazonic acid (CPA) abolished airway peristalsis and branching morphogenesis. However, its mechanism of action is not fully understood and merits further investigation. The observed effects may be due to inhibition of the cell cycle (Short *et al.* 1993; Shukla *et al.*, 1997), abolition of smooth muscle development or development of increased tension within the smooth muscle (Moore *et al.* 2005).

3. It is well-established that lung liquid production is related to lung growth. Chronic drainage of lung fluid via a tracheostomy in utero results in lung hypoplasia (Alcorn *et al.* 1977). In contrast, congenital laryngeal obstruction results in hyperplastic lungs (Fewell *et al.* 1983). Fetal tracheal occlusion has been utilised to correct lung growth in utero (Hedrick *et al.* 1994; Bealer *et al.* 1995; Skarsgard *et al.* 1996; VanderWall *et al.* 1996; Beierle *et al.* 1996; Harrison *et al.* 2003; Heerema *et al.* 2003; Keller *et al.* 2004; Deprest *et al.* 2005; Saura *et al.* 2007). However its effects upon airway peristalsis are not clear. In these studies we have shown that niflumic acid, an inhibitor of Cl^- channels, increases both lung growth and airway peristalsis (i.e. 'coupled growth'). In contrast, the use of sucrose to manipulate the osmotic concentration of the culture medium increases lung growth, but the frequency of airway peristalsis is reduced (i.e. 'uncoupled growth'). Could airway peristalsis-related Cl^--efflux perhaps drive Cl^--led lung fluid production (Figure 7.1), explaining these differences?

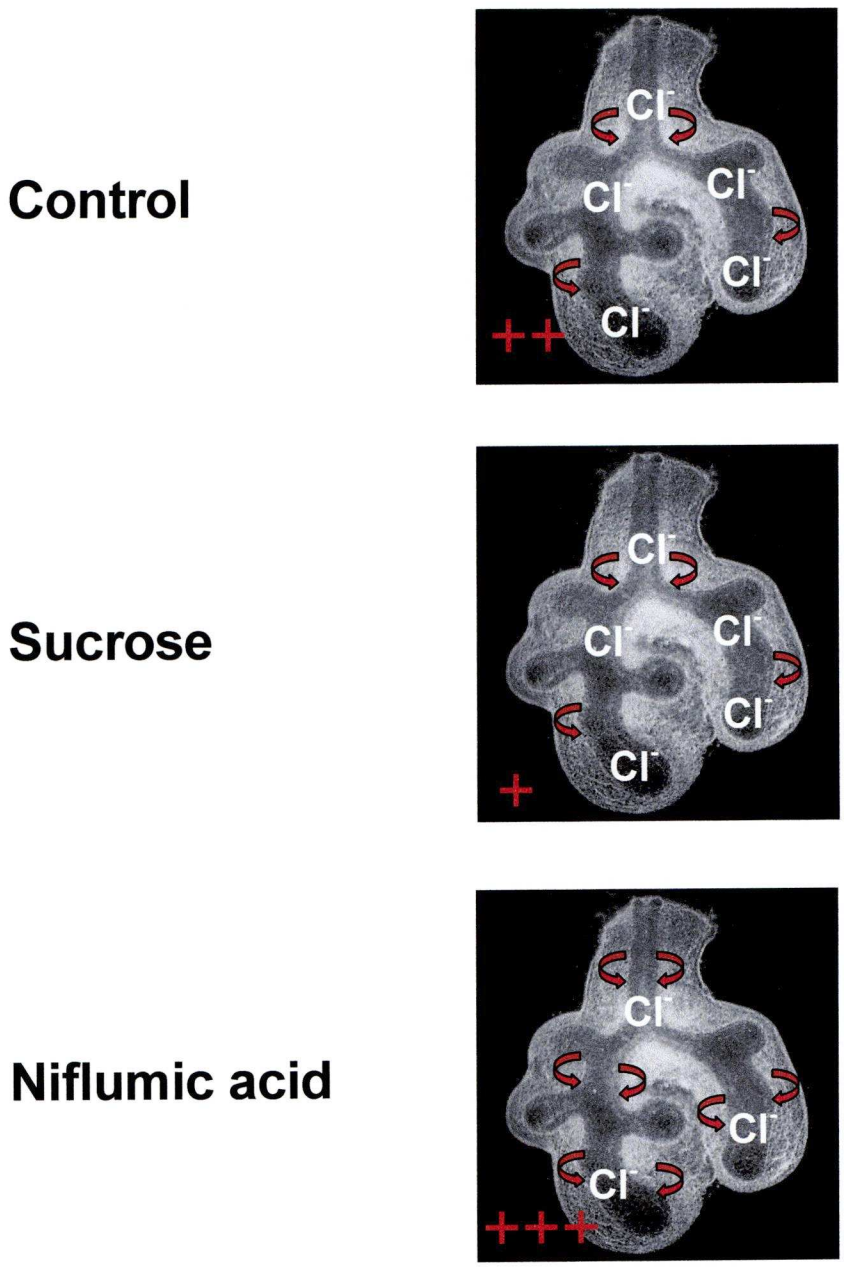

Figure 7.1. Airway peristalsis-related Cl^- efflux (from ASM) may drive Cl^--led lung fluid production. Whilst both sucrose and niflumic acid reduce lung fluid (and here favour airway branching over dilatation), interference with Cl^- transport (niflumic acid) prompts homeostatic increases in AP (+++) whereas osmotic manipulation (sucrose) does not (+).

Further research is required to elucidate how airway peristalsis and lung growth are related. Further investigations could also look at the relationship between lung liquid production and Ca^{2+}_i transients. When niflumic acid is used to improve lung growth, the amplitude of Ca^{2+}_i transients became less in our preliminary experiments. This is in-keeping with the findings within the hypoplastic lung, in which the amplitude of Ca^{2+}_i transients were greater than normal lung, but the frequency of peristalsis was less. One may therefore hypothesise that airway fluid production, airway peristalsis and lung growth is intimately related (Figure 7.2). Perhaps, balloon tracheal occlusion may affect airway peristalsis and therefore lung growth in a detrimental manner.

7.3 Closing Remarks

The care of newborns with congenital diaphragmatic hernia remains a challenge to all involved. Advances have been made in ventilatory techniques and clinical research demonstrated improved outcomes as a result (Wung *et al.* 1995). New ventilatory therapies (e.g. liquid ventilation) merit further investigation as they may ameliorate barotrauma and promote lung growth (Hirschl *et al.* 2003). Fetal interventions are under trial (having been translated from 'bench to bedside') to improve hypoplastic lung function and growth (Harrison *et al.* 2003; Deprest *et al.* 2005). Despite promising experimental and preliminary clinical data,

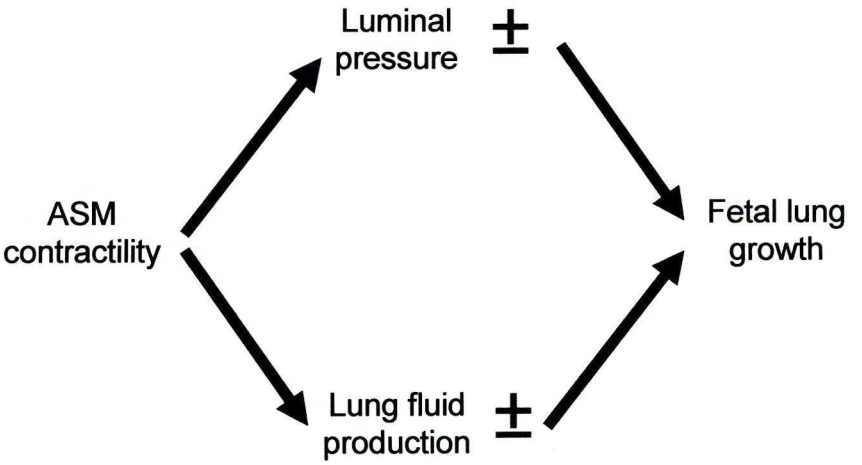

Figure 7.2. Putative regulation of lung growth by ASM activity via feedback regulation of intraluminal pressure and AP-related Cl^- efflux (from ASM) in the expanding lung.

conclusive evidence to back these interventions is awaited. Further scientific investigations may in time help optimize such prenatal therapies by providing a better understanding of the determinants of lung growth. Enthusiasm, dedication and lateral thinking from researchers and surgeons of the future may provide solutions to the ongoing high mortality and morbidity seen in CDH.

Appendix I – Prizes / Distinctions

1. Poster Prize, British Association for the Advancement of Science Annual Meeting Exeter, 2004

2. Poster Prize, Medical Research Society / Academy of Medical Sciences, London, 2005

3. Front cover, American Journal of Respiratory Cell and Molecular Biology, 2005

4. Runner-up Peter Paul Rickham prize, BAPS Annual International Congress, Dublin, Ireland, 2005

Appendix II - Publications Resulting From This Research

1. Spontaneous propagating calcium waves underpin airway peristalsis in embryonic rat lung.

NC Featherstone, EC Jesudason, MG Connell, DG Fernig, S Wray, PD Losty and TV Burdyga.

Am J Respir Cell Mol Biol 2005; 33: 153-160

2. Airway smooth muscle dysfunction precedes teratogenic congenital diaphragmatic hernia and may contribute to hypoplastic lung morphogenesis.

NC Featherstone, MG Connell, DG Fernig, S Wray, TV Burdyga, PD Losty and EC Jesudason.

Am J Respir Cell Mol Biol 2006; 35: 571-8.

Appendix III - Published Abstracts Resulting From This Research

1. Periodic Ca^{2+} oscillations underpin prenatal airway peristalsis

NC Featherstone, EC Jesudason, NP Smith, MG Connell, DG Fernig, S Wray, PD Losty and TV Burdyga. J Physiol 2004; 557P: C25

2. Sarcoplasmic reticulum regulates calcium transients, airway peristalsis and branching morphogenesis of lung explants in vitro

NC Featherstone, EC Jesudason, MG Connell, DG Fernig, S Wray, PD Losty and TV Burdyga. Proc Am Thorac Soc 2005; 2: A503

3. Carbachol and high-k^{+} depolarisation-induced Ca^{2+} transients in airway smooth muscle in normal and hypoplastic lungs

NC Featherstone, EC Jesudason, MG Connell, DG Fernig, S Wray, TV Burdyga and PD Losty. Proc Am Thorac Soc 2005; 2: A503

4. Physiology of spontaneous Ca^{2+} waves in developing lung – innovative concepts towards developing new fetal therapies in congenital diaphragmatic hernia

NC Featherstone, **EC Jesudason, MG Connell, DG Fernig, S Wray, TV Burdyga, PD Losty. Surgeon 2005; 3(suppl): S21**

5. Airway smooth muscle calcium signalling is abnormal in prenatal lung hypoplasia (Poster)

NC Featherstone, PD Losty, MG Connell, DG Fernig, S Wray, TV Burdyga, EC Jesudason

Proc Am Thorac Soc Abstracts Issue 2006; 3: A170

6. A New Regulator of Chloride-Led Lung Liquid Production?

NC Featherstone, M Connell, D Fernig, P Losty, E Jesudason

Am J Crit Care Med Abstracts Issue 2008; 177: A315

Appendix IV - Presentations Resulting From This Research

1. Periodic Ca^{2+} oscillations underpin prenatal airway peristalsis

NC Featherstone, EC Jesudason, NP Smith, MG Connell, DG Fernig, S Wray, PD Losty and TV Burdyga

Presented to the Physiological Society, Glasgow, March 2004

2. Rescuing lung growth in CDH babies (Poster)

NC Featherstone**, EC Jesudason and PD Losty**

Presented to the Annual Meeting of The British Association for the Advancement of Science, Exeter, September 2004

3. Calcium flux and airway contractility are abnormal in experimental lung hypoplasia

NC Featherstone, EC Jesudason, MG Connell, DG Fernig, S Wray, TV Burdyga and PD Losty

Presented to the XVIIth International Symposium of Paediatric Surgical Research, Liverpool, October 2004.

4. Airway peristalsis: a new regulator of prenatal lung growth (Poster)

NC Featherstone, EC Jesudason, MG Connell, DG Fernig, S Wray, TV Burdyga and PD Losty

Presented to the Medical Research Society, Academy of Medical Sciences and Royal College of Physicians meeting for Clinical Scientists in Training, The Royal College of Physicians, London, February 2005.

5. Sarcoplasmic reticulum regulates calcium transients, airway peristalsis and branching morphogenesis of lung explants in vitro (Poster)

NC Featherstone, EC Jesudason, MG Connell, DG Fernig, S Wray, PD Losty and TV Burdyga

Presented to the 100th International Conference of The American Thoracic Society, San Diego, USA, May 2005.

6. Carbachol and high-k^+ depolarisation-induced Ca^{2+} transients in airway smooth muscle in normal and hypoplastic lungs (Poster)

NC Featherstone, EC Jesudason, MG Connell, DG Fernig, S Wray, TV Burdyga and PD Losty

Presented to the 100th International Conference of The American Thoracic Society, San Diego, USA, May 2005.

7. Physiology of spontaneous Ca^{2+} waves in developing lung - innovative concepts towards developing new fetal therapies in congenital diaphragmatic hernia

NC Featherstone, EC Jesudason, MG Connell, DG Fernig, S Wray, TV Burdyga and PD Losty

Presented to the Quincentennial Meeting of The Royal College of Surgeons of Edinburgh, Edinburgh, June 2005.

8. Ca^{2+} waves underpin airway peristalsis, propagate via airway smooth muscle and are abnormal in lung hypoplasia

NC Featherstone, EC Jesudason, MG Connell, DG Fernig, S Wray, TV Burdyga and PD Losty

Presented to the 52nd International Congress of The British Association of Paediatric Surgeons, Dublin, July 2005.

9. Ca^{2+} imaging of airway contractility (airway peristalsis) in embryonic lung primordia

NC Featherstone, EC Jesudason, MG Connell, DG Fernig, S Wray, PD Losty and TV Burdyga

Presented to the 5th International Young Investigators Symposium 'Smooth Muscle in airway and Vascular Disease', Malmo, September 2005

10. An embryonic lesion of airway smooth muscle in lung hypoplasia

NC Featherstone, MG Connell, DG Fernig, S Wray, TV Burdyga, PD Losty and EC Jesudason

Presented to the XVIIIth International Symposium of Paediatric Surgical Research, Stockholm, October 2005.

11. Calcium imaging identifies growth-coupled pacemaker activity (Poster / 3 minute paper)

NC Featherstone, TV Burdyga, MG Connell, DG Fernig, S Wray, PD Losty and EC Jesudason

Presented to the 75th American Academy of Pediatrics (Surgical Section), Washington DC, October 2005.

12. An embryonic lesion of airway smooth muscle in lung hypoplasia (Poster)

NC Featherstone, MG Connell, DG Fernig, S Wray, TV Burdyga, PD Losty and EC Jesudason Presented to the Medical Research Society,

Academy of Medical Sciences and Royal College of Physicians meeting for Clinical Scientists in Training, The Royal College of Physicians, London, February 2006.

13. Airway smooth muscle calcium signalling is abnormal in prenatal lung hypoplasia (Poster)

NC Featherstone, PD Losty, MG Connell, DG Fernig, S Wray, TV Burdyga, EC Jesudason

Presented to the 101st International Conference of The American Thoracic Society, San Diego, USA, May 2006.

14. A New Regulator of Chloride-Led Lung Liquid Production?

NC Featherstone, M Connell, D Fernig, P Losty, E Jesudason

Presented to the 103rd International Conference of The American Thoracic Society, Toronto, Canada, May 2006.

Appendix V - Funding Received For This Research

1. The Royal College of Surgeons of England One Year Research Fellowship (Cazenove & Co Research Fellowship): 2003 – 2004.

2. Medical Research Council (MRC) Clinical Training Fellowship: 2004 – 2006.

REFERENCES

Acosta, J.M,, Thébaud, B., Castillo, C., Mailleux, A., Tefft, D., Wuenschell, C., Anderson, K.D., Bourbon, J., Thiery, J.P., Bellusci, S. and Warburton, D. (2001). Novel mechanisms in murine nitrofen-induced pulmonary hypoplasia: FGF-10 rescue in culture. Am J Physiol Lung Cell Mol Physiol **281**, L250-L257.

Adzick, N.S., Harrison, M.R., Glick, P.L., Nakayama, D.K., Manning, F.A. and deLorimier, A.A. (1985). Diaphragmatic hernia in the fetus: prenatal diagnosis and outcome in 94 cases. J Pediatr Surg **20**, 357-61.

Adzick, N. S., Outwater, K. M., Harrison, M. R., Davies, P., Glick, P. L., deLorimier, A. A., and Reid, L. M. (1985). Correction of congenital diaphragmatic hernia in utero. IV. An early gestational fetal lamb model for pulmonary vascular morphometric analysis. J Pediatr Surg **20,** 673-80.

Adzick, N. S., Vacanti, J. P., Lillehei, C. W., O'Rourke, P. P., Crone, R. K., and Wilson, J. M. (1989). Fetal diaphragmatic hernia: ultrasound diagnosis and clinical outcome in 38 cases. J Pediatr Surg **24,** 654-7.

Ahmad, A., Gangitano, E., Odell, R. M., Doran, R., and Durand, M. (1999). Survival, intracranial lesions, and neurodevelopmental outcome in infants with congenital diaphragmatic hernia treated with extracorporeal membrane oxygenation. J Perinatol **19,** 436-40.

Ahn, H.Y., Shin, J.C., Kim, Y.H., Ko, H.S., Park, I.Y., Kim, S.J., Rha, J.G. and Kim, S.P. (2005). Prenatal diagnosis of congenital diaphragmatic hernia in a fetus with 46,XY/46,X,-Y,+der(Y)t(Y;1)(q12;q12) mosaicism: a case report. J Korean Med Sci **20**, 895-8.

Albanese, C.T., Lopoo, J., Goldstein, R.B., Filly, R.A., Feldstein, V.A., Calen, P.W., Jennings, R.W., Farrell, J.A. and Harrison, M.R. (1998). Fetal liver position and perinatal outcome for congenital diaphragmatic hernia. Prenat Diagn **18**, 1138-1142.

Alcorn, D., Adamson, T.M., Lambert, T.F., Maloney, J.E., Ritchie, B.C. and Robinson, P.M. (1977). Morphological effects of chronic tracheal ligation and drainage in the fetal lamb lung. J Anat **123**, 649-60.

Alescio, T. (1968). The effect of the mesenchyme on epithelial morphogenesis in the in vitro development of mouse embryonal lung. Arch Ital Anat Embriol **73,** 295-319.

Alfanso, L.F., Arnaiz, A., Alvarez, F.J., Qi, B., Diez-Pardo, J.A., Vallis-i-Soler, A. and Tovar, J.A. (1995). Lung hypoplasia and surfactant system immaturity induced in the fetal rat by prenatal exposure to nitrofen. Biol Neonate **69**, 94-100.

Arca, M.J., Barnhart, D.C., Lelli, J.L. Jr., Greenfeld, J., Harmon, C.M., Hirschl, R.B. and Teitelbaum, D.H. (2003). Early experience with minimally invasive repair of congenital diaphragmatic hernias: results and lessons learned. J Pediatr Surg **38**, 1563-1568.

Arkovitz, M.S., Russo, M., Devine, P., Budhorick, N. and Stolar, C.J. (2007). Fetal lung-head ratio is not related to outcome for antenatal diagnosed congenital diaphragmatic hernia. J Pediatr Surg **42**, 107-10.

Arnold, J.H. (2000). High-frequency ventilation in the pediatric intensive care unit. Pediatr Crit Care Med **1**, 93-99.

Atkinson, J.B., Ford, E.G., Humphries, B., Kitagawa, H., Lew, C., Garg, M. and Bui, K. (1995). The impact of extracorporeal membrane support in the treatment of congenital diaphragmatic hernia. J Pediatr Surg **30**, 10-15.

Azarow, K., Messineo, A., Pearl, R., Filler, R., Barker, G. and Bohn, D. (1997). Congenital diaphragmatic hernia--a tale of two cities: the Toronto experience. J Pediatr Surg **32**, 395-400.

Ba'ath, M.E., Jesudason, E.C. and Losty, P.D. (2007). How useful is the lung-to-head ratio in predicting outcome in the fetus with congenital diaphragmatic hernia? A systematic review and meta-analysis. Ultrasound Obstet Gynecol **30**, 897-906.

Bagolan, P., Casaccia, G., Crescenzi, F., Nahom, A., Trucchi, A. and Giorlandino, C. (2004). Impact of a current treatment protocol on outcome of high-risk congenital diaphragmatic hernia. J Pediatr Surg **39**, 313-8.

Baird, G.S., Zacharias, D.A. and Tsien, R.Y. (1999). Circular permutation and receptor insertion within green fluorescent proteins. Proc Natl Acad Sci USA **96**, 11241-11246.

Baran, E. M., Houston, H. E., Lynn, H. B., and O'Connell, E. J. (1967). Foramen of Morgagni hernias in children. Surgery **62,** 1076-81.

Bartlett, R.H., Gazzaniga, A.B., Jefferies, M.R., Huxtable, R.F., Haiduc, N.J. and Fong, S.W. (1976). Extracorporeal membrane oxygenation (ECMO) cardiopulmonary support in infancy. Trans Am Soc Artif Intern Organs **22**, 80-93.

Bealer, J.F., Skarsgard, E.D., Hedrick, M.H., Meuli, M., VanderWall, K.J., Flake, A.W., Adzick, N.S. and Harrison, M.R. (1995). The 'PLUG' odyssey: adventures in experimental fetal tracheal occlusion. J Pediatr Surg **30**,361-4.

Beierle, E.A., Langham, M.R. Jr. and Cassin, S. (1996). In utero lung growth of fetal sheep with diaphragmatic hernia and tracheal stenosis. J Pediatr Surg **31**, 141-6.

Belaguli, N.S., Schildmeyer, L.A. and Schwartz, R.J. (1997). Organization and myogenic restricted expression of the murine serum response factor gene. A role for autoregulation. J Biol Chem **18**, 18222-31.

Belik, J., Davidge, S.T., Zhang, W., Pan, J. and Greer, J.J. (2003). Airway smooth muscle changes in the nitrofen-induced congenital diaphragmatic hernia rat model. Pediatr Res **22**, 295-304.

Bellusci, S., Grindley, J., Emoto, H., Itoh, N., and Hogan, B. L. (1997). Fibroblast growth factor 10 (FGF10) and branching morphogenesis in the embryonic mouse lung. Development **124,** 4867-78.

Benjamin, D. R., Juul, S., and Siebert, J. R. (1988). Congenital posterolateral diaphragmatic hernia: associated malformations. J Pediatr Surg **23,** 899-903.

Beresford, M. W., Shaw, N. J. (2000). Outcome of congenital diaphragmatic hernia. Pediatr Pulmonol **30,** 249-256.

Bergner, A. and Sanderson, M.J. (2002). Acetylcholine-induced calcium signaling and contraction of airway smooth muscle cells in lung slices. J Gen Physiol **119**, 187-98.

Berridge, M.J. (1997). The AM and FM of calcium signalling. Nature **386**, 759-760.

Berridge, M.J., Bootman, M.D. and Roderick, H.L. (2003). Calcium signalling: dynamics, homeostasis and remodelling. Nat Rev Mol Cell Biol **4**, 517-29.

Bhatt, A.J., Amin, S.B., Chess, P.R., Watkins, R.H. and Maniscalco, W.M. (2000). Expression of vascular endothelial growth factor and Flk-1 in developing and glucocorticoid-treated mouse lung. Pediatr Res **47**, 606-613.

Bianchi, A., Doig, C.M. and Cohen, S.J. (1983). The reverse latissimus dorsi flap for congenital diaphragmatic hernia repair. J Pediatr Surg **18**, 560-563.

Bilmen, J.G., Wootton, L.L., Godfrey, R.E., Smart, O.S. and Michelangeli, F. (2002). Inhibition of SERCA Ca^{2+} pumps by 2-aminoethoxydiphenyl borate (2-APB). 2-APB reduces both Ca^{2+} binding and phosphoryl transfer from ATP, by interfering with the pathway leading to the Ca^{2+}-binding sites. Eur J Biochem **269**, 3678-3687.

Blaisdell, C.J., Edmonds, R.D., Wang, X.T., Guggino, S. and Zeitlin, P.L. (2000). pH-regulated chloride secretion in fetal lung epithelia. Am J Physiol Lung Cell Mol Physiol **278**, L1248-55.

Blaisdell, C.J., Morales, M.M., Andrade, A.C., Bamford, P., Wasicko, M. and Welling, P. (2004). Inhibition of CLC-2 chloride channel expression interrupts expansion of fetal lung cysts. Am J Physiol Lung Cell Mol Physiol **286**, L420-6.

Bloss, R. S., Turmen, T., Beardmore, H. E., and Aranda, J. V. (1980). Tolazoline therapy for persistent pulmonary hypertension after congenital diaphragmatic hernia repair. J Pediatr **97,** 984-8.

Boas, S.R., Kurland, G., Greally, P.G. and Motoyama, E.K. (1996). Evolution of airway hyperresponsiveness in infants with severe congenital diaphragmatic hernia. Pediatr Pulmonol **22**, 295-304.

Bochdalek, V. A. (1848). Einige Betrachtungen uber die Entstehung des angeborenen Zwerchfellbruches. Als Beitrag zur pathologischen Anatomie der Ilernien. Vierteljahrschrift fur die praktische Heilkunde **19,** 89-97.

Boloker, J., Bateman, D.A., Wung, J.T. and Stolar, C.J. (2002). Congenital diaphragmatic hernia in 120 infants treated consecutively with permissive hypercapnea/spontaneous respiration/elective repair. J Pediatr Surg **37**, 357-366.

Borys, D. and Taxy, J.B. (2004). Congenital diaphragmatic hernia and chromosomal anomalies: autopsy study. Pediatr Dev Pathol **7**, 35-8.

Bos, A.P., Pattenier, A.M., Grobbee, R.E., Lindhout, D., Tibboel, D. and Molenaar, J.C. (1994). Etiological aspects of congenital diaphragmatic hernia: results of a case comparison study. Hum Genet **94**, 445-6.

Boyden, E.A. (1977) Development and growth of the airways. In: Hodson, W.A. ed. Lung Biology in Health and Disease. Development of the Lung. Vol 6. New York: Dekker, 3-35.

Boyle, J.P., Tomasic, M. and Kotlikoff, M.I. (1992). Delayed rectifier potassium channels in canine and porcine airway smooth muscle cells. J Physiol **447**, 329-50.

Brandsma, A. E., Tenbrinck, R., Ijsselstijn, H., Scheffers, E. C., Gaillard, J. L. J., Kluth, D., Have-Opbroek, A. A. W., Lachmann, B. and Tibboel, D. (1995). Congenital diaphragmatic hernia: new models, new ideas. Pediatr Surg Int **10**, 10-15.

Browning, C.L., Culberson, D.E., Aragon, I.V., Fillmore, R.A., Croissant, J.D., Schwartz, R.J. and Zimmer, W.E. (1998). The developmentally regulated expression of serum response factor plays a key role in the control of smooth muscle-specific genes. Dev Biol **194**, 18-37.

Buch, S., Jones, C., Sweezey, N., Tanswell, K. and Post, M. (1991). Platelet-derived growth factor and growth-related genes in rat lung. I. Developmental expression. Am J Respir Cell Mol Biol **5**, 371-376.

Burdyga, T., Shmygol, A., Eisner, D.A. and Wray, S. (2003). A new technique for simultaneous and in situ measurements of Ca2+ signals in arteriolar smooth muscle and endothelial cells. Cell Calcium **34**, 27-33.

Burdyga, T.V. and Wray, S. (1999). The relationship between the action potential, intracellular calcium and force in intact phasic, guinea-pig uretic smooth muscle. J Physiol **520**, 867-883.

Burdyga, T.V. and Wray, S. (2002). On the mechanisms whereby temperature affects excitation-contraction coupling in smooth muscle. J Gen Physiol **119**, 93-104.

Burge, D.M., Atwell, J.D. and Freeman, N.V. (1989). Could the stomach site help predict outcome in babies with left sided congenital diaphragmatic hernia diagnosed antenatally? J Pediatr Surg **24**, 567-9.

Burnstock, G. (1979). Structure of smooth muscle and its innervation. In: Brading, A., Jones, A.E. and Tomita, T. (eds) Smooth Muscle, Arnold, London, pp 1-69.

Cacciari, A., Ruggeri, G., Mordenti, M., Ceccarelli, P.L., Baccarini, E., Pigna, A. and Gentili, A. (2001). High-frequency oscillatory ventilation versus conventional mechanical ventilation in congenital diaphragmatic hernia. Eur J Pediatr Surg **11**, 3-7.

Cannie, M., Jani, J., De Keyzer, F., Van Kerkhove, F., Meersschaert, J., Lewi, L., Deprest, J. and Dymarkowski, S. (2008). Magnetic resonance imaging of the fetal lung: a pictorial essay. Eur Radiol (epub ahead of print).

Chalfie, M., Tu, Y., Euskirchen, G., Ward, W.W. and Prasher, D.C. (1994). Green fluorescent protein as a marker for gene expression. Science **263**, 802-805.

Chen, J., Knowles, H. J., Herbert, J. L., and Hackett, B. P. (1998). Mutation of the mouse hepatocyte nuclear factor / forkhead homologue 4 gene results in absence of cilia and random left-right assymmetry. J Clin Invest **102,** 1077-1082.

Clark, R. H., Hardin, W. D., Jr., Hirschl, R. B., Jaksic, T., Lally, K. P., Langham, M. R., Jr., and Wilson, J. M. (1998). Current surgical management of congenital diaphragmatic hernia: a report from the Congenital Diaphragmatic Hernia Study Group. J Pediatr Surg **33,** 1004-9.

Clarke, L.L., Grubb, B.R., Yankaskas, J.R., Cotton, C.U., McKenzie, A. and Boucher, R.C. (1994). Relationship of a non-cystic fibrosis transmembrane conductance regulator-mediated chloride conductance to organ-level disease in Cftr(-/-) mice. Proc Natl Acad Sci USA **91**, 479-83.

Colen, K.L., Crisera, C.A., Rose, M.I., Connelly, P.R., Longaker, M.T. and Gittes, G.K. (1999). Vascular development in the mouse embryonic pancreas and lung. J Pediatr Surg **34**, 781-785.

Colvin, J., Bower, C., Dickinson, J.E., and Sokol, J. (2005). Outcomes of congenital diaphragmatic hernia: a population-based study in Western Australia. Pediatrics **116**, e356-63.

Copland, I. and Post, M. (2004). Lung development and fetal lung growth. Paediatr Respir Rev **5**, S259-64.

Crapo, R.O., Morris, A.H. and Gardner, R.M. (1982). Reference values for pulmonary tissue volume, membrane diffusing capacity, and pulmonary capillary blood volume. Bull Eur Physiopathol Respir **18**, 893-9.

D'Agostino, J. A., Bernbaum, J. C., Gerdes, M., Schwartz, I. P., Coburn, C. E., Hirschl, R. B., Baumgart, S., and Polin, R. A. (1995). Outcome for infants with congenital diaphragmatic hernia requiring extracorporeal membrane oxygenation: the first year. J Pediatr Surg **30,** 10-5.

de Lorimier, A. A., Tierney, D. F., and Parker, H. R. (1967). Hypoplastic lungs in fetal lambs with surgically produced CDH. Surgery **62,** 12-16.

De Paepe, M.E., Johnson, B.D., Papadakis, K., Sueishi, K. and Luks, F.I. (1998). Temporal pattern of accelerated lung growth after tracheal occlusion in the fetal rabbit. Am J Pathol **152**, 179-90.

Der-Silaphet, T., Malysz, J., Hagel, S., Larry Arsenault, A. and Huizinga, J.D. (1998). Interstitial cells of cajal direct normal propulsive contractile activity in the mouse small intestine. Gastroenterology **114**, 724-36.

de Vries JI, Visser GH, Prechtl HF (1986). Fetal behaviour in early pregnancy. Eur J Obstet Gynecol Reprod Biol **21**, 271-276.

Deprest, J., Jani, J., Gratacos, E., Vandecruys, H., Naulaers, G., Delgado, J., Greenough, A. and Nicolaides, K.; FETO Task Group (2005). Fetal intervention for congenital diaphragmatic hernia: the European experience. Semin Perinatol **29**, 94-103.

Diegelmann, S., Fiala, A., Leibold, C., Spall, T. and Buchner, E. (2002). Transgenic flies expressing the fluorescence calcium sensor Cameleon 2.1 under UAS control. Genesis **34**, 95-98.

DiFiore, J. W., Fauza, D. O., Slavin, R., Peters, C. A., Fackler, J. C., and Wilson, J. M. (1994). Experimental fetal tracheal ligation reverses the structural and physiological effects of pulmonary hypoplasia in congenital diaphragmatic hernia. J Pediatr Surg **29,** 248-56.

Dillon, E., Renwick, M. and Wright, C. (2000). Congenital diaphragmatic herniation: antenatal detection and outcome. Br J Radiol **73**, 360-5.

Downard, C.D., Jaksic, T., Garza, J.J., Dzakovic, A., Nemes, L., Jennings, R.W. and Wilson, J.M. (2003). Analysis of an improved survival rate for congenital diaphragmatic hernia. J Pediatr Surg **38**, 729-732.

Duthie, H.L. (1974). Electrical activity of gastrointestinal smooth muscle. Gut **15**, 669-81.

Edmonds, R.D., Silva, I.V., Guggino, W.B., Butler, R.B., Zeitlin, P.L. and Blaisdell, C.J. (2002). ClC-5: ontogeny of an alternative chloride channel in respiratory epithelia. Am J Physiol Lung Cell Mol Physiol **282**, L501-7.

Elbourne, D., Field, D. and Mugford, M. (2002. Extracorporeal membrane oxygenation for severe respiratory failure in newborn infants. Cochrane Database Syst Rev **1**, CD001340.

Endo, M. (1977). Calcium release from the sarcoplasmic reticulum. Physiol Rev **57**, 71-108.

Fauza, D.O., Hirschl, R.B. and Wilson, J.M. (2001). Continuous intrapulmonary distension with perfluorocarbon accelerates lung growth in infants with congenital diaphragmatic hernia: initial experience. J Pediatr Surg **36**,1237-40.

Fauza, D. O., Tannuri, U., Ayoub, A. A., Capelozzi, V. L., Saldiva, P. H., and Maksoud, J. G. (1994). Surgically produced congenital diaphragmatic hernia in fetal rabbits. J Pediatr Surg **29,** 882-6.

Featherstone, N.C., Jesudason, E.C., Connell, M.G., Fernig, D.G., Wray, S., Losty, P.D. and Burdyga, T.V. (2005). Spontaneous propagating calcium waves underpin airway peristalsis in embryonic rat lung. Am J Respir Cell Mol Biol **33**, 153-60.

Featherstone, N.C., Connell, M.G., Fernig, D.G., Wray, S., Burdyga, T.V., Losty, P.D. and Jesudason, E.C. (2006). Airway smooth muscle dysfunction precedes teratogenic congenital diaphragmatic hernia and may contribute to hypoplastic lung morphogenesis. Am J Respir Cell Mol Biol **35**, 1-8.

Fewell JE, Hislop AA, Kitterman JA, Johnson P (1983). Effect of tracheostomy on lung development in fetal lambs. J Appl Physiol **55**, 1103-1108.

Fiala, A., Spall, T., Diegelmann, S., Eisermann, B., Sachse, S., Devaud, J.M., Buchner, E. and Galizia, C.G. (2002). Genetically expressed cameleon in Drosophila melanogaster is used to visualize olfactory information in projection neurons. Curr Biol **12**, 1877-1884.

Fill, M. and Copello, J.A. (2002). Ryanodine receptor calcium release channels. Physiol Rev **82**, 893-922.

Finer, N.N. and Barrington, K.J. (2000). Nitric oxide for respiratory failure in infants born at or near term. Cochrane Database Syst Rev **2**, CD000399.

Gabriel, S.E., Clarke, L.L., Boucher, R.C. and Stutts, M.J. (1993). CFTR and outward rectifying chloride channels are distinct proteins with a regulatory relationship. Nature **363**, 263-8.

Garne, E., Haeusler, M., Barisic, I., Gjergja, R., Stoll, C. and Clementi, M.; Euroscan Study Group (2002). Congenital diaphragmatic hernia: evaluation of prenatal diagnosis in 20 European regions. Ultrasound Obstet Gynecol **19**, 329-33.

Garne, E., Loane, M., Dolk, H., De Vigan, C., Scarano, G., Tucker, D., Stoll, C., Gener, B., Pierini, A., Nelen, V., Rösch, C., Gillerot, Y., Feijoo, M., Tincheva, R., Queisser-Luft, A., Addor, M.C., Mosquera, C., Gatt, M. and Barisic, I. (2005). Prenatal diagnosis of severe structural congenital malformations in Europe. Ultrasound Obstet Gynecol **25**, 6-11.

Gebb, S. A., and Shannon, J. M. (2000). Tissue interactions mediate early events in pulmonary vasculogenesis. Dev Dyn **217,** 159-69.

Gee, K.R., Brown, K.A., Chen, W.N., Bishop-Stewart, J., Gray, D, and Johnson, I. (2000). Chemical and physiological characterization of fluo-4 $Ca^{(2+)}$-indicator dyes. Cell Calcium **27**, 97-106.

Gehr, P., Bachofen, M. and Weibel, E.R. (1978). The normal human lung: ultrastructure and morphometric estimation of diffusion capacity. Respir Physiol **32**, 121-40.

Ghabrial, A., Luschnig, S., Metzstein, M.M. and Krasnow, M.A. (2003). Branching morphogenesis of the Drosophila tracheal system. Annu Rev Cell Dev Biol **19**, 623-47.

Goldstein, J.D. and Reid, L.M. (1980). Pulmonary hypoplasia resulting from phrenic nerve agenesis and diaphragmatic amyoplasia. J Pediatr **97**, 282-287.

Greenwood, I.A. and Large, W.A. (1995). Comparison of the effects of fenamates on Ca-activated chloride and potassium currents in rabbit portal vein smooth muscle cells. Br J Pharmacol **116**, 2939-48.

Greenwood, I.A. and Leblanc, N. (2007). Overlapping pharmacology of Ca2+-activated Cl- and K+ channels. Trends Pharmacol Sci **28**, 1-5.

Greer, J.J., Babiuk, R.P. and Thebaus, B. (2003). Etiology of congenital diaphragmatic hernia: the retinoid hypothesis. Pediatr Res **53**: 726-730.

Griscom, N.T., Harris, G.B., Wohl, M.E., Vawter, G.F. and Eraklis, A.J. (1969). Fluid-filled lung due to airway obstruction in the newborn. Pediatrics **43**, 383-390.

Gross, I., and Wilson, C. M. (1983). Fetal rat lung maturation: initiation and modulation. J Appl Physiol **55,** 1735-1732.

Gross, R.E. (1946). Congenital hernia of the diaphragm. Am J Dis Child 71, 579-592.Hall, S.M., Hislop, A.A. and Haworth, S.G. (2002). Origin, differentiation, and maturation of human pulmonary veins. Am J Respir Cell Mol Biol **26**, 333-340.

Grynkiewicz, G., Poenie, M. and Tsien, R.Y. (1985). A new generation of Ca^{2+} indicators with greatly improved fluorescence properties. J Biol Chem **260**, 3440-50.

Haller, J.A. Jr., Signer, R.D., Golladay, E.S., Inon, A.E., Harrington, D.P. and Shermeta, D.W. (1976). Pulmonary and ductal hemodynamics in studies of simulated diaphragmatic hernia of fetal and newborn lambs. J Pediatr Surg **11**, 675-680.

Harding, R. (1991). Fetal breathing movements. in The Lung: Scientific Foundations. Crystal, R.G. and West, J.B. editors. Raven Press, New York. 1655-1663.

Harding, R., Bocking, A.D. and Sigger, J.N. (1986). Influence of upper respiratory tract on liquid flow to and from fetal lungs. J Appl Physiol **61**, 68-74.

Harding, R., and Hooper, S. B. (1996). Regulation of lung expansion and lung growth before birth. J Appl Physiol **81,** 209-224.

Harrison, M. R., Adzick, N. S., Bullard, K. M., Farrell, J. A., Howell, L. J., Rosen, M. A., Sola, A., Goldberg, J. D., and Filly, R. A. (1997). Correction of congenital diaphragmatic hernia in utero VII: a prospective trial. J Pediatr Surg **32,** 1637-42.

Harrison, M. R., Adzick, N. S., Flake, A. W., Jennings, R. W., Estes, J. M., MacGillivray, T. E., Chueh, J. T., Goldberg, J. D., Filly, R. A., Goldstein, R. B., et al. (1993). Correction of congenital diaphragmatic hernia in utero: VI. Hard-earned lessons. J Pediatr Surg **28,** 1411-7.

Harrison, M. R., Bressack, M. A., Churg, A. M., and de Lorimier, A. A. (1980a). Correction of congenital diaphragmatic hernia in utero. II. Simulated correction permits fetal lung growth with survival at birth. Surgery **88,** 260-8.

Harrison, M. R., Jester, J. A., and Ross, N. A. (1980b). Correction of congenital diaphragmatic hernia in utero. I. The model: intrathoracic balloon produces fatal pulmonary hypoplasia. Surgery **88,** 174-82.

Harrison, M.R., Keller, R.L., Hawgood, S.B., Kitterman, J.A., Sandberg, P.L., Farmer, D.L., Lee, H., Filly, R.A., Farrell, J.A. and Albanese, C.T. (2003). A randomized trial of fetal endoscopic tracheal occlusion for severe fetal congenital diaphragmatic hernia. N Engl J Med **349**, 1916-24.

Hashitani, H., Fukuta, H., Takano, H., Klemm, M.F. and Suzuki, H. (2001). Origin and propagation of spontaneous excitation in smooth muscle of the guinea-pig urinary bladder. J Physiol **530**, 273-86.

Hashitani, H., Yanai, Y. and Suzuki, H. (2004). Role of interstitial cells and gap junctions in the transmission of spontaneous Ca2+ signals in detrusor smooth muscles of the guinea-pig urinary bladder. J Physiol **559**, 567-81.

Haugen, S.E., Linker, D., Eik-Nes, S., Kufaas, T., Vik, T., Eggen, B.M. and Brubakk, A.M. (1991). Congenital diaphragmatic hernia: determination of the optimal time for operation by echocardiographic monitoring of the pulmonary arterial pressure. J Pediatr Surg **26**, 560-2.

Healy, A.M., Morgenthau, L., Zhu, X., Farber, H.W. and Cardoso, W.V. (2000). VEGF is deposited in the subepithelial matrix at the leading edge of branching airways and stimulates neovascularization in the murine embryonic lung. Dev Dyn **219**, 341-352.

Hedrick, M.H., Estes, J.M., Sullivan, K.M., Bealer, J.F., Kitterman, J.A., Flake, A.W., Adzick, N.S. and Harrison, M.R. (1994). Plug the lung until it grows (PLUG): a new method to treat congenital diaphragmatic hernia in utero. J Pediatr Surg **29**, 612-7.

Heerema, A.E., Rabban, J.T., Sydorak, R.M., Harrison, M.R. and Jones, K.D. (2003). Lung pathology in patients with congenital diaphragmatic hernia treated with fetal surgical intervention, including tracheal occlusion. Pediatr Dev Pathol **6**, 536-46.

Hentsch, B., Lyons, I., Li, R., Hartley, L., Lints, T. J., Adams, J. M., and Harvey, R. P. (1996). *Hlx* homeo box gene is essential for an inductive tissue interaction that drives expansion of embryonic liver and gut. Genes Dev **10,** 70-79.

Hirschl, R.B., Philip, W.F., Glick, L., Greenspan, J., Smith, K., Thompson, A., Wilson, J. and Adzick, N.S. (2003). A prospective, randomized pilot trial of perfluorocarbon-induced lung growth in newborns with congenital diaphragmatic hernia. J Pediatr Surg **38**, 283-9.

Hirst, G.D. and Ward, S.M. (2003). Interstitial cells: involvement in rhythmicity and neural control of gut smooth muscle. J Physiol **550**, 337-46.

Holbolth, N. (1962). Drugs and congenital abnormalities. Lancet **2**, 1333-1334.

Hogan, B. L. (1999). Morphogenesis. Cell **96,** 225-33.

Holzapfel, C.W. (1968). The isolation and structure of cyclopiazonic acid, a toxic metabolite of Penicillium cyclopium Westling. Tetrahedon **24**, 2101-19.

Hoffmann, C. and Faure, A. (1966). Reactions de l'acide chloro-2 nicotinique (1er memoire). Condesations avec les amines aromatiques. Bull Soc Chim France **7**, 2316-2319.

Hubbard, A.M., Crombleholme, T.M., Adzick, N.S., Coleman, B.G., Howell, L.J., Meyer, J.S. and Flake, A.W. (1999). Prenatal MRI evaluation of congenital diaphragmatic hernia. Am J Perinatol **16**, 407-413.

Huizinga, J.D. and Lammers, W.J. (2009). Gut peristalsis is governed by a multitude of cooperating mechanisms. Am J Physiol Gastrointest Liver Physiol **296**, G1-8.

Ikeda, K., Clark, J.C., Shaw-White, J.R., Stahlman, M.T., Boutell, C.J. and Whitsett, J.A. (1995). Gene structure and expression of human thyroid transcription factor-1 in respiratory epithelial cells. J Biol Chem **270**, 8108-8114.

Iritani, I. (1984). Experimental study on embryogenesis of congenital diaphragmatic hernia. Anat Embryol (Berl) **169,** 133-9.

Jesudason, E.C. (2001). Embryonic lung development in an experimental model of congenital diaphragmatic hernia (CDH). MD Thesis, University of Liverpool, UK.

Jesudason, E.C. (2002). Challenging embryological theories on congenital diaphragmatic hernia: future therapeutic implications for paediatric surgery. Ann R Coll Surg Engl **84**, 252-9.

Jesudason, E.C. (2006). Small lungs and suspect smooth muscle. J Pediatr Surg **41**, 431-435.

Jesudason, E. C., Connell, M. G., Fernig, D. G., Lloyd, D. A., and Losty, P. D. (2000). Early lung malformations in congenital diaphragmatic hernia. *J Pediatr Surg* **35,** 124-7.

Jesudason, E.C., Smith, N.P., Connell, M.G., Spiller, D.G., White, M.R., Fernig, D.G. and Losty, P.D. (2005). Developing rat lung has a sided pacemaker region for morphogenesis-related airway peristalsis. Am J Respir Cell Mol Biol **32**, 118-27.

Jesudason, E.C., Smith, N.P., Connell, M.G., Spiller, D.G., White, M.R., Fernig, D.G. and Losty, P.D. (2006). Peristalsis of airway smooth muscle is developmentally regulated and uncoupled from hypoplastic lung growth. Am J Physiol Lung Cell Mol Physiol **291**, L559-65.

Jobe, A.H. and Bancalari, E. (2001). Bronchopulmonary dysplasia. Am J Respir Crit Care Med **163**, 1723-1729.

Jostarndt-Fögen, K., Djonov, V. and Draeger, A. (1998). Expression of smooth muscle markers in the developing murine lung: potential contractile properties and lineal descent. Histochem Cell Biol **110**, 273-84.

Kang, Y. J., Zolna, L., and Manson, J. M. (1986). Strain differences in response of Sprague-Dawley and Long Evans Hooded rats to the teratogen nitrofen. Teratology **34,** 213-23.

Karl, S.R., Ballantine, T.V. and Snider, M.T. (1983). High-frequency ventilation at rates of 375 to 1800 cycles per minute in four neonates with congenital diaphragmatic hernia. J Pediatr Surg **18**, 822-828.

Kao, J.P. (1994). Practical aspects of measuring [Ca2+] with fluorescent indicators. Methods Cell Biol **40**, 155-81.

Kays, D. W., Langham, M. R., Jr., Ledbetter, D. J., and Talbert, J. L. (1999). Detrimental effects of standard medical therapy in congenital diaphragmatic hernia. *Ann Surg* **230,** 340-8.

Keijzer, R., Liu, J., Deimling, J., Tibboel, D., and Post, M. (2000). Dual-Hit Hypothesis ExplainsPulmonary Hypoplasia in the Nitrofen Model of Congenital Diaphragmatic Hernia. Am J Pathol **156,** 1299-1306.

Keijzer, R., van Tuyl, M., Meijers, C., Post, M., Tibboel, D., Grosveld, F. and Koutsourakis, M. (2001). The transcription factor GATA6 is essential for branching morphogenesis and epithelial cell differentiation during fetal pulmonary development. Development **128**, 503-11.

Keller, R.L., Glidden, D.V., Paek, B.W., Goldstein, R.B., Feldstein, V.A., Callen, P.W., Filly, R.A. and Albanese, C.T. (2003). The lung-to-head ratio and fetoscopic temporary tracheal occlusion: prediction of survival in severe left congenital diaphragmatic hernia. Ultrasound Obstet Gynecol **21**, 244-9.

Keller, R.L., Hawgood, S., Neuhaus, J.M., Farmer, D.L., Lee, H., Albanese, C.T., Harrison, M.R. and Kitterman, J.A. (2004). Infant pulmonary function in a randomized trial of fetal tracheal occlusion for severe congenital diaphragmatic hernia. Pediatr Res **56**, 818-25.

Kieffer, J., Sapin, E., Berg, A., Beaudoin, S., Bargy, F., and Helardot, P. G. (1995). Gastroesophageal reflux after repair of congenital diaphragmatic hernia. J Pediatr Surg **30,** 1330-3.

Kim, S., Ip, H.S., Lu, M.M., Clendenin, C. and Parmacek, M.S. (1997). A serum response factor-dependent transcriptional regulatory program identifies distinct smooth muscle cell sublineages. Mol Cell Biol **17**, 2266-78.

Kimura, S., Hara, Y., Pineau, T., Fernandez-Salguero, P., Fox, C.H., Ward, J.M. and Gonzalez, F.J. (1996). The T/ebp null mouse: thyroid-specific enhancer-binding protein is essential for the organogenesis of the thyroid, lung, ventral forebrain, and pituitary. Genes Dev **10**, 60-69.

Kitagawa, M., Hislop, A., Boyden, E. A., and Reid, L. (1971). Lung hypoplasia in congenital diaphragmatic hernia. A quantitative study of airway, artery, and alveolar development. Br J Surg **58,** 342-6.

Kitano Y (2007). Prenatal intervention for congenital diaphragmatic hernia. Semin Pediatr Surg **16**, 101-8.

Kitterman, J.A. (1986). Physical factors and fetal lung growth. *In* Respiratory Control and Lung Development in the Fetus and Newborn. Johnston, B.M. and Gluckman, P.D., editors. Perinatology Press, Ithica, NY, 63-85.

Kluth, D., Kangah, R., Reich, P., Tenbrinck, R., Tibboel, D., and Lambrecht, W. (1990). Nitrofen-induced diaphragmatic hernias in rats: an animal model. J Pediatr Surg **25,** 850-4.

Kluth, D., Tenbrinck, R., von Ekesparre, M., Kangah, R., Reich, P., Brandsma, A., Tibboel, D., and Lambrecht, W. (1993). The natural history of congenital diaphragmatic hernia and pulmonary hypoplasia in the embryo. J Pediatr Surg **28,** 456-62.

Kluth, D., Keijzer, R., Hertl, M., and Tibboel, D. (1996a). Embryology of congenital diaphragmatic hernia. Semin Pediatr Surg **5,** 224-33.

Kluth, D., Losty, P. D., Schnitzer, J. J., Lambrecht, W., and Donahoe, P. K. (1996b). Toward understanding the developmental anatomy of congenital diaphragmatic hernia. Clin Perinatol **23,** 655-69.

Koblizek, T.I., Weiss, C., Yancopoulos, G.D., Deutsch, U., Risau, W. (1998). Angiopoietin-1 induces sprouting angiogenesis in vitro. Curr Biol **8**, 529-532.

Kohler, G., Tressel, W., Dell, H.D., Doersing, M., Fischer, R., Kamp, R., Langer, M., Richter, B. and Wirzbach, E. (1992). Plasm- and tissue concentrations following intramuscular administration of etofenamat. Pharmacokinetics of etofenamat and flufenamic acid in plasma, synovium, and tissues of patients with chronic polyarthritis after administration of an oily solution of etofenamat. Arzneimittelforschung **42**, 1487-1491.

Korn, S.J., Bolden, A. and Horn, R. (1991). Control of action potentials and Ca^{2+} influx by the Ca2+-dependent chloride current in mouse pituitary cells. J Physiol **439**, 423-437.

Kosterin, S.A., Babich, L.G., Shlykov, S.G. and Rovenets, N.A. (1996). Mg^{2+},ATP-dependent transport of Ca^{2+} in the endoplasmic reticulum of myometrial cells. Biokhimiia **61**, 73-81.

Kotlikoff, M.I. and Wang, Y.X. (1998). Calcium release and calcium-activated chloride channels in airway smooth muscle cells. Am J Crit Care Med **158**, S109--S114.

Kreidberg, J. A., Sariola, H., Loring, J. M., Maeda, M., Pelletier, J., Housman, D., and Jaenisch, R. (1993). WT-1 is required for early kidney development. Cell **74,** 679-691.

Kufeji, D.I. and Crabbe, D.C. (1999). Familial bilateral congenital diaphragmatic hernia. Pediatr Surg Int **15**, 58-60.

Lally, K.P., Bagolan, P., Hosie, S., Lally, P.A., Stewart, M., Cotton, C.M., Van Meurs, K.P. and Alexander, G.; Congenital Diaphragmatic Hernia Study Group (2006). Corticosteroids for fetuses with congenital diaphragmatic hernia: can we show benefit?. J Pediatr Surg **41**, 668-74.

Lamb, F.S., Graeff, R.W., Clayton, G.H., Smith, R.L., Schutte, B.C. and McCray, P.B. Jr. (2001). Ontogeny of CLCN3 chloride channel gene expression in human pulmonary epithelium. Am J Respir Cell Mol Biol **24**, 376-81.

Lang, R.J., Hashitani, H., Tonta, M.A., Parkington, H.C. and Suzuki, H. (2007). Spontaneous electrical and Ca2+ signals in typical and atypical smooth muscle cells and interstitial cell of Cajal-like cells of mouse renal pelvis. J Physiol **583**, 1049-1068.

Lang, R.J., Tonta, M.A., Zoltkowski, B.Z., Meeker, W.F., Wendt, I. and Parkington, H.C. (2006). Pyeloureteric peristalsis: role of atypical smooth muscle cells and interstitial cells of Cajal-like cells as pacemakers. J Physiol **576**, 695-705.

Langer, J.C., Filler, R.M., Bohn, D.J., Shandling, B., Ein, S.H., Wesson, D.E. and Superina, R.A. (1988). Timing of surgery for congenital diaphragmatic hernia: is emergency operation necessary? J Pediatr Surg **23**, 731-4.

Langston, C., Kida, K., Reed, M. and Thurlbeck, W.M. (1984). Human lung growth in late gestation and in the neonate. Am Rev Respir Dis **129**, 607-13.

Laudy, J.A., Van Gucht, M., Van Dooren, M.F., Wladimiroff, J.W. and Tibboel, D. (2003). Congenital diaphragmatic hernia: an evaluation of the prognostic value of the lung-to-head ratio and other prenatal parameters. Prenat Diagn **23**, 634-9.

Lebeche D, Malpel S and Cardoso WV (1999). Fibroblast growth factor interactions in the developing lung. Mech Dev **86**, 125-136.

Lewis, M. (1924). Spontaneous rhythmical contraction of the muscles of the bronchial tubes and air sacs of the chick embryo. Am J Physiol **68**, 385-388.

Levine, D., Barnewolt, C.E., Mehta, T.S., Trop, I., Estroff, J. and Wong, G. (2003). Fetal thoracic abnormalities: MR imaging. Radiology **228**, 379-388.

Liggins, G.C., Vilos, G.A., Campos, G.A., Kitterman, J.A. and Lee, C.H. (1981a). The effect of bilateral thoracoplasty on lung development in fetal sheep. J Dev Physiol **3**, 275-82.

Liggins, G.C., Vilos, G.A., Campos, G.A., Kitterman, J.A. and Lee, C.H. (1981b). The effect of spinal cord transection on lung development in fetal sheep.. J Dev Physiol **3**, 267-74.

Lipsett, J., Cool, J.C., Runciman, S.I., Ford, W.D., Kennedy, J.D. and Martin, A.J. (1998). Effect of antenatal tracheal occlusion on lung development in the sheep model of congenital diaphragmatic hernia: a morphometric analysis of pulmonary structure and maturity. Pediatr Pulmonol **25**, 257-69.

Lipsett, J., Cool, J. C., Runciman, S. I., Ford, W. D., Kennedy, J. D., Martin, A. J., and Parsons, D. W. (2000). Morphometric analysis of preterm fetal pulmonary development in the sheep model of congenital diaphragmatic hernia. Pediatr Dev Pathol **3,** 17-28.

Lipshutz, G.S., Albanese, C.T., Feldstein, V.A., Jennings, R.W., Housley, H.T., Beech, R., Farrell, J.A. and Harrison, M.R. (1997). Prospective analysis of lung-to-head ratio predicts survival for patients with prenatally diagnosed congenital diaphragmatic hernia. J Pediatr Surg **32**, 1634-6.

Lipskaia, L. and Lompré, A.M. (2004). Alteration in temporal kinetics of Ca2+ signaling and control of growth and proliferation. Biol Cell **96**, 55-68.

Lipskaia, L., Pourci, M.L., Deloménie, C., Combettes, L., Goudounèche, D., Paul, J.L., Capiod, T. and Lompré, A.M. (2003). Phosphatidylinositol 3-kinase and calcium-activated transcription pathways are required for VLDL-induced smooth muscle cell proliferation. Circ Res **92**, 1115-22.

Liu HN, Ohya S, Furuzono S, Wang J, Imaizumi Y, Nakayama S (2005a). Co-contribution of IP3R and Ca2+ influx pathways to pacemaker Ca2+ activity in stomach ICC. J Biol Rhythms **20**, 15-26.

Liu, H.N., Ohya, S., Wang, J., Imaizumi, Y. and Nakayama, S. (2005b). Involvement of ryanodine receptors in pacemaker Ca2+ oscillation in murine gastric ICC. Biochem Piophys Res Commun **328**, 640-646.

Liu, J., Zhang, L., Wang, D., Shen, H., Jiang, M., Mei, P., Hayden, P.S., Sedor, J.R. and Hu, H. (2003). Congenital diaphragmatic hernia, kidney agenesis and cardiac defects associated with Slit3-deficiency in mice. Mech Dev **120**, 1059-1070.

Liu, M., Skinner, S.J., Xu, J., Han, R.N., Tanswell, A.K. and Post, M. (1992). Stimulation of fetal rat lung cell proliferation in vitro by mechanical stretch. Am J Physiol **263**, L376-83.

Liu, M., Qin, Y., Liu, J., Tanswell, A.K. and Post, M. (1996). Mechanical strain induces pp60src activation and translocation to cytoskeleton in fetal rat lung cells. J Biol Chem **271**, 7066-71.

Liu, M., Xu, J., Souza, P., Tanswell, B., Tanswell, A.K. and Post, M. (1995). The effect of mechanical strain on fetal rat lung cell proliferation: comparison of two- and three-dimensional culture systems. In Vitro Cell Dev Biol Anim **31**, 858-66.

Logan, J.W., Rice, H.E., Goldberg, R.N. and Cotton, C.M. (2007). Congenital diaphragmatic hernia: a systematic review and summary of best-evidence practice strategies. J Perinatol **27**, 535-49.

Lohnes, D., Mark, M., Mendelsohn, C., Dolle, P., Dierich, A., Gorry, P., Gansmuller, A., and Chambon, P. (1994). Function of the retinoic acid receptors (RARs) during development (I). Craniofacial and skeletal abnormalities in RAR double mutants. Development **120,** 2723-48.

Losty, P. D., Pacheco, B. A., Manganaro, T. F., Donahoe, P. K., Jones, R. C., and Schnitzer, J. J. (1996b). Prenatal hormonal therapy improves pulmonary morphology in rats with congenital diaphragmatic hernia. J Surg Res **65,** 42-52.

Lund, D. P., Mitchell, J., Kharasch, V., Quigley, S., Kuehn, M., and Wilson, J. M. (1994). Congenital diaphragmatic hernia: the hidden morbidity. J Pediatr Surg **29,** 258-62.

Mailleux, A.A., Kelly, R., Veltmaat, J.M., De Langhe, S.P., Zaffran, S., Thiery, J.P. and Bellusci, S. (2005). Fgf10 expression identifies parabronchial smooth muscle cell progenitors and is required for their entry into the smooth muscle cell lineage. Development **132**, 2157-66.

Maisonpierre, P.C., Suri, C., Jones, P.F., Bartunkova, S., Wiegand, S.J., Radziejewski, C., Compton, D., McClain, J., Aldrich, T.H., Papadopoulos, N., Daly, T.J., Davis, S., Sato, T.N. and Yancopoulos, G.D. (1997). Angiopoietin-2, a natural antagonist for Tie2 that disrupts in vivo angiogenesis. Science **277**, 55-60.

Maruyama, T., Kanaji, T., Nakade, S., Kanno, T. and Mikoshiba, K. (1997). 2APB, 2-aminoethoxydiphenyl borate, a membrane-penetrable modulator of Ins(1,4,5)P3-induced Ca^{2+} release. J Biochem (Tokyo) **122**, 498-505.

Masters, J. R. (1976). Epithelial-mesenchymal interaction during lung development: the effect of mesenchymal mass. *Dev Biol* **51,** 98-108.

McAteer, J. A., Cavanagh, T. J., and Evan, A. P. (1983). Submersion culture of the intact fetal lung. In Vitro **19,** 210-218.

McCarty, N.A., McDonough, S., Cohen, B.N., Riordan, J.R., Davidson, N. and Lester, H.A. (1993). Voltage-dependent block of the cystic fibrosis transmembrane conductance regulator Cl- channel by two closely related arylamaminobenzoates. J Gen Physiol **102**, 1-23.

McCray, P.B. Jr. (1993). Spontaneous contractility of human fetal airway smooth muscle. Am J Respir Cell Mol Biol **8**, 573-80.

McCray, P.B. Jr., Bettencourt, J.D. and Bastacky, J. (1992). Secretion of lung fluid by the developing fetal rat alveolar epithelium in organ culture. Am J Respir Cell Mol Biol **6**, 609-16.

McGahren, E.D., Mallik, K. and Rodgers, B.M. (1997). Neurological outcome is diminished in survivors of congenital diaphragmatic hernia requiring extracorporeal membrane oxygenation. J Pediatr Surg **32**, 1216-20.

Mendelsohn, C., Lohnes, D., Decimo, D., Lufkin, T., LeMeur, M., Chambon, P., and Mark, M. (1994). Function of the retinoic acid receptors (RARs) during development (II). Multiple abnormalities at various stages of organogenesis in RAR double mutants. Development **120,** 2749-71.

Metkus, A. P., Filly, R. A., Stringer, M. D., Harrison, M. R., and Adzick, N. S. (1996). Sonographic predictors of survival in fetal diaphragmatic hernia. J Pediatr Surg **31,** 148-51.

Metzger, R.J., Klein, O.D., Martin, G.R., and Krasnow, M.A. (2008). The branching programme of mouse lung development. Nature **453**, 745-50.

Michalevicz, D., and Chaimoff, C. (1989). Use of a Silastic sheet for widening the abdominal cavity in the surgical treatment of diaphragmatic hernia. J Pediatr Surg **24,** 265-6.

Miller, L.A., Wert, S.E. and Whitsett, J.A. (2001). Immunolocalization of sonic hedgehog (Shh) in developing mouse lung. J Histochem Cytochem **49**, 1593-1604.

Missiaen, L., Callewaert, G., De Smedt, H. and Parys, J.B. (2001). 2-Aminoethoxydiphenyl borate affects the inositol 1,4,5-trisphosphate receptor, the intracellular Ca^{2+} pump and the non-specific Ca^{2+} leak from the non-mitochondrial Ca^{2+} stores in permeabilized A7r5 cells. Cell Calcium **29**, 111-116.

Mitchell JJ, Reynolds SE, Leslie KO, Low RB, Woodcock-Mitchell J (1990). Smooth muscle cell markers in developing rat lung. Am J Respir Cell Mol Biol **3**, 515-23.

Mitzner, W. (2004). Airway smooth muscle: the appendix of the lung. Am J Respir Crit Care Med **169**, 787-90.

Miyawaki, A., Llopis, J., Heim, R., McCaffery, J.M., Adams, J.A., Ikura, M. and Tsien, R.Y. (1997). Fluorescent indicators for Ca^{2+} based on green fluorescent proteins and calmodulin. Nature 388, 882-887.

Moessinger, A.C., Harding, R., Adamson, T.M., Singh, M. and Kiu, G.T. (1990). Role of lung fluid volume in growth and maturation of the fetal sheep lung. J Clin Invest 86, 1270-7.

Moore, K.A., Polte, T., Huang, S., Shi, B., Alsberg, E., Sunday, M.E. and Ingber, D.E. (2005). Control of basement membrane remodeling and epithelial branching morphogenesis in embryonic lung by Rho and cytoskeletal tension. Dev Dyn **232**, 268-281.

Morise, H., Shimomura, O, Johnson, F.H. and Winant, J. Intermolecular energy transfer in the bioluminescent system of Aequorea. Biochemistry **13**, 2656-2662.

Moss, R.L., Chen, C.M. and Harrison, M.R. (2001). Prosthetic patch durability in congenital diaphragmatic hernia: a long-term follow-up study. J Pediatr Surg **36**, 152-154.

Motoyama, J., Liu, J., Mo, R., Ding, Q., Post, M., and Hui, C. C. (1998). Essential function of Gli2 and Gli3 in the formation of lung, trachea and oesophagus. Nat Genet **20,** 54-7.

Moya, F.R., Thomas, V.L., Romaguera, J., Mysore, M.R., Maberry, M., Bernard, A. and Freund, M. (1995). Fetal lung maturation in congenital diaphragmatic hernia. Am J Obstet Gynecol **173**, 1401-5.

Moyer, V., Moya, F., Tibboel, R., Losty, P., Nagaya, M. and Lally, K.P. (2000). Late versus early surgical correction for congenital diaphragmatic hernia in newborn infants. Cochrane Database Syst Rev **3**, CD001695.

Murray, C.B., Morales, M.M., Flotte, T.R., McGrath-Morrow, S.A., Guggino, W.B. and Zeitlin, P.L. (1995). CIC-2: a developmentally dependent chloride channel expressed in the fetal lung and downregulated after birth. Am J Respir Cell Mol Biol **12**, 597-604.

Nagai, T., Sawano, A., Park, E.S. and Miyawaki, A. (2001). Circularly permuted green fluorescent proteins engineered to sense Ca^{2+}. Proc Natl Acad Sci USA 98, 3197-3202.

Nakamura, T., Liu, M., Mourgeon, E., Slutsky, A. and Post, M. (2000). Mechanical strain and dexamethasone selectively increase surfactant protein C and tropoelastin gene expression. Am J Physiol Lung Cell Mol Physiol **278**, L974-80.

Nakamura, Y., Yamatoto, I., Fukuda, S., and Hashimoto, T. (1991). Pulmonary acinar development in diaphragmatic hernia. Arch Pathol Lab Med **115,** 372-376.

Neff, K.W., Kilian, A.K., Schaible, T., Schütz, E.M. and Büsing, K.A. (2007). Prediction of mortality and need for neonatal extracorporeal membrane oxygenation in fetuses with congenital diaphragmatic hernia: logistic regression analysis based on MRI fetal lung volume measurements. AJR Am J Roentgenol **189**, 1307-11.

Nelson, S.M., Hajivassiliou, C.A., Haddock, G., Cameron, A.D., Robertson, L., Olver, R.E. and Hume, R. (2005). Rescue of the hypoplastic lung by prenatal cyclical strain. Am J Respir Crit Care Med **171**, 1395-1402.

Neonatal Inhaled Nitric Oxide Study Group (1997). Inhaled nitric oxide and hypoxic respiratory failure in infants with congenital diaphragmatic hernia. Pediatrics **99,** 838-45.

Neville, H.L., Jaksic, T., Wilson, J.M., Lally, P.A., Hardin, W.D. Jr., Hirschl, R.B. and Lally, K.P.; Congenital Diaphragmatic Hernia Study Group (2003). Bilateral congenital diaphragmatic hernia.J Pediatr Surg **38**, 522-4.

Nio, M., Haase, G., Kennaugh, J., Bui, K., and Atkinson, J. B. (1994). A prospective randomized trial of delayed versus immediate repair of congenital diaphragmatic hernia. J Pediatr Surg **29,** 618-21.

Noble, B.R., Babiuk, R.P., Clugston, R.D., Underhill, T.M., Sun, H., Kawaguchi, R., Walfish, P.G., Blomhoff, R., Gundersen, T.E., and Greer, J.J. (2007). Mechanisms of

action of the congenital diaphragmatic hernia-inducing teratogen nitrofen. Am J Physiol Lung Cell Mol Physiol **293**, L1079-L1087.

Nogawa, H. and Hasegawa, Y. (2002). Sucrose stimulates branching morphogenesis of embryonic mouse lung in vitro: a problem of osmotic balance between lumen fluid and culture medium. Dev Growth Differ **44**, 383-90.

Ohkawa, H., Matsumoto, M., Hori, T., and Kashiwa, H. (1993). Familial congenital diaphragmatic hernia in the pig--studies on pathology and heredity. *Eur J Pediatr Surg* **3,** 67-71.

Ontario Congenital Anomalies Study Group (2004). Apparent truth about congenital diaphragmatic hernia: a population-based database is needed to establish benchmarking for clinical outcomes for CDH. J Pediatr Surg **39**, 661-5.

O'Toole, S.J., Sharma, A., Karamanoukian, H.L., Holm, B., Azizkhan, R.G. and Glick, P.L. (1996). Tracheal ligation does not correct the surfactant deficiency associated with congenital diaphragmatic hernia. J Pediatr Surg **31**, 546-50.

Palmer, R.M., Ferrige, A.G. and Moncada, S. (1987). Nitric oxide release accounts for the biological activity of endothelium-derived relaxing factor. Nature **327**, 524-526.

Pepicelli, C.V., Lewis, P.M. and McMahon, A.P. (1998). Sonic hedgehog regulates branching morphogenesis in the mammalian lung. Curr Biol **8**, 1083-1086.

Potter, E. (1946). Bilateral renal agenesis. J Pediatr **29**, 68-76.

Powell, P.D. and Johnstone, J.M.. (1962). Phenometrazine and fetal abnormalities. BMJ **2**, 1327.

Prasher, D., McCann, R.O. and Cormier, M.J. (1985). Cloning and expression of the cDNA coding for aequorin, a bioluminescent calcium-binding protein. Biochem Biophys Res Commun **126**, 1259-1268.

Proctor, A.V. and Fry, C.H. (1999). The actions of altered osmolarity on guinea-pig detrusor smooth muscle contractility and intracellular calcium. Pflugers Arch **438**, 531-7.

Quaggin, S.E., Vanden Heuvel, G.B. and Igarashi, P. (1998). Pod-1, a mesoderm-specific basic-helix-loop-helix protein expressed in mesenchymal and glomerular epithelial cells in the developing kidney. Mech Dev **71**, 37-48.

Rankin, J., Pattenden, S., Abramsky, L., Boyd, P., Jordan, H., Stone, D., Vrijheid, M., Wellesley, D. and Dolk, H. (2005). Prevalence of congenital anomalies in five British regions, 1991-99. Arch Dis Child Fetal Neonatal Ed **90**, F374-9.

Rasheed, A., Tindall, S., Cueny, D.L., Klein, M.D. and Delaney-Black, V. (2001). Neurodevelopmental outcome after congenital diaphragmatic hernia: Extracorporeal membrane oxygenation before and after surgery. J Pediatr Surg **36**, 539-44.

Reiff, D.F., Thiel, P.R. and Schuster, C.M. (2002). Differential regulation of active zone density during long-term strengthening of Drosophila neuromuscular junctions. J Neurosci **22**, 9399-9409.

Rembold, C.M., Kendall, J.M. and Campbell, A.K. (1997). Measurement of changes in sarcoplasmic reticulum [Ca^{2+}] in rat tail artery with targeted apoaequorin delivered by an adenoviral vector. Cell Calcium **21**, 69-79.

Rizzuto R, Brini M and Pozzan T (1994). Targeting recombinant aequorin to specific intracellular organelles. Methods Cell Biol **40**, 339-358.

Rizzuto, R., Simpson, A.W., Brini, M. and Pozzan, T. (1992). Rapid changes of mitochondrial Ca^{2+} revealed by specifically targeted recombinant aequorin. Nature **358**, 325-327.

Robertson, C.M., Cheung, P.Y., Haluschak, M.M., Elliott, C.A. and Leonard, N.J. (1998). High prevalence of sensorineural hearing loss among survivors of neonatal congenital diaphragmatic hernia. Western Canadian ECMO Follow-up Group. Am J Otol **19**, 730-6.

Roman, J. (1995). Effects of calcium channel blockade on mammalian lung branching morphogenesis. Exp Lung Res **21**, 489-502.

Romoser, V.A., Hinkle, P.M. and Persechini, A. (1997). Detection in living cells of Ca^{2+}-dependent changes in the fluorescence emission of an indicator composed of two green fluorescent protein variants linked by a calmodulin-binding sequence. A new class of fluorescent indicators. J Biol Chem **272**, 13270-13274.

Roubliova, X., Verbeken, E., Wu, J., Yamamoto, H., Lerut, T., Tibboel, D. and Deprest, J. (2004). Pulmonary vascular morphology in a fetal rabbit model for congenital diaphragmatic hernia. J Pediatr Surg **39**, 1066-72.

Rudolf, R., Mongillo, M., Rizzuto, R. and Pozzan, T. (2003). Looking forward to seeing calcium. Nat Rev Mol Cell Biol 4, 579-86.

Ruocco, S., Lallemand, A., Tournier, J.M. and Gaillard, D. (1996). Expression and localization of epidermal growth factor, transforming growth factor-alpha, and localization of their common receptor in fetal human lung development. Pediatr Res **39**, 448-455.

Sanchez-Esteban, J., Tsai, S.W., Sang, J., Qin, J., Torday, J.S. and Rubin, L.P. (1998). Effects of mechanical forces on lung-specific gene expression. Am J Med Sci **316**, 200-4.

Sanders, K.M. (2001). Invited review: Mechanisms of calcium handling in smooth muscles. J Appl Physiol **91**, 1438-1449.

Saura, L., Castañón, M., Prat, J., Albert, A., Caceres, F., Moreno, J. and Gratacós, E. (2007). Impact of fetal intervention on postnatal management of congenital diaphragmatic hernia. Eur J Pediatr Surg **17**, 404-7.

Scaife, E.R., Johnson, D.G., Meyers, R.L., Johnson, S.M. and Matlak, M.E. (2003). The split abdominal wall muscle flap--a simple, mesh-free approach to repair large diaphragmatic hernia. J Pediatr Surg **38**, 1748-1751.

Schaarschmidt, K., Strauss, J., Kolberg-Schwerdt, A., Lempe, M., Schlesinger, F. and Jaeschke, U. (2005). Thoracoscopic repair of congenital diaphragmatic hernia by inflation-assisted bowel reduction, in a resuscitated neonate: a better access? Pediatr Surg Int **21**, 806-8.

Schittny, J.C., Miserocchi, G. and Sparrow, M.P. (2000). Spontaneous peristaltic airway contractions propel lung liquid through the bronchial tree of intact and fetal lung explants. Am J Respir Cell Mol Biol **23**, 11-18.

Schoeman, L., Pierro, A., Macrae, D., Spitz, L., Kiely, E.M. and Drake, D.P. (1999). Late death after extracorporeal membrane oxygenation for congenital diaphragmatic hernia. J Pediatr Surg **34**, 357-9.

Schopper, W. (1935). Embryonales und erwachsenes Lungengewebe vom Meerschweinchen und Huhn in der Kultur mit Zeitrafferbeobachtungen an Flimmerepithel, sog. Alveolarphagocyten und von Kontraktionen der Bronchialmuskulatur. Virchows Arch **295**, 644.

Schopper, W. (1937). uber das Verhalten des Lungengewebes in der Gewebe-kultur (Filmdemonstration). Arch Exp Zellforsch **19**, 326-328.

Schuger, L. (1997). Laminins in lung development. Exp Lung Res **23,** 119-29.

Sekine, K., Ohuchi, H., Fujiwara, M., Yamasaki, M., Yoshizawa, T., Sato, T., Yagishita, N., Matsui, D., Koga, Y., Itoh, N., and Kato, S. (1999). Fgf10 is essential for limb and lung formation. Nat Genet **21,** 138-41.

Shah, A.V. and Shah, A.A. (2002). Laparoscopic approach to surgical management of congenital diaphragmatic hernia in the newborn. J Pediatr Surg 37, 548-550.

Shanbhogue, L.K., Tam, P.K., Ninan, G., and Lloyd, D.A. (1990). Preoperative stabilisation in congenital diaphragmatic hernia. Arch Dis Child **65**, 1043-4.

Shannon, J.M. and Hyatt, B.A. (2004). Epithelial-mesenchymal interactions in the developing lung. Annu Rev Physiol **66**, 625-645.

Shimomura, O., Johnson, F.H. and Saiga, Y. (1962). Extraction, purification and properties of aequorin, a bioluminescent protein from the luminous hydromedusan, Aequorea. J Cell Comp Physiol **59**, 223-239.

Short, A.D., Bian, J., Ghosh, T.K., Waldron, R.T., Rybak, S.L. and Gill, D.L. (1993). Intracellular Ca2+ pool content is linked to control of cell growth. Proc Natl Acad Sci USA **90**, 4986-90.

Shukla, N., Jeremy, J.Y., Nicholl, P., Krijgsman, B., Stansby, G. and Hamilton, G. (1997). Short-term exposure to low concentrations of thapsigargin inhibits replication of cultured human vascular smooth muscle cells. Br J Surg **84**, 325-30.

Shmygol, A., Blanks, A.M., Bru-Mercier, G., Gullam, J.E. and Thornton, S. (2007) Control of uterine Ca^{2+} by membrane voltage: toward understanding the excitation-contraction coupling in human myometrium. Ann N Y Acad Sci **1101**, 97-109.

Silver, M.M., Thurston, W.A. and Patrick, J.E. (1988). Perinatal pulmonary hyperplasia due to laryngeal atresia. Hum Pathol **19**, 110-3.

Skari, H., Bjornland, K., Frenckner, B., Friberg, L.G., Heikkinen, M., Hurme, T., Loe, B., Mollerlokken, G., Nielsen, O.H., Qvist, N., Rintala, R., Sandgren, K., Serlo, W., Wagner, K., Wester, T. and Emblem, R. (2004). Congenital diaphragmatic hernia: a survey of practice in Scandinavia. Pediatr Surg Int **20**, 309-13.

Skari, H., Bjornland, K., Haugen, G., Egeland, T., and Emblem, R. (2000). Congenital diaphragmatic hernia: a meta-analysis of mortality factors. J Pediatr Surg **35,** 1187-97.

Skarsgard ED, Meuli M, VanderWall KJ, Bealer JF, Adzick NS, Harrison MR (1996). Fetal endoscopic tracheal occlusion ('Fetendo-PLUG') for congenital diaphragmatic hernia. J Pediatr Surg **31**, 1335-8.

Skinner, S.J., Somervell, C.E. and Olson, D.M. (1992). The effects of mechanical stretching on fetal rat lung cell prostacyclin production. Prostaglandins **43**, 413-33.

Slavotinek, A.M., Warmerdam, B., Lin, A.E. and Shaw, G.M. (2007). Population-based analysis of left- and right-sided diaphragmatic hernias demonstrates different frequencies of selected additional anomalies. Am J Med Genet A **143**, 3127-36.

Smith, N.P., Jesudason, E.C. and Losty, P.D. (2002). Congenital diaphragmatic hernia. Pediatr Respir Rev **3**, 339-48.

Smith, N.P., Jesudason, E.C., Featherstone, N.C., Corbett, H.J. and Losty, P.D. (2005). Recent advances in congenital diaphragmatic hernia. Arch Dis Child **90**, 426-8.

Solmann, T. and Gilbert, A.J. (1937). Microscopic observations on bronchiolar reactions. J Pharmacol Exp Ther **61**, 272-285.

Somlyo, A.P. and Somlyo, A.V. (1994). Signal transduction and regulation in smooth muscle. Nature **372**, 231-236.

Sorokin, S. (1961). A study of development in organ cultures of mammalian lungs. Dev Biol **3**, 60-83.

Sparrow, M.P. and Lamb, J.P. (2003). Ontogeny of airway smooth muscle: structure, innervation, myogenesis and function in the fetal lung. Respir Physiol Neurobiol **16**, 261-72.

Sparrow, M.P., Warwick, S.P. and Mitchell, H.W. (1994). Foetal airway motor tone in prenatal lung development of the pig. Eur Respir J **7**, 1416-1424.

Sparrow, M.P., Warwick, S.P. and Everett, A.W. (1995). Innervation and function of the distal airways in the developing bronchial tree of fetal pig lung. Am J Respir Cell Mol Biol **13**, 518-25.

Sparrow, M.P., Weichselbaum, M. and McCray, P.B. (1999). Development of the innervation and airway smooth muscle in human fetal lung. Am J Respir Cell Mol Biol **20**, 550-60.

Spooner, B. S., and Wessells, N. K. (1970). Mammalian lung development: interactions in primordium formation and bronchial morphogenesis. J Exp Zool **175,** 445-54.

Stege, G., Fenton, A. and Jaffray, B. (2003). Nihilism in the 1990s: the true mortality of congenital diaphragmatic hernia. Pediatrics **112**, 532-5.

Stephens, N.L. (2002). Airway smooth muscle. Lung **179**, 333-373.

Stevens, D. C., Schreiner, R. L., Bull, M. J., Bryson, C. Q., Lemons, J. A., Gresham, E. L., Grosfeld, J. L., and Weber, T. R. (1980). An analysis of tolazoline therapy in the critically-ill neonate. J Pediatr Surg **15,** 964-70.

Stevens, R.J., Weinert, J.S. and Publicover, N.G. (1999). Visualization of origins and propagation of excitation in canine gastric smooth muscle. Am J Physiol **277**, C448-C460.

Sturgess, J. and Imrie, J. (1982). Quantitative evaluation of the development of tracheal submucosal glands in infants with cystic fibrosis and control infants. Am J Pathol **106**, 303-11.

Sweed, Y., and Puri, P. (1993). Congenital diaphragmatic hernia: influence of associated malformations on survival. *Arch Dis Child* **69,** 68-70.

Sydorak, R.M., Hoffman, W., Lee, H., Yingling, C.D., Longaker, M., Chang, J., Smith, B., Harrison, M.R. and Albanese, C.T. (2003). Reversed latissimus dorsi muscle flap for repair of recurrent congenital diaphragmatic hernia. J Pediatr Surg **38**, 296-300.

Taderera, J.V. (1967). Control of lung differentiation in vitro. Dev Biol **16**, 489-512.

Taggart, M.J. and Wray, S. (1998). Contribution of sarcoplasmic reticular calcium to smooth muscle contractile activation: gestational dependence in isolated rat uterus. J Physiol **511**, 133-144.

Taleporos, P., Salgo, M. P., and Oster, G. (1978). Teratogenic action of bis(dichloroacetyl)diamine on rats: patterns of malformations produced in high incidence at time-limited periods of development. *Teratology* **18,** 5-15.

Taskin, M., Zengin, K., Unal, E., Eren, D. and Korman, U. (2002). Laparoscopic repair of congenital diaphragmatic hernias. Surg Endosc **16**, 869.

Taylor, C.W. and Laude, A.J. (2002). IP3 receptors and their regulation by calmodulin and cystolic Ca^{2+}. Cell Calcium **32**, 321-334.

Teixeira, J., Sepulveda, W., Hassan, J., Cox, P.M. and Singh, M.P. (1997). Abdominal circumference in fetuses with congenital diaphragmatic hernia: correlation with hernia content and pregnancy outcome. J Ultrasound Med **16**, 407-10.

Ten Have-Opbroek, A. A. W. (1981). The development of the lung in mammals: an analysis of concepts and findings. Am J Anat **162,** 201-219.

The Congenital Diaphragmatic Hernia Study Group (1999). Does extracorporeal membrane oxygenation improve survival in neonates with congenital diaphragmatic hernia? The Congenital Diaphragmatic Hernia Study Group. J Pediatr Surg **34**, 720-724.

Thilaganathan, B. (2002). Routine ultrasound for the prenatal diagnosis of congenital diaphragmatic hernia: the 'isms'. Ultrasound Obstet Gynecol **19**, 327-8.

Thurlbeck, W.M. (1982). Postnatal human lung growth. Thorax **37**, 564-71.

Tibboel, D., and Gaag, A. V. (1996). Etiologic and genetic factors in congenital diaphragmatic hernia. Clin Perinatol **23,** 689-99.

Ting, A., Glick, P. L., Wilcox, D. T., Holm, B. A., Gil, J., and DiMaio, M. (1998). Alveolar vascularization of the lung in a lamb model of congenital diaphragmatic hernia. Am J Respir Crit Care Med **157,** 31-4.

Tollet, J., Everett, A.W. and Sparrow, M.P. (2001). Spatial and temporal distribution of nerves, ganglia, and smooth muscle during the early pseudoglandular stage of fetal mouse lung development. Dev Dyn **221**, 48-60.

Toma C, Greenwood IA, Helliwell RM, Large WA (1996). Activation of potassium currents by inhibitors of calcium-activated chloride conductance in rabbit portal vein smooth muscle cells. Br J Pharmacol **118**, 513-20.

Torday, J.S., Sanchez-Esteban, J. and Rubin, L.P. (1998). Paracrine mediators of mechanotransduction in lung development. Am J Med Sci **316**, 205-8.

Tovar, J.A., Qi, B., Diez-Pardo, J.A., Alfonso, L.F., Aranaiz, A., Alvarez, F.J., Valls-i-Soler, A., and Morreale de Escobar, G. (1997). Thyroid hormones in the pathogenesis of lung hypoplasia and immaturity induced in fetal rats by prenatal exposure to nitrofen. J Pediatr Surg **32**, 1395-1397.

Tsien, R.Y. (1980). New calcium indicators and buffers with high selectivity against magnesium and protons: design, synthesis, and properties of prototype structures. Biochemistry **19**, 2396-2404.

Tsien, R.Y. (1981). A non-disruptive technique for loading calcium buffers and indicators into cells. Nature **290**, 527- 528.

UK Collaborative ECMO Trail Group (1996). UK collaborative randomised trial of neonatal extracorporeal membrane oxygenation. Lancet **348**, 75-82.

Urase, K., Mukasa, T., Igarashi, H., Ishii, Y., Yasugi, S., Momoi, M.Y. and Momoi, T. (1996). Spatial expression of Sonic hedgehog in the lung epithelium during branching morphogenesis. Biochem Biophys Res Commun **225**, 161-166.

Valls-i-Soler, A., Alfonso, L. F., Arnaiz, A., Alvarez, F. J., and Tovar, J. A. (1996). Pulmonary surfactant dysfunction in congenital diaphragmatic hernia: experimental and clinical findings. Biol Neonate **69,** 318-26.

VanderWall, K.J., Bruch, S.W., Meuli, M., Kohl, T., Szabo, Z., Adzick, N.S. and Harrison, M.R. (1996). Fetal endoscopic ('Fetendo') tracheal clip. J Pediatr Surg **31**, 1101-3.

Van Meurs, K.; Congenital Diaphragmatic Hernia Study Group (2004). Is surfactant therapy beneficial in the treatment of the term newborn infant with congenital diaphragmatic hernia? J Pediatr **145**, 312-6.

van Tuyl, M., Liu, J., Groenman, F., Ridsdale, R., Han, R.N., Venkatesh, V., Tibboel, D. and Post, M. (2006). Iroquois genes influence proximo-distal morphogenesis during rat lung development. Am J Respir Crit Care Med **290**, L777-L789.

Vilos, G.A. and Liggins, G.C. (1982). Intrathoracic pressures in fetal sheep. J Dev Physiol **4**, 247-256.

Wang, J., Campos, B., Kaetzel, M.A. and Dedman, J.R. (1996). Expression of a calmodulin inhibitor peptide in progenitor alveolar type II cells disrupts lung development. Am J Physiol **271**, L245-L250.

Warburton, D., Schwarz, M., Tefft, D., Flores-Delgado, G., Anderson, K. D., and Cardoso, W. V. (2000). The molecular basis of lung morphogenesis. Mech Dev **92,** 55-81.

Ward, S.M. and Sanders, K.M. (2001). Physiology and pathophysiology of the interstitial cell of Cajal: from bench to bedside. I. Functional development and plasticity of interstitial cells of Cajal networks. Am J Physiol Gastrointest Liver Physiol **281**, G602-11.

Weber, T.R., Connors, R.H., Pennington, D.G., Westfall, S., Keenan, W., Kotagal, S. and Lewis, J.E. (1987). Neonatal diaphragmatic hernia. An improving outlook with extracorporeal membrane oxygenation. Arch Surg **122**, 615-618.

Weiss, R.M., Tamarkin, F.J. and Wheeler, M.A. (2006). Pacemaker activity in the upper urinary tract. J Smooth Muscle Res **42**, 103-15.

Wellman, G.C. and Nelson, M.T. (2003). Signaling between SR and plasmalemma in smooth muscle: sparks and the activation of Ca^{2+}-sensitive ion channels. Cell Calcium **34**, 211-229.

Wessells, N. K. (1970). Mammalian lung development: interactions in formation and morphogenesis of tracheal buds. J Exp Zool **175,** 455-66.

White, M.M. and Aylwin, M. (1990). Niflumic and flufenamic acids are potent reversible blockers of Ca^{2+}-activated Cl^- channels in *Xenopus* oocytes. Mol Pharmacol **37**, 720-724.

Wigglesworth, J.S. and Desai, R. (1979). Effect on lung growth of cervical cord section in the rabbit fetus. Early Hum Dev **3**, 51-65.

Wilson, J., Roth, C. B., and Waekany, J. (1953). An analysis of the syndromes of malformation induced by maternal vitamin A deficiency. Effects of restoration of vitamin A at various times during gestation. Am J Anat **92,** 189-217.

Wilson, J.M., Lund, D.P., Lillehei, C.W. and Vacanti, J.P. (1997). Congenital diaphragmatic hernia--a tale of two cities: the Boston experience. J Pediatr Surg **32**, 401-405.

Wirtz, H.R. and Dobbs, L.G. (1990). Calcium mobilization and exocytosis after one mechanical stretch of lung epithelial cells. Science **250**, 1266-9.

Witters, I., Legius, E., Moerman, P., Deprest, J., Van Schoubroeck, D., Timmerman, D., Van Assche, F.A. and Fryns, J.P. (2001). Associated malformations and chromosomal anomalies in 42 cases of prenatally diagnosed diaphragmatic hernia. Am J Med Genet **103**, 278-82.

Wray, S. and Noble, K. (2008). Sex hormones and excitation-contraction coupling in the uterus: the effects of oestrous and hormones. J Neuroendocrinol **20**, 451-61

Wright, C., Strauss, S., Toole, K., Burt, A.D. and Robson, S.C. (1999). Composition of the pulmonary interstitium during normal development of the human fetus. Pediatr Dev Pathol **2**, 424-31.

Wu, J., Ge, X., Verbeken, E.K., Gratacós, E., Yesildaglar, N. and Deprest, J.A. (2002). Pulmonary effects of in utero tracheal occlusion are dependent on gestational age in a rabbit model of diaphragmatic hernia. J Pediatr Surg **37**, 11-17.

Wung, J.T., James, L.S., Kilchevsky, E. and James, E. (1985). Management of infants with severe respiratory failure and persistence of the fetal circulation, without hyperventilation. Pediatrics **76**, 488-494.

Wung, J.T., Sahni, R., Moffitt, S.T., Lipsitz, E. and Stolar, C.J. (1995). Congenital diaphragmatic hernia: survival treated with very delayed surgery, spontaneous respiration, and no chest tube. J Pediatr Surg **30**, 406-409.

Xu, J., Liu, M., Tanswell, A. K., and Post, M. (1998). Mesenchymal determination of mechanical strain-induced fetal lung cell proliferation. Am J Physiol **275,** L545-L550.

Yamada, T., Suzuki, E., Gejyo, F. and Ushiki, T. (2002). Developmental changes in the structure of the rat fetal lung, with special reference to the airway smooth muscle and vasculature. Arch Histol Cytol **65**, 55-69.

Yamazawa, T. and Iino, M. (2002). Simultaneous imaging of Ca2+ signals in interstitial cells of Cajal and longitudinal smooth muscle cells during rhythmic activity in mouse ileum. J Physiol **538**, 823-835.

Yang, S.H., Nobuhara, K.K., Keller, R.L., Ball, R.H., Goldstein, R.B., Feldstein, V.A., Callen, P.W., Filly, R.A., Farmer, D.L., Harrison, M.R. and Lee, H. (2007). Reliability of

the lung-to-head ratio as a predictor of outcome in fetuses with isolated left congenital diaphragmatic hernia at gestation outside 24-26 weeks. Am J Obstet Gynecol **197**, 30.e1-7.

Yang, Y., Beqaj, S., Kemp, P., Ariel, I. and Schuger, L. (2000). Stretch-induced alternative splicing of serum response factor promotes bronchial myogenesis and is defective in lung hypoplasia. J Clin Invest **106**, 1321-30.

Yang, Y., Palmer, K.C., Relan, N., Diglio, C. and Schuger, L. (1998). Role of laminin polymerization at the epithelial mesenchymal interface in bronchial myogenesis. Development **125**, 2621-9.

Yang, Y., Relan, N.K., Przywara, D.A. and Schuger, L. (1999). Embryonic mesenchymal cells share the potential for smooth muscle differentiation: myogenesis is controlled by the cell's shape. Development **126**, 3027-33.

You, L-R, Takamoto, N., Yu, C-T., Tanaka, T., Kodama, T., DeMayo, F.J., Tsai, S.Y., and Tsai, M-J. (2005). Mouse lacking COUP-TFII as an animal model of Bochdalek-type congenital diaphragmatic hernia. PNAS **102**, 16351-16356.

Young, R.C. (2007). Myocytes, myometrium, and uterine contractions. Ann N Y Acad Sci **1101**, 72-84.

Yu, D., Baird, G.S., Tsien, R.Y. and Davis, R.L. (2003). Detection of calcium transients in Drosophila mushroom body neurons with camgaroo reporters. J Neurosci **23**, 64-72.

Yuan, Y. and Atchison, W.D. (2007). Methylmercury-induced increase of intracellular Ca^{2+} increases spontaneous synaptic current frequency in rat cerebellar slices. Mol Pharmacol **71**, 1109-21.

Zeltner, T.B. and Burri, P.H. (1987a). The postnatal development and growth of the human lung. II. Morphology. Respir Physiol **67**, 269-82.

Zeltner, T.B., Caduff, J.H., Gehr, P., Pfenninger, J. and Burri, P.H. (1987b). The postnatal development and growth of the human lung. I. Morphometry. Respir Physiol **67**, 247-67.

Zhang, J., O'Shea, S., Liu, J. and Schuger, L. (1999). Bronchial smooth muscle hypoplasia in mouse embryonic lungs exposed to a laminin beta1 chain antisense oligonucleotide. Mech Dev **89**, 15-23.

Zhou, L., Dey, C.R., Wert, S.E., Yan, C., Costa, R.H. and Whitsett, J.A. (1997). Hepatocyte nuclear factor-3beta limits cellular diversity in the developing respiratory epithelium and alters lung morphogenesis in vivo. Dev Dyn **210**, 305-314.

Zhou, L., Lim, L., Costa, R.H. and Whitsett, J.A. (1996). Thyroid transcription factor-1, hepatocyte nuclear factor-3beta, surfactant protein B, C, and Clara cell secretory protein in developing mouse lung. J Histochem Cytochem **44**, 1183-93.